REFERENCE VOLUME CONSIDERATION IN LIMIT LOAD DETERMINATION

PHANI SURESH REDDY, GUDIMETLA

Reference Volume Consideration in Limit Load Determination

By

Phani Suresh Reddy, Gudimetla., B.Tech., M.E.

A thesis submitted to the School of Graduate Studies

In partial fulfillment of the requirement for the degree of
Doctor of Philosophy in Engineering

Faculty of Engineering & Applied Science
Memorial University

St. John's, Newfoundland and Labrador, Canada
26th Aug 2010.

ABSTRACT

Reference volume plays an important role in finding out the limit loads of mechanical components and structures. In the current research work, new and simplified methods are proposed in order to determine the reference volume (i.e., elastic and plastic reference volumes) for any given general mechanical component or structure.

Many methods have been developed for estimating limit loads in general components and structures; these methods depend on an upper bound multiplier which takes the total volume into consideration. Considering total volume results in overestimating the upper bound multiplier. To overcome this deficiency, two methods are proposed in this research to find reliable estimate of limit load using the reference volume.

The Elastic Reference Volume Method is developed by extending the well established pressure bulb concepts in soil mechanics to general mechanical components. This method is basically for second category components, like components with notches or cracks. The results obtained are within the range of 2 to 5 percent lower bounded to non-linear results. On the other hand, for the first category components which are well designed, the Plastic Reference Volume Method is developed. The results obtained are with in the range of 2 to 7 percent lower bounded to non-linear results.

To obtain a reliable lower bounded limit loads, other than the dead volume effect peak stress effect is also need to be corrected. A new method which can correct both the reference volume effect and the peak stress effect is developed. This method given a lower bounded m_α tangent multiplier for all the examples. The results are compared with the non-linear analysis results and results are found to be very close estimates (< 2 percent) to the non-linear results.

Taking the practical material usage in industry into consideration, a new method is developed for finding out limit loads of components or structures made of anisotropic materials by incorporating the reference volume correction. The usage of anisotropic materials in industries is increasing day by day, and so is the need for finding out accurate limit loads for components considering such material properties. The results are found to be in good agreement with the non-linear results.

Whenever a component or a structure is subjected to continuous loading and the stress exceeds the yield limit, the component undergoes strain hardening. It is very important to consider this strain hardening effect while obtaining the limit loads for optimal utilization of material. A new method developed in this research will take the strain hardening effect upto a 5% strain limit into consideration, while calculating the limit loads. Multipliers obtained using this approach are found higher then the ones obtained by regular limit analysis, suggesting the usage of reserved strength.

ACKNOWLEDGEMENTS

I would like to express my deep gratitude to my supervisor, Dr. R. Seshadri, for his intellectual guidance, tireless support and valuable discussions during the course of my Doctorial program. His vast knowledge and immense expertise in diversified areas provided me with working in industrial projects. I would also like to thank Dr. K. Munaswamy for all his support and co-supervision. I would also like to thank Dr. Bipul Hawaldar, Dr. A. S. J. Swamidas and Dr. S. M. R. Adluri for their help and support. I am also thankful to Dr. Reza Adibi-asl and Dr. Mosharraf Hossain from Nuclear Safety Solutions (NSS) for their valuable technical discussions.

The financial support provided by the School of Graduate Studies and the Faculty of Engineering and Applied Science, Memorial University is gratefully acknowledged. I also thank Dr. Leonard Lye, Associated Dean of Graduate Studies, and acknowledge Ms. Moya Crocker, office of the Associate Dean, for her administrative assistance during the course of my program.

I would like to extend my acknowledgements to my friends in the Asset Integrity Management Research Group for their cooperation. I would like to thank all my friends for their support and encouragement. I also would like to thank Ms. Heather O'Brien, Canada Research Chairs office, for her administrative assistance during the course of my program.

I owe my deepest thanks to Dr. S. P. Reddy and Ms. Parvati Reddy for their continuous support and encouragement throughout my program. I also owe my thanks to my family members, Dr. G. P. R. Vittal Reddy and G. Rama Devi for their inspiration and understanding through all these years.

TABLE OF CONTENTS

LIST OF TABLES

LIST OF FIGURES

NOMENCLATURE

Symbols

$\dot{D}$	Increment of plastic dissipation for unit volume
E	Modulus of elasticity
E_0	Initial modulus
E_t	Tangent modulus
$f(s_{ij})$	Yield function
F	Peak stress
L	Length of beam
m	Exact limit load multiplier
m^0	Upper bound multiplier
$m^0(V_{re})$	Upper bound multiplier with elastic reference volume method correction
$m^0(V_{rp})$	Upper bound multiplier with plastic reference volume method correction
m_α	Improved lower bound multiplier
m_α^T	m-alfa tangent multiplier
$m_\alpha^T(V_{re})$	m-alfa tangent multiplier with elastic reference volume method correction
$m_\alpha^T(V_{rp})$	m-alfa tangent multiplier with plastic reference volume method correction
m^*	Kinematically admissible multiplier
m_L	Classical lower bound limit load multiplier
m_u	Classical upper bound limit load multiplier
M	Bending moment
p	Internal pressure
P	Primary stress, Normal force
q	Modulus adjustment index
Q	Secondary stresses
r_1, r_2, r_3	Fillet radius

R, r	Radius
R_i	Inner radius
R_0	Outer radius
R^0	Ratio of m^0 / m
R_L	Ratio of m_L / m
R_α	Ratio of m_α / m
s_{ij}	Deviatoric stress field
s_{ij}^0	Statically admissible deviatoric stress field under applied load $m^0 T_i$
$\bar{s}_{ij}^0$	Statically admissible deviatoric stress field under applied load T_i
s_{eq}	Equivalent stress
S_T	Surface of the body where surface traction is prescribed
S_V	Surface of the body where velocity is applied
t_n	Required minimum wall thickness
T_i	Applied surface traction
$\dot{u}$	Velocity field
V	Volume of the component
V_R	Reference volume
V_η	Sub-volume
$\bar{V}_\eta$	Sub-volume ratio
V_T	Total volume
w	Width

Greek Symbols

δ_{ij}	Kronecker's delta
ε	Strain
$\dot{\varepsilon}$	Strain rate
$d\varepsilon_{ij}^p$	Plastic strain increment

$\dot{\varepsilon}_{ij}^{*}$	Kinematically admissible strain rate
v_i^{*}	Kinematically admissible velocity field
φ^{0}	Point function introduced in the yield criterion
$d\lambda$	Positive scalar of proportionality in the flow rule
μ	Plastic flow parameter
v	Poisson's ratio
σ_{ij}	Stress tensor
$\sigma_{\max}$	Maximum stress
σ_{eq}	von-Mises equivalent stress
σ_{ref}	Reference stress
$\sigma_1, \sigma_2, \sigma_3$	Principle stresses
σ_y	Yield strength
σ_y^{*}	Equivalent yield strength
ζ	ratio of m^0 / m_L
ξ	Iteration Variable

Subscripts

e	von-Mises equivalent
i, j	Tensorial indices
k	Element number
L	Limit, lower bound
u	Upper bound
α	Parameters based on m_α method
y	Yield

Superscripts

0	Statically admissible quantities
T	Tangent
*	Kinematically admissible quantities

Acronyms

ASME	American Society of Mechanical Engineers
DBA	Design by Analysis
EMAP	Elastic Modulus Adjustment Procedure
ERVM	Elastic Reference Volume Method
FEA	Finite Element Analysis
LEFEA	Linear Elastic Finite Element Analysis
NFEA	Nonlinear Finite Element Analysis
PRVM	Plastic Reference Volume Method
TBM	Two Bar Model

CHAPTER 1
INTRODUCTION

1.1 General Background

Mechanical components and structures could be designed based on elastic analysis and elastic-plastic analysis or limit analysis. Among these design philosophies, limit analysis is of considerable interest as it provides protection against gross plastic deformation i.e., catastrophic failure of the components or structures. In addition, it provides a measure of reserve strength of the structure. The limit analysis could be defined as the determination of load that results in cross-sectional plasticity in the structure, which leads to uncontained plastic flow (plastic collapse).

The limit load could be determined either by analytical methods, numerical methods or by using simplified methods. Approximate methods use the bounding theorems to estimate the limit loads. Numerical methods include the nonlinear finite element analysis (FEA) which is a permitted method for limit analysis by the codes and standards (e.g., ASME Boiler and Pressure Vessel Code [1]). Nonlinear FEA is quite complicated as it is carried out in an iterative and incremental manner. It requires detailed information about the material properties at respective operating conditions. Finally, the analysis and interpretation of nonlinear analysis results require in-depth knowledge and expertise in nonlinear analysis techniques. Nonlinear analysis for a complex problem takes longer duration and there is always the possibility shear and volumetric locking [2].

In order to avoid the complicated elastic-plastic limit analysis in designing mechanical components and structures, the development of robust and simplified methods is considered to be an attractive alternative. The advantage of these methods being able to estimate the limit loads by using linear elastic FEA. These methods significantly overcome the limitations of the time consuming and costly nonlinear FEA. In recent years, significant efforts are directed in developing the robust and simplified methods in limit analysis. For any simplified method developed so far finding out the reference volume of the structure has been a challenge. In this thesis the efforts are focused on developing the methods for finding the reference volume for any general component.

1.2 Objectives of Research

The primary set of objectives of the proposed research work is as follows:

1. To develop new and simplified approaches for reference volume determination.
2. To achieve lower bound limit load multipliers for any given general component by incorporating above reference volume approaches.
3. To achieve a lower bounded m_α tangent multiplier by correcting the peak stress and dead volume effects.
4. To achieve lower bound estimates for anisotropic materials components using reference volume concepts.
5. To develop new and simplified method for accurately incorporating the strain hardening effects into the limit load analysis.

1.3 Scope of Research

Estimation of limit loads using simplified methods is of considerable interest due to the simplicity and cost effectiveness, the m_α-method proposed by Seshadri and Mangalaramanan [3], and m_α-tangent methods proposed by Seshadri and Hossain [4] for predicting the limit loads are able to obtain reasonably close estimates of limit load in most of the cases.

These methods depend on upper bound multiplier which takes the total volume into consideration. By considering total volume, we are overestimating the upper bound multiplier. This over estimated upper bound multiplier leads to inaccurate limit load estimates. To overcome this difficulty two methods are developed in this research to find the reference volume. The objective of the present research is to develop simplified methods for estimation of good lower bound limit loads of a general class of mechanical components and structures.

For getting good approximations of the limit loads we need a proper method of finding the reference volume. In the current literature there are reference volume methods developed for certain set of specific components. P. Tantichattanont *et al.* [5], [6] developed reference volume calculation for hot spots and corrosion damages in spherical and cylindrical vessels, F.Ahmad *et al,* [7] developed reference volume calculations for hydrostatic storage tanks. The new approaches of finding the reference volumes are being developed in the current research. These methods are developed to predict reference volumes of any given mechanical component and structure.

Modern components are made not only of materials that can be considered as isotropic, but also of anisotropic materials, due to there mechanical and strength advantages. When compared to isotropic material, the anisotropic materials show appreciable difference in material properties in different directions. Some examples for such components are rolled sheets in pressure vessels, composites and directionally solidified super-alloys in gas turbine blades. The knowledge of the limit load is useful in design and sizing of components and structures made from these materials. The Li Pan and Seshadri [8] proposed a method for determining limit loads in anisotropic material using m_α method. In certain cases the overestimated upper bound multiplier leads to inaccurate limit load estimates. So a new method is developed to obtain reliable reference volume to estimate the lower bound limit loads of any given general component or structure made of anisotropic materials.

In general when ever a component or a structure is subjected to monotonic loading, once the stress crosses the yield limit, the component starts to experience strain hardening. In the general limit analysis this strain hardening effect is not considered while calculating the limit load multipliers, which leads to the under utilization of the material strength. If the strain hardening effect is incorporated into limit analyses while calculating limit loads, the material can be used to its optimal strength level. A new method is developed in this research which will take strain hardening into consideration while calculating more reliable limit loads.

1.4 Organization of the Thesis

This research thesis is composed of nine chapters,

Chapter 1: It covers general background, objectives and scope of the proposed research work.

Chapter 2: Provides a brief literature review related to the current research work. The chapter covers the theoretical aspects of classical elasticity and plasticity including bounding theorems and admissible limit load multiplier.

Chapter 3: It gives an overall review of development of various multipliers. It discusses m_α and m_α-tangent methods in more detail. It discusses the limitations of these methods which will lead way to the necessity of the current developed methods. In this chapter 2-Bar method is generalized to any given component.

Chapter 4: Reference volume concepts in a component is Introduced. The effect of the reference volume on the limit load estimates is discussed. *Elastic Reference Volume method*, its theories and general procedure for incorporation of this method is discussed in detail. The method is applied on different mechanical components and there results are discussed

Chapter 5: *Plastic Reference Volume method*, its theories and general procedures for incorporation of this method is discussed in detail. The method is applied on different mechanical components and there results are discussed.

Chapter 6: A method to obtain the lower bounded *m-alfa* tangent multiplier using a simultaneous correction of dead volume and peak stress effects is introduced. Its theories and general procedure for incorporation of this method is discussed in detail. This method is applied on different mechanical components and the results are discussed.

Chapter 7: In this chapter constitutive Relationships and Multipliers of Anisotropic Material are discussed. The method for incorporating reference volume approach for calculating lower bound limit loads for any general anisotropic material is introduced. General procedure for incorporation of this method is presented. Method is tested on different mechanical components and its results are discussed.

Chapter 8: In this chapter concepts of strain hardening in materials are presented. Different strain hardening material models are studied in detail. The method for incorporating strain hardening effect into limit analysis, its general procedure and its applications are discussed in detail.

Chapter 9: In this chapter achievement of the research work, original contributions are summarized followed with a discussion on the future research scope in these areas.

CHAPTER 2
THEORETICAL BACKGROUND REVIEW

2.1 Introduction

In this chapter the theoretical concepts of the current research are presented. The research work covers an extensive volume of literature covering the areas of elasticity, plasticity and limit analysis. A brief review of the basic theories in elasticity, plasticity and limit analysis including limit load multipliers are presented. A brief overview of variational principles in limit analysis is also presented. These theories and concepts form the background for the current research work.

2.2 Elasticity Concepts

The theory of elasticity deals with those bodies which can recover back to their original shape after the external loads have been removed. The elastic analysis of a mechanical component or structure essentially means the determination of stress and strain fields that simultaneously satisfies the equilibrium equations, compatibility conditions and constitutive relationships. The equilibrium equations are basic physical laws that represent a balance between the applied external forces and/or moments with that of the internal resistive forces and/or moments. Where as, compatibility conditions are the geometric relationships that express the continuity of the structure.

The stresses and strains within the elastic limit are more of instantaneous and are independent of the loading history. The stresses are related to the strains using constitutive relationships. The principles and mathematical interpretations of the theory of Elasticity are available in number of standard texts Timoshenko and Gere [9], Shames and Cozzarelli [10].

The constitutive relationship for a linear elastic body can be established by generalized Hooke's law. The most generalized relationship between the stresses and strains could be expressed by,

$$\sigma_{ij} = C_{ijkl}\, \varepsilon_{kl} \tag{2.1}$$

where, σ_{ij} is the stress tensor, ε_{kl} is the strain tensor and C_{ijkl} are the material dependent elastic constants.

In case of isotropic materials, where all possible symmetries are considered, the elastic strains are related to the stresses according to the following relationship,

$$\varepsilon_{ij} = \frac{1+\nu}{E}\sigma_{ij} - \frac{\nu}{E}\sigma_{kk}\,\delta_{ij} \tag{2.2}$$

where, ε_{ij} is the strain tensor, σ_{ij} is the stress tensor, E is the Young's modulus, ν is the Poisson's ratio and δ_{ij} is the Kronecker's delta.

In design using the theory of elasticity, the maximum stress based on certain specified conditions is limited to the *allowable stress* of the material. The allowable stress is usually defined on the basis of design *safety factor* and *yield strength* of the material.

2.3 Plasticity Concepts

The theory of plasticity deals with those bodies which can not recover back to their original shape after the external loads have been removed. The principles and mathematical interpretations of the theory of plasticity are available in a number of standard texts Mendelson [11], Calladine [12], Hill [13] and Kachanov [14]. In the plastic range; the strains are dependent on the history of the loading. In order to determine the final strain, the incremental strains are accumulated over the full loading history. The stress-strain relationship in plastic range is generally expressed by *Prandtl-Reuss* equation and is characterized as *flow rule*.

In the plastic theory it is assumed that the solids are isotropic and homogeneous and onset of yielding is identical in tension and compression. Volume changes are considered to be negligible and hydrostatic stress state does not influence yielding.

Theory of plasticity is the basis for limit analysis. The limit analysis is an idealized form of elastic-plastic analysis, where an elastic perfectly plastic material model is assumed with out considering any strain hardening.

2.4 Incremental and Deformation Theories

When the material is loaded with in the elastic range, the strains are linearly related to stresses by Hooke's law. In this case, the stresses can be computed directly from the current state of strain regardless of the loading history. But in the plastic range, the relationship between stresses and strains are nonlinear and the final strain depends on history of loading. Therefore, the total strain can be computed by summing the increments of plastic strain through out the loading history. The onset of yielding is defined by the appropriate yield criterion and the subsequent plastic strain increment is prescribed by the corresponding plastic *flow rule*. The most general form of the plastic flow rule for ideal plasticity is as follows,

$$d\varepsilon_{ij}^{p} = d\lambda \frac{\partial f(\sigma_{ij})}{\partial \sigma_{ij}} \tag{2.3}$$

where, $d\varepsilon_{ij}^{p}$ is the plastic increment at any instant of loading, $d\lambda$ is the plastic flow parameter, f is the yield function and σ_{ij} is the stress tensor.

The plastic flow parameter $d\lambda$ is equal to zero when the material behaves elastically i.e., $f(\sigma_{ij}) < k$ and takes a positive value when the material behaves plastically i.e., $f(\sigma_{ij}) = k$. The direction cosine of the normal to the yield surface is proportional to $\partial f(\sigma_{ij}) / \partial \sigma_{ij}$. Therefore, Eq. (2.3) implies that the plastic flow vector is directed along the normal to the yield surface when plastic flow takes place.

As mentioned earlier, onset of plastic flow is characterized by the appropriate yield criterion. For instance, von Mises yield criterion can be expressed as,

$$f(s_{ij}) = \frac{1}{2} s_{ij} s_{ij} - k^{2} \tag{2.4}$$

The associated flow rule corresponding to von Mises yield criterion can be expressed as,

$$d\varepsilon_{ij}^{p} = d\lambda \times s_{ij} \tag{2.5}$$

where, s_{ij} is the deviatoric stress tensor.

The plastic strains and stresses are related by the infinitesimal strain increments and deviatoric stresses; Eq. (2.5) is called *incremental stress-strain relations* because they relate the increments of plastic strain to the stress. To obtain the total plastic strain components, one must integrate these equations over the whole history of loading. Hencky [11] proposed total stress-strain relations whereby the total strain components are related to the current stress. This can be expressed in the form of the equation as follows:

$$\varepsilon_{ij}^{p} = \phi \times s_{ij} \tag{2.6}$$

where ϕ is an unspecified proportionality factor, analogous to $d\lambda$ in Eq. (2.5). The plastic strains then are functions of the current state of stress and are independent of the history of loading. Such theories are called *total* or *deformation theories*. In contrast to the incremental or flow theories previously described, this type of assumption greatly simplifies the problem.

In case of proportional or radial loading, the incremental theory reduces to the deformation theory. $\sigma_{ij} = K\sigma_{ij}^{0}$, where σ_{ij}^{0}an arbitrary reference state of stress and K is the monotonically increasing function of time, and then Eq. (2.5) on integration leads to Eq. (2.6). So the plastic strain is a function only of the current state of stress and is independent of the loading path.

From a practical viewpoint, there are a great many engineering problems where the loading path is not far from proportional loading, provided one is careful when unloading occurs to separate the problem into separate parts, the loading parts and the unloading parts.

2.5 Bounding Theorems in plasticity

Most of the practical engineering components and structures are complicated in nature and hence the complete plastic analyses of these structures are generally more involved and time consuming. The complexity arises from the irreversibility of plastic flow and dependency on the history of loading. Since the failure prevention is the primary objective of any structural design, therefore, it is justified to concentrate on the collapse state of the structure, which results in a considerable saving of effort. The plasticity theory offers the well known bounding theorems in order to estimate the collapse load of the structure. There are two approaches, the *equilibrium approach* for lower bound estimate and the *geometry approach* for upper bound estimate. The load at plastic collapse is termed as limit load of the structure. In the classical limit analysis, material nonlinearity is included by assuming perfectly plastic material model, while the geometric nonlinearity is not taken into account.

2.5.1 Classical Lower Bound Theorem

It states: "If any stress distribution throughout the structure can be found, which is everywhere in equilibrium internally and balances the external loads and at the sane time does not violate the yield condition, those loads will be carried safely by the structure" [12].

Therefore, the load estimated by the lower bound theorem will be less then or at most equal to the exact limit load. In lower bound theorem, the equilibrium equations (statically admissible stress field) and yield conditions are satisfied with out considering the mode of deformation of the structure.

2.5.2 Classical Upper Bound Theorem

It states: "If the estimation of the plastic collapse load of a body is made by equating the internal rate of dissipation of energy to the rate at which external forces do work in any postulated mechanism of deformation of body, the estimate will be either high or correct" [12].

In upper bound theorem, only the mode of deformation (kinematically admissible velocity fields) and energy balance are considered with out considering the equilibrium equations. Applying the principle of virtual work, the upper-bound theorem can be expressed as,

$$\int_{S_T} T_i \dot{u}_i \, dS \leq \int_{V_T} \dot{D} \, dV \tag{2.7}$$

where, T_i is the surface traction acting on the surface S_T. $\dot{u}_i$ is the rate of displacement. $\dot{D}$ is the corresponding plastic dissipation rates per unit volume and V_T is the total volume.

2.6 Limit Load Multipliers

Consider a structure with volume V and surface S (as shown in Fig 2.1), which is in equilibrium under surface traction T_i applied on the surface S_T and the geometric constraint $v_i = 0$ applied on the surface S_V. It is assumed that the surface traction is applied in proportional loading, i.e. the external traction is assumed to be mT_i, where m is the monotonically increasing parameter. For sufficiently small value of m, the structure will be in a purely elastic state. As m gradually increases, plastic flow starts to occur at a certain point in the structure. If the value of the m continues to increase, the plastic region spreads further and the structure will reach a state of impending plastic collapse.

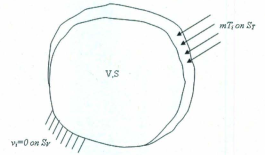

Figure 2.1 A Body Subjected to Traction Load

The set of loads corresponding to the impending plastic collapse state is called the *limit load* of the structure and the corresponding value of m is the *safety factor*. Therefore, the safety factor is the ratio of the limit load to the actual applied load.

2.6.1 Classical Plasticity - Statically Admissible Multiplier

A given stress field, σ_{ij}^{0} is said to be *statically admissible* when it is in equilibrium internally, balances the external load mT_i, and nowhere violates the yield criterion. The multiplier m, corresponding to such a stress field is called the *statically admissible multiplier*. Therefore, a statically admissible stress field should satisfy the following conditions,

$$\sigma_{ij,j}^{0} = 0 \qquad \text{in V,} \tag{2.8}$$

$$\sigma_{ij}^{0} n_j = mT_i \qquad \text{on } S_T, \tag{2.9}$$

$$f(s_{ij}^{0}) = \frac{1}{2} s_{ij}^{0} s_{ij}^{0} - k^2 \le 0 \qquad \text{in V,} \tag{2.10}$$

where, k is the yield stress in pure shear and s_{ij}^{0} is the statically admissible deviatoric stress tensor which can be defined as,

$$s_{ij}^{0} = \sigma_{ij}^{0} - \delta_{ij}\sigma^{0} \tag{2.11}$$

$$\sigma^{0} = \frac{1}{3}\sigma_{kk}^{0} \tag{2.12}$$

where, δ_{ij} is the Kronecker's delta. Eqs. (2.8 and 2.9) are the equilibrium equations and Eq. (2.10) is the yield function.

2.6.2 Classical Plasticity - Kinematically Admissible Multiplier

A given velocity v_i^{*} is said to be Kinematically admissible if it satisfies the displacement (velocity) boundary conditions and also the rate of total external work done by the applied loads on this velocity field is positive. Therefore, a kinematically admissible velocity field should satisfy the following conditions,

$$\delta_{ij} v_{ij}^{*} = 0 \qquad \text{in V,} \tag{2.13}$$

$$v_i^{*} = 0 \qquad \text{on S,} \tag{2.14}$$

$$\int_{S_T} T_i \, v_i^{*} \, dS > 0 \tag{2.15}$$

where, δ_{ij} is the Kronecker's delta. Here, Eq. (2.13) is the condition of incompressibility. The generalized strain-rate vector associated with a given kinematically admissible velocity field can be defined by $\dot{\varepsilon}^*$, where the asterisk is used to indicate that it is not necessarily the actual strain-rate vector but is kinematically admissible. If von Mises yield criterion is applied, plastic strain occurs when deviatoric stresses are on the yield surface i.e., $\frac{1}{2} s_{ij}^0 s_{ij}^0 = k^2$ where k is the yield stress in the pure shear. The Kinematically admissible multiplier, m^* can now be expressed as,

$$m^* = \frac{k \int_V \left(2 \dot{\varepsilon}_{ij} \dot{\varepsilon}_{ij}\right)^{1/2} dV}{\int_{S_T} T_i v_i^* \, dS} \qquad (2.16)$$

where,

$$\varepsilon_{ij}^* = \frac{1}{2}(v_{i,j}^* + v_{j,i}^*) \qquad \text{in V,} \qquad (2.17)$$

According to the classical limit theorem the following relation holds,

$$m_s < m < m^* \qquad (2.18)$$

where, m is the actual collapse load multiplier.

2.7 Closure

A review of the classical theories of elasticity, plasticity and limit analysis is presented in this chapter. The admissible limit load multipliers are also been discussed in this chapter. In the next chapter plastic multipliers using the variational concepts are discussed.

CHAPTER 3
REVIEW OF LIMIT LOAD MULTIPLIERS

3.1 Introduction

A review of how the multipliers in limit analysis have been developed so for is presented in this chapter. Using Mura's extended variational formulation [15] as an alternative to the classical limit theorem, Seshadri and Mangalaramanan [3] proposed the m_α method, which provides better lower bound limit load over Mura's lower bound estimation. m_α - Tangent Method proposed by Seshadri and Hossain [4] which gives better estimates of limit loads when compared to m_α method and over comes certain limitations of m_α method. These methods and there limitations which lead the way to the current research are discussed in more detail in this chapter.

3.2 Mura's Extended Variational Formulation

Mura *et al.* [16] showed by using the variational principles, that the safety factors the statically admissible lower bound multiplier and Kinematically admissible upper bound multiplier for a component or structure made of perfectly plastic material and subjected to prescribed surface tractions are actually extremum values of the same functional under different constraint conditions.

In classical theory of limit analysis, the statically admissible stress field (equilibrium set) can not lie outside the yield surface and the stress associated with a kinematically admissible strain rate field (compatibility set) in calculating the plastic dissipation should lie on the yield surface. Mura *et al.* [16] proposed an approach that eliminates such a requirement and replaced it by the concept of integral mean of yield criterion based on a variational formulation. The integral mean of yield criterion can be expressed as,

$$\int_{V_T} \mu^0 \, [f(\bar{s}_{ij}^0) + (\varphi^0)^2] dV = 0 \tag{3.1}$$

where, the superscript '0' refers to the statically admissible equilibrium stress fields and μ^0 is the plastic flow parameter. The deviatoric stress $\bar{s}_{ij}^0$ corresponds to the impending limit state, where $\bar{s}_{ij}^0 = m^0 s_{ij}^0$. Here, m^0 is the limit load multiplier and s_{ij}^0 is the deviatoric stress field that is in equilibrium with the applied loads. The parameter φ^0 is a point function that takes a value of zero if s_{ij}^0 is at yield and remains positive below yield.

3.3 Upper Bound Limit Load Multipliers

3.3.1 Multiplier m_1^0

Since $\bar{s}_{ij}^0$ corresponds to the deviatoric stress state for impending plastic flow, s_{ij}^0 represents the deviatoric stress state for applied traction T_i. The von Mises yield criterion is given by,

$$f(\bar{s}_{ij}) = \frac{3}{2}\bar{s}_{ij}^0\,\bar{s}_{ij}^0 - \sigma_y^2 \tag{3.2}$$

and the associated flow rule can be expressed as

$$\dot{\varepsilon}_{ij} = \mu\left(\frac{\partial f}{\partial s_{ij}}\right) \quad \text{where, } \mu \text{P0.} \tag{3.3}$$

Mura et al. [15] and [16] have shown that m^0, μ^0 and φ^0 can be determined by rendering the functional F stationary in

$$F = m^0 - \int_{V_T} \mu^0 [f(\bar{s}_{ij}^0) + (\varphi^0)^2] dV \tag{3.4}$$

Leading to set of equations

$$\frac{\partial F}{\partial m^0} = 0, \; \frac{\partial F}{\partial \mu^0} = 0, \; \frac{\partial F}{\partial \varphi^0} = 0 \tag{3.5}$$

For the von Mises yield criterion, the functional becomes

$$F = m^0 - \int_{V_T} \mu^0 [\frac{3}{2}(m^0)^2 s_{ij}^0 s_{ij}^0 + (\varphi^0)^2]\, dV \tag{3.6}$$

Assuming a constant flow parameter μ^0 and setting $\delta F = 0$, the foregoing functional can be written in a finite element scheme, for $\varphi^0 = 0$, as

$$m_1^0 = \frac{\sigma_y \sqrt{V_T}}{\sqrt{\int_{V_T} (\sigma_{eq})^2 dV}} \Leftrightarrow \frac{\sigma_y \sqrt{V_T}}{\sqrt{\sum_{k=1}^{N} (\sigma_{ek})^2 \Delta V_k}} \tag{3.7}$$

where N is the total number of elements, σ_y is the yield stress, σ_{ek} and ΔV_k are the equivalent stress and volume of elements k, and V_T is the total volume of the component.

The m_1^0 limit load multiplier has been shown to be greater than the classical lower bound (m_L) and classical upper bound (m_U) limit load multiplier [19].

3.3.2 Multiplier m_2^0

Eq. (3.7) implies that the calculation of m_1^0 is based on the total volume V_T. If plastic collapse occurs over a localized region of the structure m_1^0 will be significantly overestimated. To overcome this problem, Li Pan and Seshadri [17] have proposed a new formulation for evaluating m^0, namely m_2^0.

On the basis of deformation theory of plasticity, the flow rule can be expressed as,

$$e_{ij} = \mu s_{ij} \tag{3.8}$$

where e_{ij} and s_{ij} are the deviatoric strain and stress, respectively. Therefore, μ can be defined as,

$$\mu = \frac{3}{2}\frac{\bar{\varepsilon}}{\bar{\sigma}} \tag{3.9}$$

where $\bar{\sigma} = \sqrt{(3/2) s_{ij}\, s_{ij}}$ is the effective stress and $\bar{\varepsilon} = \sqrt{(2/3) e_{ij} e_{ij}}$ is the effective strain.

Substituting Eq. (3.9) into the integral mean of yield criterion, the m_2^0 limit load multiplier can be obtained as

$$m_2^0 = \sigma_y \frac{\sqrt{\int_{V_T} (\varepsilon_{eq} / \sigma_{eq}) dV}}{\sqrt{\int_{V_T} \sigma_{eq} \varepsilon_{eq} \, dV}} \Leftrightarrow \sigma_y \frac{\sqrt{\sum_{k=1}^{N} (\varepsilon_{eq} / \sigma_{eq})_k \, \Delta V_k}}{\sqrt{\sum_{k=1}^{N} (\sigma_{eq} \varepsilon_{eq})_k \, \Delta V_k}} \tag{3.10}$$

3.4 Lower Bound Limit Load Multipliers

3.4.1 Classical Lower Bound Multiplier, m_L

The lower bound limit load can be calculated by invoking the lower bound limit load theorem that states that if a statically admissible stress distribution throughout a given body can be found in which the stress nowhere exceeds yield under given loading and everywhere is in equilibrium internally and balances certain external loads the applied load is a lower bound on the limit [3]. A lower bound load can therefore be established by estimating the load required to give a maximum equivalent stress equal to the nominal yield strength, σ_y. Therefore, the classical lower bound multiplier m_L is given by,

$$m_L = \frac{\sigma_y}{(\sigma_{eq})_{\max}} \tag{3.11}$$

3.4.2 Multiplier m'

Mura's extended principle leads to a new lower bound multiplier m' smaller then the unknown actual collapse load multiplier m and can be expressed as,

$$m' = \frac{m^0}{1 + \frac{1}{2k^2} \max[f(\bar{s}_{ij}^0) + (\varphi^0)^2]} \leq m \tag{3.12}$$

Eq.(3.12) includes the classical definition of lower bound multiplier where the use of $\max[f(\bar{s}_{ij}^0) + (\varphi^0)^2]$ with Eq.(3.12) leads to $m_L \leq m$. Eq. (3.12) for m' can be rewritten in terms of the classical limit load multiplier m_L in a component as:

$$m' = \frac{2m^0}{1+(m^0/m_L)^2} \tag{3.13}$$

3.4.3 Multiplier m''

Based on the "Integral mean of yield criterion", Eq. (3.1) the Mura's lower bound multiplier is stated as an inequality, which can be expressed as,

$$m^0 \le m + \int_{V_T} \mu [f(\bar{s}_{ij}^0) + (\varphi^0)^2] dV \tag{3.14}$$

Eq.(3.14) can be rewritten as

$$m^0 \le m + \int_{V_T} \mu f^0 dV \tag{3.15}$$

A lower bound multiplier m'' can be obtained from Eq.(3.15) in terms of m_2^0 upper bound limit load multiplier

$$m'' = \frac{m_2^0}{1+G} \tag{3.16}$$

where G is calculated from the following expression,

$$G = \sqrt{\frac{\int_{V_T} \left(\left(m_2^0 \frac{\sigma_{eq}}{\sigma_y} \right)^2 - 1 \right)^2 dV}{4V_T}} \Leftrightarrow \sqrt{\frac{\sum_{k=1}^{N} \left(\left(m_2^0 \frac{\sigma_{eq}}{\sigma_y} \right)^2 - 1 \right)_k^2 \Delta V_k}{4V_T}} \tag{3.17}$$

The parameter G acts as a convergence parameter, and is indicative of any deviation of statically admissible stress distributions from the limit state. That is, $G \to 0$ corresponds to the converged exact solution.

3.5 m_α Multiplier Method

The m_α Method, invokes the notion of reference volume to account for localized collapse and the technique of "leap-frogging" to a limit state. These concepts are used in conjunction with the elastic modulus adjustment technique, described by Seshadri and Fernando [18], for obtaining improved lower and upper bound limit load estimates.

Differentiating Mura's lower bound limit load multiplier, $m' = f(m^0, m_L)$, with respect to iteration variable, ξ, leads to the expression

$$\frac{dm'}{d\xi} = \left(\frac{\partial m'}{\partial m^0}\right)_{\xi=\xi_i} \frac{dm^0}{d\xi} + \left(\frac{\partial m'}{\partial \frac{1}{m_L}}\right)_{\xi=\xi_i} \frac{\partial \frac{1}{m_L}}{d\xi} \tag{3.18}$$

In terms of finite differential Eq.(3.18) can be expressed as,

$$\Delta m' = \left(\frac{\partial m'}{\partial m^0}\right)\Bigg|_{\xi=\xi_i} \times \Delta m^0 + \left(\frac{\partial m'}{\partial \frac{1}{m_L}}\right)\Bigg|_{\xi=\xi_i} \times \Delta\left(\frac{1}{m_L}\right) \tag{3.19}$$

where $\Delta m' = m' - m_\alpha$, $\Delta m^0 = m^0 - m_\alpha$, $\Delta m_L = m_L - m_\alpha$.

The limit load multiplier m_α is assumed to be the estimated actual limit load [3]. Therefore,

$$m' - m_\alpha = 2\frac{1-\left(\frac{m^0}{m_L}\right)}{\left(1+\left(\frac{m^0}{m_L}\right)^2\right)^2}(m^0 - m_\alpha) - 4\frac{(m^0)^3}{m_L\left(1+\left(\frac{m^0}{m_L}\right)^2\right)^2}\left(\frac{1}{m_L} - \frac{1}{m_\alpha}\right) \tag{3.20}$$

Eq.(3.20) is a polynomial of second degree in m_α, which can be shown in general form as

$$A m_\alpha^2 + B m_\alpha + C = 0 \tag{3.21}$$

where

$$A = \left(\frac{m^0}{m_L}\right)^4 + 4\left(\frac{m^0}{m_L}\right)^2 - 1,\ B = -8m^0\left(\frac{m^0}{m_L}\right)^2,\ C = 4(m^0)^2\left(\frac{m^0}{m_L}\right)$$

The parameters A, B and C can be calculated from the results of linear elastic FEA. Therefore,

$$m_\alpha = \frac{-B \pm \sqrt{B^2 - 4AC}}{2A} \tag{3.22}$$

Keeping in mind that the limit load multipliers are positive, Eq. (3.22) results in following expression [3],

$$m_\alpha = 2m^0 \frac{2\left(\dfrac{m^0}{m_L}\right)^2 + \sqrt{\dfrac{m^0}{m_L}\left(\dfrac{m^0}{m_L}-1\right)^2\left(1+\sqrt{2}-\dfrac{m^0}{m_L}\right)\left(\dfrac{m^0}{m_L}-1+\sqrt{2}\right)}}{\left(\left(\dfrac{m^0}{m_L}\right)^2+2-\sqrt{5}\right)\left(\left(\dfrac{m^0}{m_L}\right)^2+2+\sqrt{5}\right)} \tag{3.23}$$

When the expression under the root in Eq. (3.22) becomes negative (i.e. $B^2 - 4AC < 0$) the solution of m_α vanishes.

Dividing both sides of Eq. (3.23) by the exact multiplier, we get

$$R_\alpha = 2R_0 \frac{2\zeta^2 + \sqrt{\zeta(\zeta-1)^2\left(1+\sqrt{2}-\zeta\right)\left(\zeta-1+\sqrt{2}\right)}}{\left(\zeta^2+2-\sqrt{5}\right)\left(\zeta^2+2+\sqrt{5}\right)} \tag{3.24}$$

where $R_\alpha = m_\alpha / m$, $\zeta = m^0 / m_L$ and $R_0 = m^0 / m$.

$R_\alpha = 1$ is the boundary between the upper bound ($R_\alpha > 1$) and the lower bound ($R_\alpha < 1$), as shown in the figure.3.1. The expression under the root in Eq. (3.24) encompasses four factors, which define the sign of the whole expression under the root. Therefore, the m_α limit load multiplier becomes imaginary foe the following conditions:

$$\begin{aligned} 0 < \zeta < \sqrt{2} - 1 \\ \zeta > \sqrt{2} + 1 \end{aligned} \tag{3.25}$$

Since $\zeta = m^0 / m_L \geq 0$, the first expression in Eq. (3.25) will never occur; therefore, the only case which causes m_α to be imaginary is $\zeta > \sqrt{2} + 1 \approx 2.4142$, as is the case for components with notches and cracks due to presence of peak stresses.

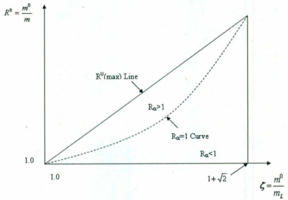

Figure 3.1 Regions of lower and upper bounds of m_α.

In Eq. (3.24), the exact multiplier m for a given component is unknown. Now $m^0 / m_L = \left((\sigma_e)_{\max} / \sigma_{ref}\right)$ is a measure of the theoretical stress-concentration factor at the notch. Therefore $m^0 / m_L \geq 1+\sqrt{2}$ represents the threshold for pronounced notch effects. The region bounded by $m^0(\max), 1 \leq m^0 / m_L \leq 1+\sqrt{2}$ and $1 \leq m^0 / m \leq 1+\sqrt{2}$ is designated as the "m_α triangle".

Reinhardt and Seshadri [20] showed that m_α estimates are lower bounds in the greater majority of the cases. But there are still cases where m_α multiplier is upper bound. Pan and Seshadri [17, 21] applied the m_α multiplier to various types of practical mechanical components.

3.6 Generalized Two-Bar Method

The two-bar method proposed by Seshadri and Adibi-Asl [22] invoking the concepts of equivalence of "static indeterminacy" that relates a multidimensional component configuration to a "reference two-bar structure". In actual method the areas of both the reference bars in the reference two bar structure is assumed to be equal. In the following section the two-bar method is more generalized by assuming unequal areas ($A_1 = X\ A_2$) and variable lengths ($L_1 = \lambda\ L_2$). A general pressure component can be related to a two bar structure as shown in Fig. 3.2.

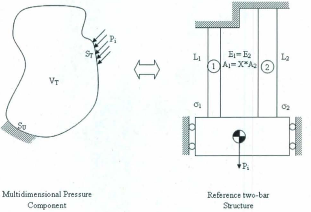

Figure 3.2 Reference two-bar structure.

For the general mechanical components from the integral mean of yield criterion can be expressed as

$$\int \mu^0 \left(f\left(\bar{s}_{ij}^0\right) + \left(\varphi^0\right)^2 \right) dV = 1 \tag{3.26}$$

where $\bar{s}_{ij}^o$ is the statically admissible deviatory stress for impending plastic flow, and φ^o is the point function that takes on a value of zero if $\bar{s}_{ij}^o$ is at the yield and remains positive below yield. Using Eq. (3.7)

$$m^0 = \frac{\sigma_y \sqrt{A_1 L_1 + A_2 L_2}}{\sqrt{\sigma_1^2 A_1 L_1 + \sigma_2^2 A_2 L_2}} \tag{3.27}$$

It is already shown by Reinhardt and Seshadri that m^0 is an upper bound except at the limit state. The classical lower bound multiplier (m_L) is given by

$$m_L = \frac{\sigma_y}{\sigma_1} \tag{3.28}$$

It is assumed that $L_1 < L_2$, $A_1 = XA_2$, as shown in Fig.3.2.

$$\frac{m^0}{m_L} = \frac{\sigma_1\sqrt{A_1L_1 + A_2L_2}}{\sqrt{\sigma_1^2 A_1L_1 + \sigma_2^2 A_2L_2}}$$

$$\frac{m^0}{m_L} = \frac{\sigma_1\sqrt{XL_1 + L_2}}{\sqrt{\sigma_1^2 XL_1 + \sigma_2^2 L_2}}$$

Taking σ_2^2 common from the denominator

$$\frac{m^0}{m_L} = \frac{\sigma_1\sqrt{XL_1 + L_2}}{\sigma_2\sqrt{\frac{\sigma_1^2}{\sigma_2^2} XL_1 + L_2}} \tag{3.29}$$

We know that $\frac{L_2}{L_1} = \frac{\sigma_1}{\sigma_2}$ since $E_1 = E_2$.

Substituting these values back in equation (3.29)

Taking $L_1/L_2 = \lambda$, clearly $\lambda \leq 1$for the range of pressure components.

$$\frac{m^0}{m_L} = \frac{1}{\sqrt{\lambda}}\sqrt{\frac{X\lambda + 1}{X + \lambda}} \tag{3.30}$$

From the equilibrium consideration $P = \sigma_1A_1 + \sigma_2A_2$

$$P = (\sigma_1A_1 + \sigma_2A_2)$$

$$P_L = (A_1 + A_2)\sigma_y$$

$$m = \frac{P_L}{P} = \frac{(A_1 + A_2)\sigma_y}{(\sigma_1A_1 + \sigma_2A_2)}$$

$$m = \frac{(X+1)\sigma_y}{(\sigma_1X + \sigma_2)} \tag{3.31}$$

Dividing Eq. (3.27) by Eq. (3.31)

$$\frac{m^0}{m} = \frac{\left(\dfrac{\sigma_y\sqrt{A_1L_1 + A_2L_2}}{\sqrt{\sigma_1^2 A_1L_1 + \sigma_2^2 A_2L_2}}\right)}{\left(\dfrac{(X+1)\sigma_y}{\sigma_1 X + \sigma_2}\right)}$$

$$\frac{m^0}{m} = \frac{(\lambda + X)}{(1+X)}\sqrt{\frac{L_2}{L_1}}\sqrt{\frac{X + \frac{L_2}{L_1}}{\frac{L_2}{L_1}X + 1}}$$

The above equation is similar to Eq. (3.29) with an extra term of (λ+X)/(1+X) the equation then becomes:

$$\frac{m^0}{m} = \frac{(\lambda + X)}{(1+X)\sqrt{\lambda}}\sqrt{\frac{X\lambda + 1}{X + \lambda}} \qquad (3.32)$$

The parameters m^0/m and m^0/m_L are useful for characterizing the state of static indeterminacy a component undergoing plastic flow.

Eq. (3.32) can be rewritten as follows:

$$\frac{m}{m^0} = \frac{(1+X)\sqrt{\lambda}\sqrt{X+\lambda}}{(X+\lambda)\sqrt{X\lambda + 1}} \qquad (3.33)$$

The value of 'X' for which the function m/m^0 is extreme can be obtained as follows:

$$\frac{d\left(\dfrac{m}{m^0}\right)}{dX} = 0$$

$$1 - \frac{(1+X)\lambda}{2(X\lambda + 1)} - \frac{(1+X)}{2(X+\lambda)} = 0$$

$$(\lambda^2 - 2\lambda + 1)X = \lambda^2 - 2\lambda + 1$$

which leads to $X = 1$, Therefore substituting $X = 1$ into Eq. (3.30) and Eq. (3.33) gives the scaling equations as :

$$\frac{m^0_{Comp}}{m_{L,Comp}} = \frac{m^0_{Bar}}{m_{L,Bar}} = \frac{1}{\sqrt{\lambda}} \tag{3.34}$$

$$\frac{m^0_{Comp}}{m_{Comp}} = \frac{m^0_{Bar}}{m_{Bar}} = \frac{\lambda+1}{2\sqrt{\lambda}} \tag{3.35}$$

These equations are similar to those proposed in the 2-bar method; hence the assumption of equal areas is proven to be valid.

3.7 m_α Tangent Method

The m_α Tangent Method proposed by Seshadri and Hossain [4] is an extension of the m_α method of analysis. The method enables evaluation based on a single linear elastic analysis or on an assumed statically admissible stress field. The formulation of the method is based on the variational principles in limit analysis.

3.7.1 The m_α tangent

The m_α multiplier method was developed on the basis of variational concepts in plasticity. The method has explicit dependency on the upper bound multiplier, m^0, and the classical lower bound multiplier, m_L. The upper bound multiplier, m^0, depends on the entire stress distribution in a component or structure where as m_L depends on the magnitude of maximum stress. Therefore, for components with sharp notches and cracks the value of m^0 / m_L will be high due to presence of peak stresses.

With respect to Fig.3.3, the following can be stated:

1. When $m \to m_L$, the domain of statically admissible m^0 is bounded by the 45-deg (R^0 (max)) line and the positive x-axis.
2. When $m \to m^0$, the domain of the statically admissible m^0 is represented by the line $m = m^0$.

3. The exact solution (m) locus would lie somewhere between the positive x-axis and the 45-deg line (R^0 (max))
4. The tangent to the $R_\alpha = 1$ curve at the limit state ($m_L = m^0 = m$) will locate the m_α tangent, which can then be used to estimate the multiplier m.

The determination of m_α tangent is as follows. Eq. (3.24) describes R_α as a function of the two variables, R^0 and ζ, where $\zeta = m^0 / m_L$. For $R_\alpha = 1$, Eq. (3.24) can be represented by a curve in two-dimensional space as shown in Fig. 3.3. The slope of the tangent at the limit state, where $m_\alpha = m_L = m^0 = m$, can be obtained as:

$$\left.\frac{dR_\alpha}{d\zeta}\right|_{\zeta=1} = 1 - \frac{1}{\sqrt{2}} \tag{3.36}$$

Therefore, the slope of the tangent ($R_\alpha^T = 1$) line at the limit state is $\tan(\theta)$ = 0.2929. Where θ is the angle made by m_α tangent with ζ axis.

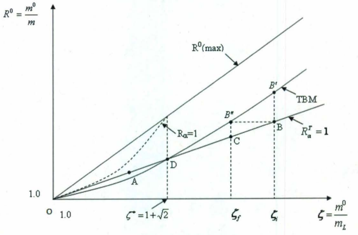

Figure 3.3 m_α tangent construction [4]

The equation corresponding to $R_\alpha^T = 1$ can be obtained as:

$$\frac{m^0}{m} = 1 + (\zeta - 1)\tan(\theta) \tag{3.37}$$

The exact limit load multiplier (m) for most of the practical components and structures being analyzed is not known a priori. For the m_α-tangent method, R^0 can be defined by making use of the tangent (R_α^T-line in Fig. 3.3) for any value of ζ. Both R^0 and ζ are greater than one, except at the limit state for which $R^0 = \zeta = 1$. In this method it is assumed that the reduction of m^0 along the $R_\alpha^T = 1$ trajectory implicitly accounts for the reference volume. Therefore, m^0 will converge to the exact multiplier as the trajectory approaches to the origin.

3.7.2 Blunting of Peak Stresses

Secondary and peak stresses are set up by redundant kinematical constraints (or static indeterminacy) in a component. ASME Boiler and pressure Vessel codes [23, 24] explicitly recognize these stresses are related to constraint effects. Fig. 3.4 shows the stress distribution in the ligament adjacent to the notch tip, where x-axis represents the distance ahead of the notch tip, and y-axis is the equivalent stress. As can be seen from the figure, the magnitude of the equivalent peak stress (σ_F) at the notch tip is considerably high; however, it is assumed that the peak stresses are very localized and that the following expression is valid [24];

$$\int_A \sigma_F \, dA = 0 \tag{3.38}$$

where A is the representative area on which σ_F acts.

With respect to constraint map, $R_\alpha^T = 1$ line can be identified as shown in Fig. 3.3. This line is tangential to the R_α=1 curve at the origin (m^0/m=1, m^0/m_L=1). The curve $\frac{m^0}{m} = \frac{1+\lambda}{2\sqrt{\lambda}}$ for reference two-bar model (TBM) can also be located as shown in Fig. 3.3.

3.7.3. Significance of $\zeta^* = 1+\sqrt{2}$

The point D (Fig. 3.3) can be determined by finding the intersection of the $R_\alpha^T = 1$ line and the reference two-bar model equation, i.e.,

$$\frac{m^0}{m} = 1 + (\zeta - 1)\ \tan(\theta) = \frac{1+\lambda}{2\sqrt{\lambda}} \tag{3.39}$$

Where $\lambda = {}^{1}\!/_{\zeta^2}$ and $\tan(\theta) = 1 - \frac{1}{\sqrt{2}}$.

The intersection point worked out to be $\zeta^* = 1$ and $1+\sqrt{2}$. The $R_\alpha^T = 1$ line represents a combination of primary and secondary stresses that exist in the pressure components. On the other hand, the TBM trajectory represents the combination of primary, secondary and peak stresses. Therefore, at point D the peak stresses are negligible (theoretically equal to zero).

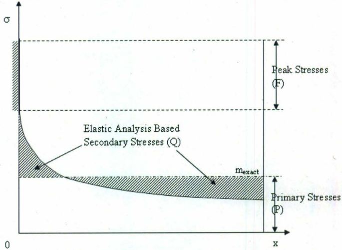

Figure 3.4 Stress distribution a head of notch tip

3.7.4 The General Procedure

Once the $R_\alpha^T = 1$ line is identified, the m_α^T value can be readily estimated by the relationship.

$$m_\alpha^T = \frac{m^0}{1 + 02929(\zeta - 1)} \tag{3.40}$$

where $\zeta = m^0 / m_L$.

The slope of the $R_\alpha^T = 1$ line is equal to $\tan(\theta) = 1 - \frac{1}{\sqrt{2}}$. The value of m^0 and ζ can be determined from statically admissible distributions obtained from liner elastic FEA.

Two cases are considered next:

Case-I: $\zeta \leq 1 + \sqrt{2}$ (negligible peak stresses)

For this case, point A (Fig. 3.3) is assumed to lie on the $R_\alpha^T = 1$ line. The value of m_α^T can be obtained from Eq. (3.45). This case usually applies to well-designed pressure components with gentle geometric transitions.

Case-II: $\zeta \geq 1 + \sqrt{2}$ (presence of peak stresses)

This case applies to well-designed components that develop flaws or cracks in service, or components with sharp notches. The aim here is to blunt the peak stresses prior to evaluating m_α^T. With respect to Fig. 3.3, the initial linear elastic FEA locates point B on the $R_\alpha^T = 1$ line and point B' on the TBM locus corresponding to $\zeta_i = m_i^0 / m_{L,i}$. The subscript "$i$" refers to the initial points B and B'. The calculation procedure is as follows:

1. Perform a linear elastic analysis.
2. Locate point B and B'. Point B represents the combination of primary and secondary stresses where as point B' represents the combination of primary, secondary and peak stresses.

3. Construct a horizontal line from point B to B'' signifying an invariant m_i^0 (blunting of peak stresses). Designate the value of m^0/m_L at B'' as ζ_f, which can be obtained by solving the equation

$$\frac{m^0}{m} = 1 + 0.2929\,(\zeta_i - 1) = \frac{1+\zeta_f^2}{2\,\zeta_f} \tag{3.41}$$

The roots of Eq.(3.41) are

$$\zeta_f = (1+C) + \sqrt{(1+C)^2 - 1} \tag{3.42}$$

where $C = 0.2929\,(\zeta_i - 1)$

4. The value of m_α^T can be evaluated by the equation

$$m_\alpha^T = \frac{m_i^0}{1 + 02929\,(\zeta_f - 1)} \tag{3.43}$$

For some geometric transitions for which $\zeta > 1+\sqrt{2}$, redistribution of secondary stresses could occur along with peak stresses. In such cases, the value of m_i^0 is not constant during the blunting of peak stresses, and there is a gradual reduction in its magnitude. There causes are usually attributed to components undergoing highly localized plastic flow such as beam and frame structures

3.8 Elastic Modulus Adjustment Procedure (EMAP)

The aim of EMAP is to establish an inelastic-like stress field by modifying the local elastic modulus in order to obtain the necessary stress redistribution [25]. Jones and Dhalla [26] were one of the earliest users of EMAP. Marriott [27] developed an iterative procedure for estimating lower-bound limit loads on the basis of linear elastic FEA by generating statically admissible stress fields and using them in conjunction with established theorems of limit analysis. Seshadri and Fernando [28] made use of the elastic modulus adjustment procedure to determine lower bounded limit loads by adopting reference stress concept in creep design [29]. Their technique, called the Redistribution

Node (R-Node) Method, is based on two linear elastic FEA in which the load control location (R-Nodes) are determined and using stresses in these locations, the limit load of the component will be achieved.

Mackenzie and Boyle [30] utilized the elastic modulus adjustment procedure suggested by Marriott [27] and Seshadri [31], named as the elastic compensation method (ECM), and obtained for every iterations lower and upper-bound limit loads by invoking the classic theorems of limit analysis. The ECM procedure has been used to estimate the lower and upper bound limit loads for different pressurized components, which are available in Mackenzie *et al.* [32] and Boyle *et al.* [33] The method has been also applied for shakedown analysis by Hamilton *et al.* [34] and Nadarajah *et al.* [35]. Ponter et al. [36] developed a formal basis for the elastic modulus adjustment and related procedures.

Numerous sets of statically admissible and kinematically admissible distributions can be generated using the EMAP, which enable calculation of both lower and upper bounds limit loads. The elastic modulus of each element in the linear elastic finite element scheme is modified as

$$E^{i+1} = \left(\frac{\sigma^i_{ref}}{\sigma^i_{eq}}\right)^q E^i \tag{3.44}$$

where q is the elastic modulus adjustment parameter, σ_{ref} is the reference stress [3], σ_{eq} is the equivalent stress and "i" is the iteration index (i=1 for the initial elastic analysis). Where,

$$\sigma^i_{ref} = \sqrt{\frac{\sum_k^n \sigma_k^2 V_k}{V_T}} \tag{3.45}$$

This formula describes how the elastic modulus at a location with the equivalent stress σ_{eq} (e.g., the von Mises equivalent stress) is updated from the i^{th} to the $(i+1)^{th}$ elastic iteration. This procedure continued until suitable convergence of a subsequent iteration is achieved. In this research a 'q' value of 0.1 is used for the EMAP, ensuring a slow but less fluctuating convergence [36]. The same 'q' is used for all the problems.

3.9 Non-linear Analyses

A system of nonlinear equilibrium equations can be written as

$$\{F\} = [K]\{u\} \tag{3.46}$$

where $[K]$ is stiffness matrix. The nonlinearity occurs in the stiffness matrix [37] and is a function of nonlinear displacement $\{u\}$and load $\{F\}$. therefore, Eq. (3.46) can be rewritten as a general form, i. e.,

$$\{F\} = [K(\{u\},\{F\})]\{u\} \tag{3.47}$$

The solution of this nonlinear Eq. (3.47) can be obtained by one of the following procedures:

- Incremental procedure
- Iterative procedure
- Mixed procedure

3.9.1 Incremental Procedure

This procedure is similar to Euler's method of solving the differential equations. In this procedure the total load is divided into a number of load increments $\{\Delta F_i\}$, and it is applied to the system incrementally. The stiffness matrix $[K]$ is assumed to be constant throughout each increment. Therefore, the equilibrium equation will be linear. The solution for each load step is obtained as an increment of the displacement $\{\Delta u_i\}$, and the total displacements will be the summation of this incremental displacement solution. At each increment the stiffness matrix is calculated using the values of $\{\Delta F_i\}$ and $\{\Delta u_i\}$. After application of the given increment (i) the load and displacement are given as

$$\{F_i\} = \{F_0\} + \sum_{j=1}^{i} \{\Delta F_j\} \tag{3.48}$$

$$\{u_i\} = \{u_0\} + \sum_{j=1}^{i} \{\Delta u_j\} \tag{3.49}$$

where $\{F_0\}$ and $\{u_0\}$ are the values of load and displacement obtained from an initial equilibrium state, which usually corresponds to the condition before load application [38]. For the next iteration $(i+1)$, the relation between load and displacement can be determined from the following equation

$$\{F_{i+1}\} = [K]\{u_{i+1}\} \tag{3.50}$$

The incremental procedure is repeated until the total load reaches to its final value.

3.9.2 Iterative Procedure

This procedure is similar to the Newton-Raphson procedure. In this iterative procedure the total load, $\{F\}$, is fully applied to the body in each iteration. Therefore the equilibrium equation is not necessarily satisfied during the iterations. After each iteration, the part of the total load that is not balanced is calculated and used in the next step to compute an additional increment of displacement [37]. For i^{th} iteration, an increment for the displacement is computed as

$$\{F_{ii}\} = [K_{i-1}]\{\Delta u_i\} \tag{3.51}$$

The procedure is repeated until the unbalanced loads become zero or within a suitable convergence range.

3.9.3 Mixed Procedure

This procedure is based on a combination of incremental and iterative procedures. The load is applied in an incremental manner, but after each increment successive iterations are applied to achieve more accurate results.

In this research, the results obtained from the nonlinear analysis are taken as the actual limit load multipliers for comparison purposes. In the non-linear analysis the elastic perfectly plastic material models are used for the calculation of limit loads. The nonlinear analysis is done on the same model with the same kind of loading with increased magnitude. The unconverged time step is taken as the limit multiplier of the component with that particular loading condition.

3.10 Closure

An overview of the development of different multipliers is given in this chapter. A detailed discussion on both m_α and m_α-tangent methods have been done. In this chapter the assumption of equal areas in two-bar method is proven valid. The choice of reference volume plays an important role in finding out the correct estimates of limit loads. Generally for the component for which $\zeta > 1 + \sqrt{2}$, finding the limit load estimates require the proper estimation of reference volume as these components have highly localized plastic regions being developed leading to larger dead volumes. In the coming chapter methods are developed which will predict the lower bound limit loads of general components or structures with the help of a systematic approach of finding reference volume.

CHAPTER 4
ELASTIC REFERENCE VOLUME METHOD

4.1 Introduction

In this Chapter the reference volume concepts are introduced. *Elastic reference volume method* for reference volume correction while finding out limit loads in the components or structures are presented. These reference volume correction concepts are used in combination with m_α Tangent method to obtain the lower bound limit load of general component or structure. The *Elastic Reference Volume Method* proposed in this paper, derived its roots from the pressure bulb concepts of soil mechanics [39]. In this method reference volume effect will be corrected based upon the maximum stress developed in the component. The proposed method is also tested on a range of components and results obtained are discussed.

4.2 Reference volume concept

It is well known that at limit load state of a component/structure, there are some regions that do not participate in inelastic action (dead volumes) and may remain rigid or elastic. On the other hand, the remaining volumes are directly active in plastic action (reference volume) are the only regions that carry the external loads at the limit state.

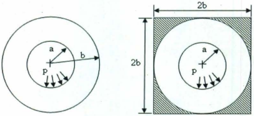

Figure 4.1 Cylinder and Square prism with a circular hole [40]

As schematically presented in Fig. 4.1, plastic spread at the collapse mechanism of an square prism with a central hole subjected to the internal pressure is a good example. The shaded regions in Fig 4.1, represents the dead volume. The remaining region is the reference volume.

In the reference volume approach, it is assumed that the plastic collapse occurs only over a kinematicaly active region of the mechanical component or structure. Clearly, m^0 (for the initial linear elastic analysis $m_2^0 = m_1^0 = m^0$) will be significantly overestimated if it is based on the total volume V_T. The concept of reference volume has been introduced to identify the "kinematically active" region of the component or structure that participates in plastic action.

Consider a component subjected to arbitrary loading condition, Fig. 4.2. The component is divided into two regions: (1) reference volume (V_R), which is kinematically active volume; and (2) the dead volume (V_D). It means only some portion of the total component takes part in plastic action, while the remaining does not. If V_T is the total volume thus,

$$V_T = V_R + V_D \tag{4.1}$$

where V_R is the reference volume, and V_D is the volume of the dead zone in the component.

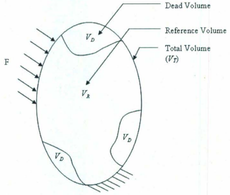

Figure 4.2 Total, Reference and Dead Volumes

Therefore, the multiplier m^0, Eq. (3.10), can be written in terms of the reference and the dead volume as

$$m^0 = \sigma_y \frac{\sqrt{\int_{V_R} (\varepsilon_{eq} / \sigma_{eq}) dV + \int_{V_D} (\varepsilon_{eq} / \sigma_{eq}) dV}}{\sqrt{\int_{V_R} \sigma_{eq} \varepsilon_{eq} \, dV + \int_{V_D} \sigma_{eq} \varepsilon_{eq} \, dV}}$$

$$m^0 = \sigma_y \frac{\sqrt{\int_{V_R} (\sigma_{eq} / E_s \sigma_{eq}) dV + \int_{V_D} (\sigma_{eq} / E_s \sigma_{eq}) dV}}{\sqrt{\int_{V_R} (\sigma^2{}_{eq} / E_s) dV + \int_{V_D} (\sigma^2{}_{eq} / E_s) dV}} \tag{4.2}$$

If we assume that the dead zone has no plastic flow occurring, then Eq. (4.2) can be simplified as

$$m^0 (V_R) = \sigma_y \frac{\sqrt{\int_{V_R} dV}}{\sqrt{\int_{V_R} \sigma_{eq}^2 \, dV}} = \sigma_y \frac{\sqrt{\sum_{\eta=1}^{R} V_\eta}}{\sqrt{\sum_{\eta=1}^{R} \sigma_{eq}^2 V_\eta}} \tag{4.3}$$

The magnitude of the upper bound multiplier, m^0, would therefore depends on the reference volume, V_R, where

$$V_R = \sum_{\eta=1}^{k} \Delta V_\eta \tag{4.4}$$

In order to identify the reference volume V_R and multiplier with reference volume correction $m^0 (V_R)$, two methods are currently being proposed.

4.3 Elastic Reference Volume Method (ERVM)

The method is named elastic reference volume method as we will be using the elastic stress profile of a component as obtained from the EMAP iterations to define the reference volume and dead volume. This method derived its roots from the pressure bulb concepts which are generally used in soil mechanics. These concepts are covered by

Smith [39], Wilun and Starzewski [41], and Helwany [42]. In the Pressure Bulb theory, using Boussinesq [43] equations, six stress components can be determined that act at a point in a semi-infinite elastic medium due to action of a vertical point load applied on the horizontal surface of the medium.

The expression for the vertical stress is given as follows:

$$\sigma_z = \frac{3P}{2\pi} * \frac{z^3}{(r^2 + z^2)^{5/2}} \tag{4.5}$$

where P = Concentrated load

r = $\sqrt{x^2 + y^2}$ = Radial distance from point of application

The expression has been simplified to:

$$\sigma_z = K * \frac{P}{z^2} \tag{4.6}$$

where K is an influence factor. Values of K against values of r/z are shown in Fig. 4.3

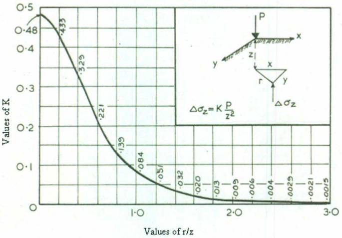

Figure 4.3 Influence coefficients for vertical stress from a concentrated load [39].

This method is only applicable for point load, which is a rare occurrence in soil mechanics. Steinbrenner [44] developed a method for finding out the vertical stress increment under a foundation of length L and width B exerting a uniform pressure p on the soil. The vertical stress increment due to the foundation at a depth z below one of the corners is given by expression:

$$\sigma_z = p \times I_\sigma \tag{4.7}$$

where I_σ is an influence factor depending upon the relative dimensions of L,B and z. I_σ can be evaluated by the Boussinesq theory and values of this factor were prepared by Fadum [45]. The variation of influence factor with m=B/z and n=L/z are shown in Fig. 4.4.

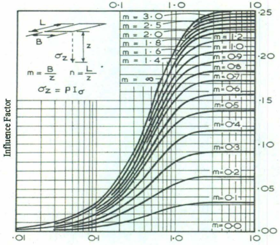

Figure 4.4 Influence factor for vertical stress beneath the corner of a rectangular Foundation [45].

If points of equal pressure are plotted on a cross section through the foundation, a diagram of the form shown in Figs 4.5 A and 4.5 B is obtained. These diagrams are known as *pressure bulbs* and helpful in determining out vertical stress at points below a foundation that is of a regular shape. The bulb of pressure for a square footing is obtained by assuming that it has the same effect on soil as that of a circular footing of a same area. In the case of a rectangular footing the bulb pressure will vary at cross sections taken along the length of the foundation, but the vertical stress at points below the center of such a foundation can still be obtained from the charts by either one of the two following ways:

(i) Assuming that the foundation is a strip footing or

(ii) Determining values for both the strip footing case and the square footing case and combining them by proportioning the length of the two foundations.

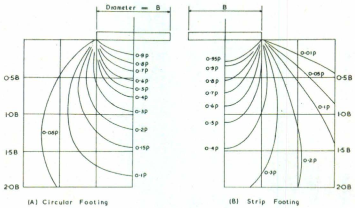

Figure 4.5 Bulbs of Pressure for vertical stresses [44].

It is sometimes necessary to evaluate the shear stresses beneath a foundation in order to determine a picture of the likely overstressing in the soil. Jurgenson [46] obtained solutions for the case of the circular footing and for the case of a strip footing (Fig.4.6). It may be noted that, in case of a strip footing, the maximum stress induced in the soil is p/π, this value occurring at points lying on a semi-circle of diameter equal to the foundation with B (diameter in circular foundation and width in rectangular foundation). Hence the maximum shear stress under the center of a continuous foundation occurs at a depth of B/2 beneath the center.

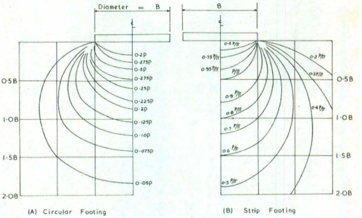

Figure 4.6 Bulbs of Pressure for shear stresses [46].

From a bulb of pressure one has some idea of the depth of soil affected by a foundation. From the plots it can be seen that significant stress values go roughly to 2.0 times the width of the foundation.

4.3.1 Cut-off Stress

Finding the elastic reference volume in mechanical components involves finding the volume in which an effective stress profile is acting. According to Boussinesq and Jurgenson theories a limit of 5% of the applied load can be used as the limit for finding out the active volume under the foundation. To extend these theories to the mechanical components an *Cut-off Stress* (σ_{ct}) is proposed which is the ratio of the equivalent stress to the maximum stress.

$$\sigma_{ct} = \frac{\sigma_{eq}}{\sigma_{\max}} \tag{4.8}$$

Different percentages of cut-off are studied and finally 5% is selected due to consistancy of lower boundedness. The other percentages are presented in plots for all the examples. The choice of the equivalent stress will include the effect of both the nominal and shear stresses into the analysis. By knowing the cut-off stress and by using multiplier (m^0) vs. sub-volume ratio ($\overline{V}_\eta$) plot, the actual volume that participates in the stress distribution can be predicted. The volume so obtained is the *Elastic reference volume*. Plots for various components are shown in coming sections. In these plots, the variation in contribution of Elastic Reference Volume with various percentages of cut-off stresses is shown. The contribution from the dead volume is shown as zero.

4.4 m^0 Vs. $\overline{V}_\eta$ plot

After the first linear elastic FEA run, the elements are sorted in the descending order of there equivalent stresses i.e., $\sigma_{eq}^1 > \sigma_{eq}^2 > \sigma_{eq}^3 > \dots\dots\dots > \sigma_{eq}^n$ [47]. The corresponding sub-volumes are calculated. The multiplier m^0 is calculated using the following equation:

$$m^0 = \frac{\sigma_y \sqrt{\sum_{\eta=1}^{k} V_\eta}}{\sqrt{\sum_{\eta=1}^{k} \sigma_\eta^2 V_\eta}} \tag{4.9}$$

Using the Eq. (4.9) the different m^0 values for different sub-volumes will be calculated as shown below.

$$m^0(V_{\eta=1}) = \frac{\sigma_y \sqrt{V_1}}{\sqrt{\sigma_1^2 V_1}} = m_L \tag{4.10}$$

$$m^0(V_{\eta=2}) = \frac{\sigma_y\sqrt{V_1+V_2}}{\sqrt{\sigma_1^2 V_1 + \sigma_2^2 V_2}} \tag{4.11}$$

In a more generalized form

$$m^0(V_{\eta=k}) = \frac{\sigma_y\sqrt{V_1+V_2+\dots\dots\dots+V_k}}{\sqrt{\sigma_1^2 V_1 + \sigma_2^2 V_2 + \dots\dots\dots + \sigma_k^2 V_k}} \tag{4.12}$$

If the "k" in Eq. (4.12) is the last element in the sorted elements of a component then $m^0(V_{\eta=k}) = m^0(V_T)$. These m^0 values are then plotted against the sub-volume ratio (i.e., $\overline{V_\eta}$).

$$\overline{V_\eta} = \frac{\sum_{\eta=1}^{k} V_\eta}{V_T} \tag{4.13}$$

The m^0 vs. $\overline{V_\eta}$ plot of a plate subjected to concentrated load with different cut-off percentages is presented in Fig. 4.9.

4.5 General Procedure for Finding Lower Bound Limit Loads Using Elastic Reference Volume Method

This section explains how to apply the above explained methods to any general component.

- Initially a linear elastic finite element analysis is performed on a given component.
- Once the equivalent stresses are obtained, the elements are arranged in the descending order of there equivalent stresses. Then the m^0 value is computed with the increasing sub-volume till the total volume.
- These m^0 values are plotted against the sub-volumes ratios $\overline{V_\eta}$.
- From the plot using cutoff stresses the dead and reference volumes are identified. Elements having less than 5% cutoff stress are considered as dead volume and the

remaining elements together are considered as the reference volume. Corresponding to this reference volume, the corrected reference volume multiplier $m^0(V_{\mathrm{Re}})$ is obtained from the plot.

- Using the corrected reference volume multiplier $m^0(V_{\mathrm{Re}})$, and lower bound multiplier m_L the value of lower bound limit load multiplier $m_\alpha^T(V_{\mathrm{Re}})$ should be calculated as explained in section 3.7.4 in chapter 3.
- The above steps are continued using the EMAP iterations until the converged solution are obtained. The results of fifty EMAP iterations and convergence criteria are provided in appendix C.

An example of a rectangular plate subjected to a uniformly distributed load on its top corner is studied in the following section. This problem is synonymous to semi infinite soil sample under a strip footing. The schematic of the problem is shown in Fig. 7. Since it's a strip loading, 2D plain strain analysis along a vertical symmetric axis through the footing and fixed bottom is performed. The footing load is applied as a Pressure of 100 KPa.

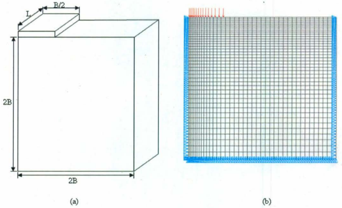

Figure 4.7 Thick plate subjected to strip loading (a) Geometry and dimensions (b) Typical finite element mesh with loading

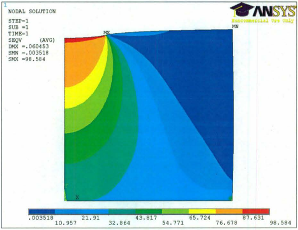

Figure. 4.8 Stress profile of plate with concentrated load

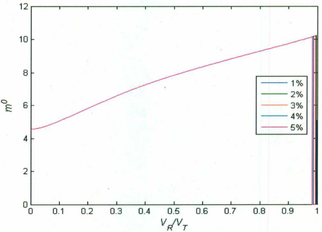

Figure. 4.9 Variation in m^0 with various cut-off percentages for Plate with a strip load

To avoid the influence of the constrain conditions sufficiently large model is considered. The young's modulus of 200 GPa and a poisons ratio of 0.47 were used. By considering 5% of peak stresses as the cutoff the contours of the stresses are plotted. The stress contours generated from initial linear elastic FEA Fig. 4.9 matches closely with the theoretical stress contours in Fig. 4.5 and Fig. 4.6.The volume covered by these contours represents the active volume which is considered to be the *elastic reference volume*. Whereas the empty spaces represent the *Dead Volume*. These volumes can be easily obtained from m^0 vs. $\overline{V}_\eta$ plot as explained in the section 4.5. The upper bound multiplier m^0 value obtained from first linear elastic run considering the total volume is 10.23 and the lower bound multiplier is 4.53. If these multipliers are used to compute m_α^T its value is 7.47. It is slightly upper bounded when compared to the non linear analysis value of 7.45. With the elastic reference volume correction the new m^0 value is $m^0(V_{\mathrm{Re}}) = 10.12$. The m_α^T value calculated with this corrected reference volume multiplier value is $m^0(V_{\mathrm{Re}})$ is 7.43, $m_\alpha^T(V_{\mathrm{Re}})$ so obtained is lower bounded.

4.6 Application to General Components

4.6.1 Thick Walled Cylinder

A thick walled cylinder (Fig.4.10) with inside radius of R = 65 mm and thickness t = 25 mm is modeled. An internal pressure of 50 MPa is applied. The material is assumed to be elastic-perfectly plastic. The modulus of elasticity is specified as 200GPa and the yield strength is assumed to be 300 MPa. For inducing a plastic flow state the Poisson ratio of 0.47 is used in elastic analysis. A 'q' value of 0.1 is used for the EMAP for ensuring a slow but less fluctuating convergence. The same 'q' value is used for all the problems. The geometry is modeled using Plane82 elements with plane strain consideration.

The variation of the upper bound multiplier with various cut-off percentages for first iteration is shown in the Fig. 4.11. Variation of $m^0(V_{\mathrm{Re}})$ and $m_\alpha^T(V_{\mathrm{Re}})$ with different iteration for thick walled cylinder are presented in Tab. 4.1 and Fig. 4.12.

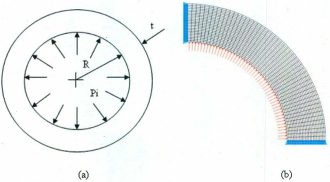

Figure 4.10 Thick walled cylinder. (a) Geometry and dimensions (b) Typical finite element mesh with loading

As the thick walled cylinder problem is not supposed to have any dead volume effect, In Fig. 4.11 we can see that no correction has been applied it can also be seen from m^0 and $m^0(V_{\text{Re}})$ columns of the Tab.4.1. both these values are equal. For the simplicity in comparison of various methods the results are presented at the equal interval sets and the raw data (i.e., m^0 and m_L values) is presented in the appendix.

Table 4.1 Comparison of Various Multipliers of Thick Walled Cylinder (EMAP)

Iteration	m^0	m_L	$m^0(V_{\text{Re}})$	$m_\alpha^T(V_{\text{Re}})$	m_{non}
1	2.294	1.706	2.294	2.081	
6	2.268	1.901	2.268	2.152	
12	2.258	2.053	2.258	2.194	2.254
18	2.255	2.142	2.255	2.223	
25	2.255	2.199	2.255	2.244	

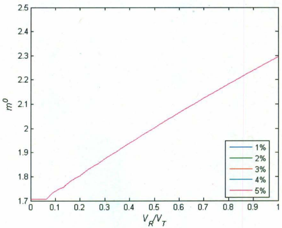

Figure. 4.11 Invariant m^0 for Thick walled Cylinder

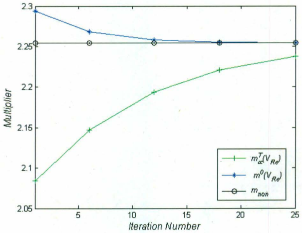

Figure. 4.12 Variation of $m^0(V_{\text{Re}})$ and $m_\alpha^T(V_{\text{Re}})$ with iterations of Thick Walled Cylinder

4.6.2 Torispherical Head (TSH)

A torispherical head (Fig.4.13) with average diameter D=2000 mm, normalized spherical cap radius $R_S / D = 0.8$, normalized knuckle radius of $R_K / D = 0.12$ and normalized thickness of $t / D = 1/40$, subjected to an internal pressure of 5 MPa is examined here. To avoid the discontinuity effect at the boundaries, the length of the cylindrical part (H) is specified as $H = 6\sqrt{Dt/2}$. The material is assumed to be elastic-perfectly plastic. The modulus of elasticity is specified as 262GPa and the yield strength is assumed to be 262 MPa. The geometry is modeled using Plane82 elements with axi-symmetric consideration.

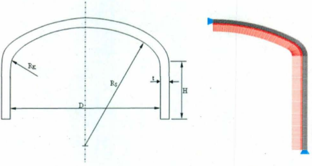

Figure 4.13. Torispherical Head (a) Geometry and dimensions (b) Typical finite element mesh with loading

The variation of the upper bound multiplier with various cut-off percentages for first iteration is shown in the Fig. 4.14. Variation of $m^0(V_{\mathrm{Re}})$ and $m_\alpha^T(V_{\mathrm{Re}})$ with different iteration for Torispherical Head are presented in Tab. 4.2 and Fig. 4.15. From the Fig. 4.14 it can be concluded that the torispherical head is a component without any dead volume effect in it. It can also be seen both m^0 and $m^0(V_{\mathrm{Re}})$ columns of the Tab.4.2. as they are equal. For such components $m_\alpha^T(V_{\mathrm{Re}})$ calculated will be equal to the regular m_α^T.

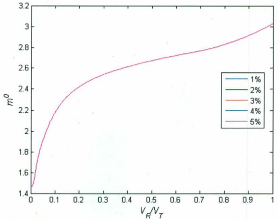

Figure. 4.14 Invariant m^0 for for Torispherical Head

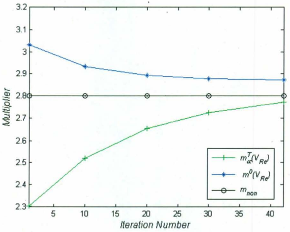

Figure. 4.15 Variation of $m^0(V_{\mathrm{Re}})$ and $m^T_\alpha(V_{\mathrm{Re}})$ with iterations of Torispherical Head

Table 4.2 Comparison of Various Multipliers of Torispherical Head (EMAP)

Iteration	m^0	m_L	$m^0(V_{Re})$	$m_\alpha^T(V_{Re})$	m_{non}
1	3.029	1.458	3.029	2.303	
10	2.932	1.883	2.932	2.521	
20	2.893	2.211	2.893	2.654	2.808
30	2.879	2.415	2.879	2.732	
42	2.871	2.559	2.871	2.775	

4.6.3 Unreinforced Axi-symmetric Nozzle (URASN)

An unreinforced axi-symmetric nozzle (Fig.4.16) is examined here. Inner radius of the head is R=914.4 mm, and the nominal wall thickness is mm. Inside radius of the nozzle is $r = 136.525$ mm and nominal wall thickness is $t_n = 25.4$ mm. The required minimum wall thickness of the head and the nozzle are $t_r = 76.835$ mm and $t_{rn} = 24.308$ mm, respectively. The material is assumed to be elastic-perfectly plastic. The modulus of elasticity is specified as 262 GPa and the yield strength is assumed to be 262 MPa.. The geometry is modeled using Plane82 elements with axi-symmetric consideration.

The variation of the upper bound multiplier with various cut-off percentages for first iteration is shown in the Fig. 4.17. Variation of $m^0(V_{Re})$ and $m_\alpha^T(V_{Re})$ with different iteration for Unreinforced Axi-symmetric Nozzle are presented in Tab. 4.3 and Fig. 4.18. From the Fig. 4.17 it can be concluded that the unreinforced axi-symmetric nozzle is a component without any dead volume effect in it. It can also be seen that both m^0 and $m^0(V_{Re})$ columns of the Tab.4.3 as they are equal.

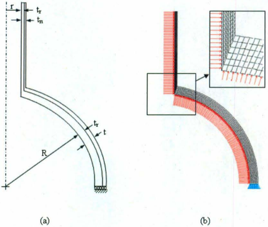

Figure 4.16 Unreinforced Axi-symmetric Nozzle. (a) Geometry and dimensions (b) Typical finite element mesh with loading.

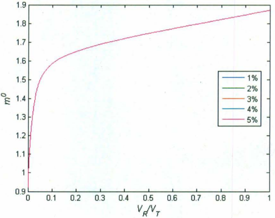

Figure. 4.17 Invariant m^0 for Unreinforced Axi-symmetric Nozzle.

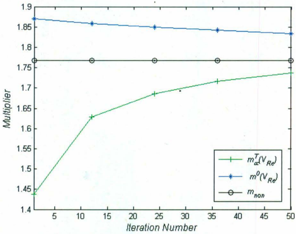

Figure. 4.18 Variation of $m^0(V_{Re})$ and $m_\alpha^T(V_{Re})$ with iterations of Unreinforced Axi-symmetric Nozzle

Table 4.3 Comparison of Various Multipliers of Unreinforced Axi-symmetric Nozzle for Elastic Reference Volume Correction (EMAP)

Iteration	m^0	m_L	$m^0(V_{Re})$	$m_\alpha^T(V_{Re})$	m_{non}
1	1.870	0.922	1.870	1.444	
12	1.858	1.254	1.858	1.632	
24	1.850	1.388	1.850	1.691	1.773
36	1.842	1.473	1.842	1.723	
50	1.834	1.539	1.834	1.744	

4.6.4 Reinforced Axi-symmetric Nozzle (RASN)

A Reinforced Axi-symmetric nozzle (Fig.4.19) is examined here. The unreinforced nozzle, modeled in the previous example is reinforced according to ASME Code VIII Div.2, AD-560.1(a) of [24].The geometric transitions of the reinforcement are modeled with fillet radius, $r_1 = 10.312$ mm, $r_2 = 83.312$ mm and $r_3 = 115.214$ mm. The other dimensions include $T_2 = 54.61\,\text{mm}$ and $\theta = 45^0$. The distribution of reinforcement is bounded by the reinforcement zone boundary specified by circle of radius $L_n = 143.51\,\text{mm}$. The other geometric dimensions are same as the previous example. The material is assumed to be elastic-perfectly plastic. The modulus of elasticity is specified as 262 GPa and the yield strength is assumed to be 262 MPa.. The geometry is modeled using Plane82 elements with Axi-symmetric consideration.

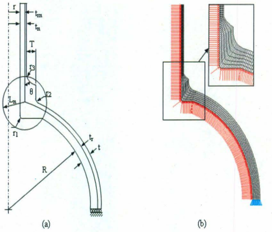

Figure 4.19 Reinforced Axi-symmetric Nozzle (a) Geometry and dimensions (b) Typical finite element mesh with loading

The variation of the upper bound multiplier with various cut-off percentages for first iteration is shown in the Fig. 4.20. Variation of $m^0(V_{\text{Re}})$ and $m_\alpha^T(V_{\text{Re}})$ with different iteration for Reinforced Axi-symmetric Nozzle are presented in Tab. 4.8 and Fig. 4.21. From the Fig. 4.20 it can be concluded that the reinforced axi-symmetric nozzle is a component without any dead volume effect in it. It can also be seen from m^0 and $m^0(V_{\text{Re}})$ columns of the Tab.4.4 as they are equal.

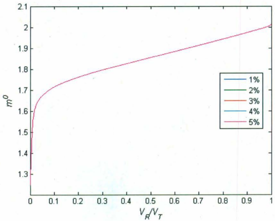

Figure. 4.20 Invariant m^0 for for Reinforced Axi-symmetric Nozzle.

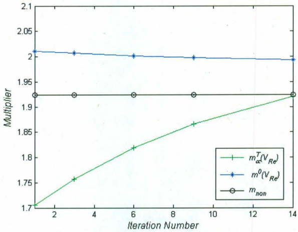

Figure. 4.21 Variation of $m^0(V_{\mathrm{Re}})$ and $m_\alpha^T(V_{\mathrm{Re}})$ with iterations of Reinforced Axi-symmetric Nozzle

Table 4.4 Comparison of Various Multipliers of Reinforced Axi-symmetric Nozzle (EMAP)

Iteration	m^0	m_L	$m^0(V_{\mathrm{Re}})$	$m_\alpha^T(V_{\mathrm{Re}})$	m_{non}
1	2.011	1.248	2.011	1.713	
3	2.006	1.351	2.006	1.762	
6	2.002	1.489	2.002	1.823	1.924
9	1.998	1.608	1.998	1.871	
14	1.993	1.764	1.993	1.922	

4.6.5 Pressure Vessel Support Skirt (PVSS)

A Pressure Vessel Support Skirt (Fig.4.22) is examined here. It's geometrically a cylinder attached to a cone. The top support ring is fixed to the rigid foundation. A blend radius is used at the cylinder-cone junction. The inner radius of cylinder $R_{cyi} = 1240$ mm and outer radius is $R_{cyo} = 1290$ mm. The cone inner radius is $R_{coi} = 1400$ mm; the blend radius at the inner radius is modeled using fillet radius, $r = 50$ mm. The height of the cylinder portion is $h_c = 760$ mm and the total height of the pressure vessel support skirt is $h = 1600$ mm. The material is assumed to be elastic-perfectly plastic. The modulus of elasticity is specified as 275.8 GPa and the yield strength is assumed to be 275.8 MPa. The bottom of the cylinder is subjected to an axial load of $P = 77.362$ MPa, and it is free to deflect and rotate. The geometry is modeled using Plane82 elements with Axi-symmetric consideration.

The variation of the upper bound multiplier with various cut-off percentages for first iteration is shown in the Fig. 4.23. Variation of $m^0(V_{\mathrm{Re}})$ and $m_\alpha^T(V_{\mathrm{Re}})$ with different iteration for Pressure Vessel Support Skirt are presented in Tab. 4.5 and Fig. 4.24. From the Fig. 4.23 it can be concluded that the pressure vessel support skirt is a component without any dead volume effect in it. It can also be seen from m^0 and $m^0(V_{\mathrm{Re}})$ columns of the Tab.4.5 as they are equal.

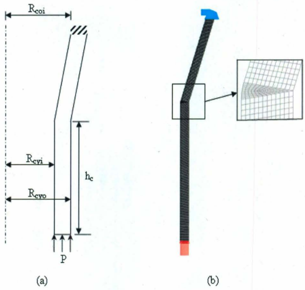

Figure 4.22 Pressure Vessel Support Skirt. (a) Geometry and dimensions (b) Typical finite element mesh with loading

Table 4.5 Comparison of Various Multipliers of Pressure Vessel Support Skirt for Elastic Reference Volume Correction (EMAP)

Iteration	m^0	m_L	$m^0(V_{Re})$	$m_\alpha^T(V_{Re})$	m_{non}
1	3.614	1.522	3.614	2.583	
12	3.463	2.064	3.463	2.891	
24	3.377	2.427	3.377	3.032	3.161
36	3.325	2.640	3.325	3.094	
50	3.288	2.800	3.288	3.132	

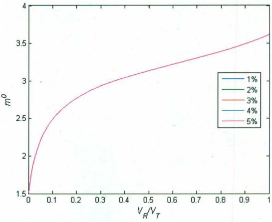

Figure 4.23 Invariant m^0 for Pressure Vessel Support Skirt

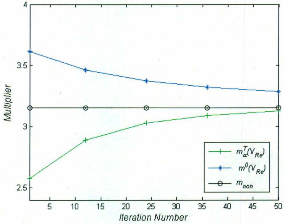

Figure 4.24 Variation of $m^0(V_{Re})$ and $m_\alpha^T(V_{Re})$ with iterations of Pressure Vessel Support Skirt

4.6.6 Compact Tension (CT) Specimen

A Compact Tension Specimen (Fig.4.25) with a width $W = 100\,\text{mm}$, height $H = 125\,\text{mm}$, thickness $t = 3\,\text{mm}$ and crack length $a = 46\,\text{mm}$ is subjected to a tensile load of $P = 10\,\text{KN}$. The material is assumed to be elastic-perfectly plastic. The modulus of elasticity is specified as 211 GPa and the yield strength is assumed to be 250 MPa. Due to symmetry in geometry and loading, only a half of the plate is modeled using Plane82 elements with plane stress with thickness consideration. Singularity elements are used around the crack-tip.

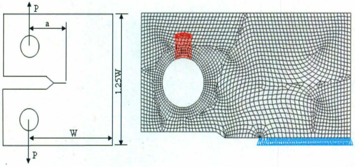

(a) (b)

Figure 4.25 CT Specimen (a) Geometry and dimensions (b) Typical finite element mesh with loading

The variation of the upper bound multiplier with various cut-off percentages for first iteration is shown in the Fig. 4.26. Variation of $m^0(V_{\text{Re}})$ and $m_\alpha^T(V_{\text{Re}})$ with different iteration for CT Specimen are presented in Tab. 4.6 and Fig. 4.27. From Fig. 4.26 it can be concluded that the CT Specimen is a component with the dead volume effect. As can be seen from m^0 and $m^0(V_{\text{Re}})$ columns of the Tab.4.6 the upper bound multiplier is corrected. Using this reference volume corrected multiplier $m_\alpha^T(V_{\text{Re}})$ is calculated. The presence of the peak stresses in the CT Specimen is causing the lower bound multiplier in the first iteration to be bit conservative, but with the EMAP iterations the results seen to be converging to nonlinear analysis solution.

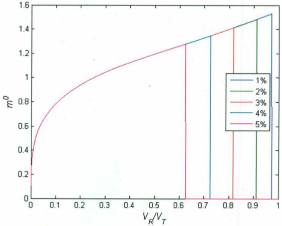

Figure 4.26 Variation of m^0 with various percentages of cut-off stress for CT Specimen

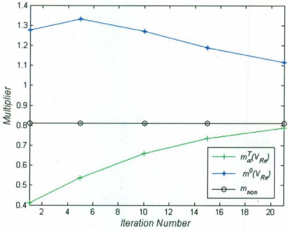

Figure 4.27 Variation of $m^0(V_{Re})$ and $m_\alpha^T(V_{Re})$ with iterations of CT Specimen

The time taken for the ERVM is 146 CPU units when compared to 186 CPU units for nonlinear analysis.

Table 4.6 Comparison of Various Multipliers of CT Specimen for Elastic Reference Volume Correction (EMAP)

Iteration	m^0	m_L	$m^0(V_{\text{Re}})$	$m_\alpha^T(V_{\text{Re}})$	m_{non}
1	1.549	0.108	1.283	0.412	
5	1.395	0.162	1.334	0.543	
10	1.273	0.248	1.272	0.664	0.812
15	1.189	0.346	1.191	0.742	
21	1.115	0.462	1.124	0.791	

4.6.7 Single Edge Notch Bend

A Single edge notch bend (Fig.4.28) with a span $S = 400\,\text{mm}$, a width $W = 100\,\text{mm}$, thickness $t = 3\,\text{mm}$ and crack length $a = 50\,\text{mm}$ is subjected to a point load of $P = 24\,\text{KN}$. The material is assumed to be elastic-perfectly plastic. The modulus of elasticity is specified as 211 GPa and the yield strength is assumed to be 488.43 MPa. Due to symmetry in geometry and loading, only a half of the specimen is modeled using Plane82 elements with plane stress with thickness consideration. Singularity elements are used around the crack-tip.

The variation of the upper bound multiplier with various cut-off percentages for the first iteration is shown in the Fig. 4.29. Variation of $m^0(V_{\text{Re}})$ and $m_\alpha^T(V_{\text{Re}})$ with different iteration for Single Edge Notch Bend are presented in Tab. 4.7 and Fig. 4.30. From Fig. 4.29 it can be concluded that the single edge notch bend is a component with the dead volume effect. As can be seen from m^0 and $m^0(V_{\text{Re}})$ columns of the Tab.4.7 the upper bound multiplier is corrected. Using this reference volume corrected multiplier $m_\alpha^T(V_{\text{Re}})$ is calculated. The presence of the peak stresses in the Single Edge Notch Bend is causing the lower bound multiplier in the first iteration to be bit conservative, but with the EMAP iterations the results seen to be converging to nonlinear analysis solution.

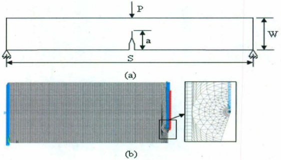

Figure 4.28 Single Edge Notch Bend (a) Geometry and dimensions (b) Typical finite element mesh with loading

The time taken for the ERVM is 250 CPU units when compared to 556 CPU units for nonlinear analysis.

Table 4.7 Comparison of Various Multipliers of Single Edge Notch Bend for Elastic Reference Volume Correction (EMAP)

Iteration	m^0	m_L	$m^0(V_{\text{Re}})$	$m_\alpha^T(V_{\text{Re}})$	m_{non}
1	4.759	0.202	2.073	0.734	
5	3.632	0.287	2.204	0.922	
10	2.709	0.417	2.252	1.141	1.353
15	2.159	0.564	2.043	1.233	
20	1.843	0.712	1.831	1.264	

4.6.8. Plate with Multiple Cracks

A plate with multiple cracks (Fig.4.32) has one horizontal crack (length $2a$=20 mm) at the center and four cracks inclined at 45° (length $2b$=21.2 mm) symmetrically located on both sides of the horizontal and vertical lines of symmetry.

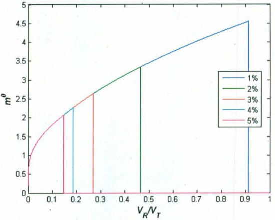

Figure 4.29 Variation of m^0 with various percentages of cut-off stress for Single Edge Notch Bend

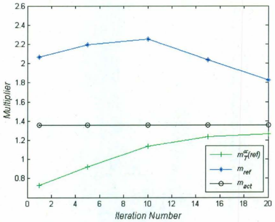

Figure 4.30 Variation of $m^0(V_{Re})$ and $m_\alpha^T(V_{Re})$ with iterations of Single Edge Notch Bend

The crack tips are spread vertically with c=20 mm and horizontally with d=40 mm. The Plate has a width W=100 mm and height H=200 mm, and is loaded by the tensile stress of $\sigma = 100$ MPa.

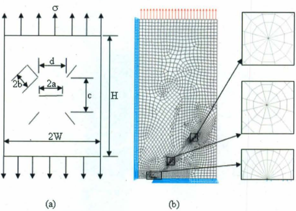

Figure 4.31 Plate with Multiple Cracks (a) Geometry and dimensions (b) Typical finite element mesh with loading

The material is assumed to be elastic-perfectly plastic. The modulus of elasticity is specified as 211 GPa and the yield strength is assumed to be 250 MPa. Due to symmetry in geometry and loading, only a quarter of the specimen is modeled using Plane82 elements with plane stress with thickness consideration. Singularity elements are used around the crack-tip.

The variation of the upper bound multiplier with various cut-off percentages for first iteration is shown in the Fig. 4.32. Variation of $m^0(V_{\text{Re}})$ and $m^T_\alpha(V_{\text{Re}})$ with different iteration for plate with multiple cracks are presented in Tab. 4.8 and Fig. 4.33. From Fig. 4.32 it can be concluded that the plate with multiple cracks is a component with the dead volume effect. As can be seen from m^0 and $m^0(V_{\text{Re}})$ columns of the Tab.4.8 the upper bound multiplier is corrected. Using this reference volume corrected multiplier $m_\alpha^T(V_{Re})$ is calculated.

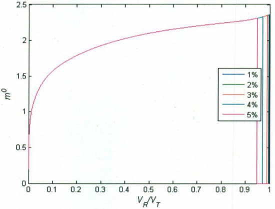

Figure 4.32 Variation of m^0 with various percentages of cut-off stress for Plate with Multiple Cracks

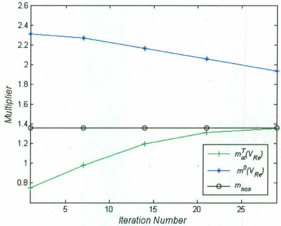

Figure 4.33 Variation of $m^0(V_{Re})$ and $m_\alpha^T(V_{Re})$ with iterations of Plate with Multiple Cracks

With the EMAP iterations the results seen to be converging to nonlinear analysis solution. The time taken for the ERVM is 139 CPU units when compared to 175 CPU units for nonlinear analysis.

Table 4.8 Comparison of Various Multipliers of Plate with Multiple cracks (EMAP)

Iteration	m^0	m_L	$m^0(V_{\text{Re}})$	$m_\alpha^T(V_{\text{Re}})$	m_{non}
1	2.359	0.197	2.314	0.752	
7	2.270	0.312	2.269	0.984	
14	2.167	0.484	2.165	1.203	1.362
21	2.059	0.645	2.058	1.312	
29	1.935	0.773	1.934	1.351	

4.6.9 Plate with a Hole

A Plate With a hole (Fig.4.34) with the following dimensions are considered: Plate width $2W = 150$ mm; length $2L = 300$ mm; hole radius $r = 23$ mm. It is subjected to a tensile load of $P = 100$ MPa. The material is assumed to be elastic-perfectly plastic. The modulus of elasticity is specified as 152.95 GPa and the yield strength is assumed to be 131.90 MPa. Due to symmetry in geometry and loading, only a quarter of the plate is modeled using Plane82 elements with plane stress consideration.

The variation of the upper bound multiplier with various cut-off percentages is shown in the Fig. 4.35. Variation of $m^0(V_{\text{Re}})$ and $m_\alpha^T(V_{\text{Re}})$ with different iteration for plate with hole are presented in Tab. 4.9 and Fig. 4.36. The Fig. 4.35 it can be concluded that the plate with a hole is a component without any dead volume effect in it. It can also be seen from m^0 and $m^0(V_{\text{Re}})$ columns of the Tab. 4.9 as they are equal. The Plate with a hole is a good example for the notch problems, as this is a notch the result from the initial analysis is much closer to the non linear analysis results when compared to the crack problems. EMAP takes less number of iterations to converge. The time taken for the ERVM is 74 CPU units when compared to 191 CPU units for nonlinear analysis.

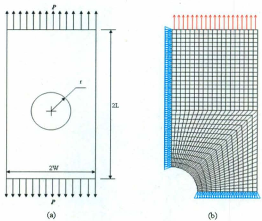

Figure 4.34 Plate with a Hole (a) Geometry and dimensions (b) Typical finite element mesh with loading

Table 4.9 Comparison of Various Multipliers of Plate with a Hole for Elastic Reference Volume Correction (EMAP)

Iteration	m^0	m_L	$m^0(V_{\text{Re}})$	$m_\alpha^T(V_{\text{Re}})$	m_{non}
1	1.221	0.481	1.221	0.852	
2	1.216	0.496	1.216	0.863	
4	1.206	0.526	1.206	0.884	0.922
6	1.197	0.556	1.197	0.902	
8	1.188	0.584	1.188	0.911	

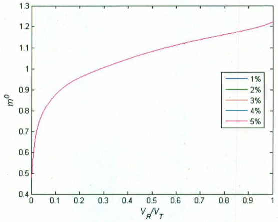

Figure 4.35 Variation of m^0 with various percentages of cut-off stress for Plate with a Hole.

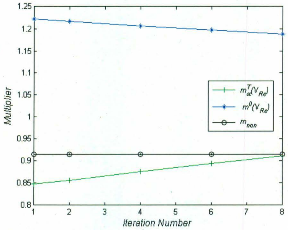

Figure 4.36 Variation of $m^0(V_{Re})$ and $m_\alpha^T(V_{Re})$ with iterations of Plate with a Hole

4.6.10 Indeterminate Beam

An Indeterminate beam (Fig.4.37) with length $L = 508$ mm; height $h = 25.4$ mm is modeled. It is subjected to uniformly distributed load of $P = 1.0$ MPa. The material is assumed to be elastic-perfectly plastic. The modulus of elasticity is specified as 206.85 GPa and the yield strength is assumed to be 206.85 MPa. The beam is modeled using Plane82 elements with plane stress consideration.

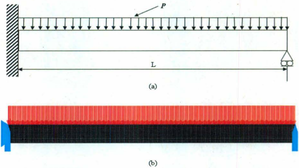

Figure 4.37 Indeterminate Beam (a) Geometry and dimensions (b) Typical finite element mesh with loading

The variation of the upper bound multiplier with various cut-off percentages is shown in the Fig. 4.38. Variation of $m^0(V_{Re})$ and $m_\alpha^T(V_{Re})$ with different iteration indeterminate beam are presented in Tab. 4.10 and Fig. 4.39. From Fig. 4.38 it can be concluded that the indeterminate beam is a component with the dead volume effect. As can be seen from m^0 and $m^0(V_{Re})$ columns of the Tab.4.8 the upper bound multiplier is corrected. Using this reference volume corrected multiplier $m_\alpha^T(V_{Re})$ is calculated. EMAP takes less number of iterations to converge. The time taken for the ERVM is 550 CPU units when compared to 583 CPU units for nonlinear analysis.

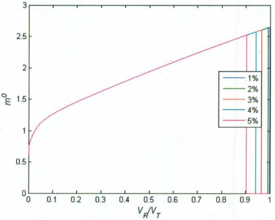

Figure 4.38 Variation of m^0 with various percentages of cut-off stress for Indeterminate Beam

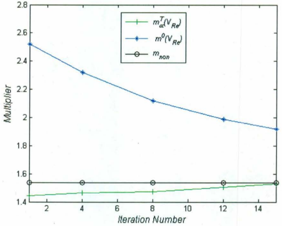

Figure 4.39 Variation of $m^0(V_{\mathrm{Re}})$ and $m_\alpha^T(V_{\mathrm{Re}})$ with iterations of Indeterminate Beam

Table 4.10 Comparison of Various Multipliers of Indeterminate Beam (EMAP)

Iteration	m^0	m_L	$m^0(V_{\mathrm{Re}})$	$m_\alpha^T(V_{\mathrm{Re}})$	m_{non}
1	2.649	0.613	2.522	1.454	
4	2.357	0.711	2.324	1.473	
8	2.124	0.837	2.121	1.471	1.543
12	1.988	0.951	1.985	1.514	
15	1.920	1.027	1.918	1.532	

4.6.11 Oblique Nozzle

An Oblique Nozzle (Fig.4.40) with length of cylinder $L_c = 2400$ mm with an internal radius $R_c = 300$ mm and length of the nozzle $L_n = 1200$ mm height $R_n = 156.5$ mm is and average thickness $t = 6$ mm with four different nozzle angles $\theta = 30^0, 45^0, 60^0$ and 90^0 is been analyzed. The cap height of the cylinder cap $H_c = 175$ mm and for the nozzle is $H_n = 106$ mm. The cylinder is mounted on supports which are separated by a distance of $S = 1600$ mm.

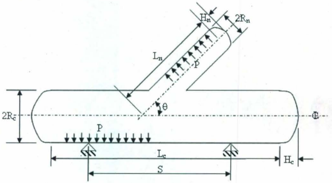

Figure 4.40 Schematic of Oblique Nozzle Geometry and dimensions

It is subjected to a uniformly distributed load of $P = 3.0\,\text{MPa}$. The material is assumed to be elastic-perfectly plastic. The modulus of elasticity is specified as 108.08 GPa and the yield strength is assumed to be 339.40 MPa. The beam is modeled using solid 95 elements.

4.6.11.1 Nozzle Angle $\theta = 30^0$

The Finite Element mesh of oblique nozzle 30^0 is presented in the Fig. 4.41. The variation of the upper bound multiplier with various cut-off percentages is shown in the Fig. 4.42. Variation of $m^0(V_{\text{Re}})$ and $m_\alpha^T(V_{\text{Re}})$ with different iteration for oblique nozzle 30^0 are presented in Tab. 4.11 and Fig. 4.43.

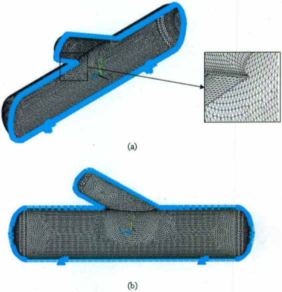

Figure 4.41 Finite Element Mesh of Oblique Nozzle 30^0 (a) Isometric View (b) Front View

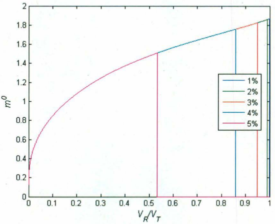

Figure 4.42 Variation of m^0 with various percentages of cut-off stress for Oblique Nozzle 30^0

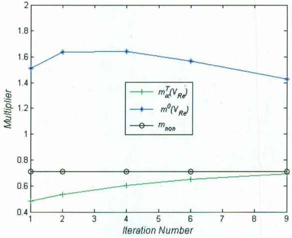

Figure 4.43 Variation of $m^0(V_{\rm Re})$ and $m_\alpha^T(V_{\rm Re})$ with iterations of Oblique Nozzle 30^0

From Fig. 4.42 it can be concluded that the oblique nozzle 30^0 is a component with the dead volume effect. As can be seen from m^0 and $m^0(V_{\mathrm{Re}})$ columns of the Tab.4.11 the upper bound multiplier is corrected. Using this reference volume corrected multiplier $m_\alpha^T(V_{\mathrm{Re}})$ is calculated. The time taken for the ERVM is 3431 CPU units when compared to 25200 CPU units for nonlinear analysis.

Table 4.11 Comparison of Various Multipliers of Oblique Nozzle 30^0 (EMAP)

Iteration	m^0	m_L	$m^0(V_{\mathrm{Re}})$	$m_\alpha^T(V_{\mathrm{Re}})$	m_{non}
1	1.867	0.127	1.514	0.483	
2	1.811	0.141	1.643	0.531	
4	1.698	0.171	1.642	0.602	0.712
6	1.589	0.201	1.571	0.652	
9	1.432	0.244	1.434	0.694	

4.6.11.2 Nozzle Angle $\theta = 45^0$

The Finite Element mesh of oblique nozzle 45^0 is presented in the Fig. 4.44. The variation of the upper bound multiplier with various cut-off percentages for first iteration is shown in the Fig. 4.45. Variation of $m^0(V_{\mathrm{Re}})$ and $m_\alpha^T(V_{\mathrm{Re}})$ with different iteration for oblique nozzle 45^0 are presented in Tab. 4.12 and Fig. 4.46.

From Fig. 4.45 it can be concluded that the oblique nozzle 45^0 is a component with the dead volume effect. As can be seen from m^0 and $m^0(V_{\mathrm{Re}})$ columns of the Tab.4.12 the upper bound multiplier is corrected. Using this reference volume corrected multiplier $m_\alpha^T(V_{\mathrm{Re}})$ is calculated. The time taken for the ERVM is 3228 CPU units when compared to 24300 CPU units for nonlinear analysis.

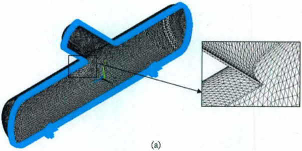

(a)

(b)

Figure 4.44 Finite Element Mesh of Oblique Nozzle 45⁰ (a) Isometric View b) Front View

Table 4.12 Comparison of Various Multipliers of Oblique Nozzle 45⁰ (EMAP)

Iteration	m^0	m_L	$m^0(V_{Re})$	$m_\alpha^T(V_{Re})$	m_{non}
1	2.400	0.242	2.362	0.864	
2	2.364	0.263	2.344	0.903	
4	2.288	0.304	2.283	0.971	1.072
6	2.210	0.343	2.201	1.022	
9	2.083	0.398	2.082	1.071	

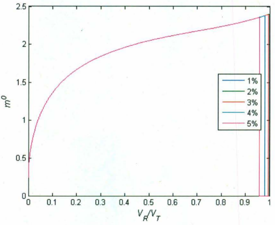

Figure 4.45 Variation of m^0 with various percentages of cut-off stress for Oblique Nozzle 45^0

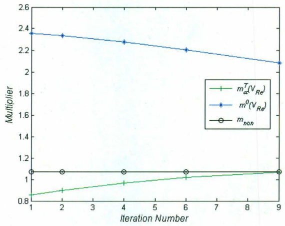

Figure 4.46 Variation of $m^0(V_{\rm Re})$ and $m_\alpha^T(V_{\rm Re})$ with iterations of Oblique Nozzle 45^0

4.6.11.3 Nozzle Angle $\theta = 60^0$

The Finite Element mesh of oblique nozzle 60^0 is presented in the Fig. 4.47. The variation of the upper bound multiplier with various cut-off percentages is shown in the Fig. 4.48. Variation of $m^0(V_{\mathrm{Re}})$ and $m_\alpha^T(V_{\mathrm{Re}})$ with different iteration for oblique nozzle 60^0 are presented in Tab. 4.13 and Fig. 4.49.

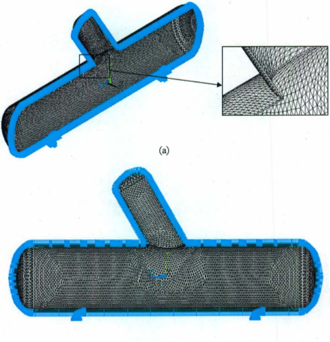

(a)

(b)

Figure 4.47 Finite Element Mesh of Oblique Nozzle 60^0 (a) Isometric View b) Front View

From Fig. 4.48 it can be concluded that the oblique nozzle 60^0 is a component with the dead volume effect. As can be seen from m^0 and $m^0(V_{Re})$ columns of the Tab.4.13 the upper bound multiplier is corrected. Using this reference volume corrected multiplier $m_\alpha^T(V_{Re})$ is calculated. The time taken for the ERVM is 3031 CPU units when compared to 23600 CPU units for nonlinear analysis.

Table 4.13 Comparison of Various Multipliers of Oblique Nozzle 60^0 (EMAP)

Iteration	m^0	m_L	$m^0(V_{Re})$	$m_\alpha^T(V_{Re})$	m_{non}
1	2.558	0.351	2.548	1.104	
4	2.476	0.420	2.467	1.202	
8	2.361	0.503	2.356	1.281	1.314
12	2.237	0.552	2.235	1.293	
15	2.141	0.594	2.140	1.304	

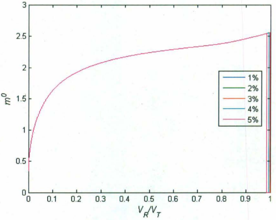

Figure 4.48 Variation of m^0 with various percentages of cut-off stress for Oblique Nozzle 60^0

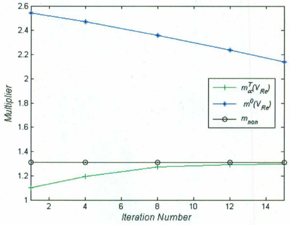

Figure 4.49 Variation of $m^0(V_{\mathrm{Re}})$ and $m_\alpha^T(V_{\mathrm{Re}})$ with iterations of Oblique Nozzle 60^0

4.6.11.4 Nozzle Angle $\theta = 90^0$

The Finite Element mesh of oblique nozzle 90^0 is presented in the Fig. 4.50. The variation of the upper bound multiplier with various cut-off percentages for first iteration is shown in the Fig. 4.51. Variation of $m^0(V_{\mathrm{Re}})$ and $m_\alpha^T(V_{\mathrm{Re}})$ with different iteration for oblique nozzle 90^0 are presented in Tab. 4.14 and Fig. 4.52.

From Fig. 4.51 it can be concluded that the oblique nozzle 90^0 is a component with the dead volume effect. As can be seen from m^0 and $m^0(V_{\mathrm{Re}})$ columns of the Tab.4.14 the upper bound multiplier is corrected. Using this reference volume corrected multiplier $m_\alpha^T(V_{\mathrm{Re}})$ is calculated. The time taken for the ERVM is 2930 CPU units when compared to 22400 CPU units for nonlinear analysis.

As can be seen from the plots of the $\boldsymbol{m}^0$ vs cut-off stress for the Oblique Nozzle problem, the reference volume of the oblique nozzle increases with the increase in the oblique angle.

Table 4.14 Comparison of Various Multipliers of Oblique Nozzle 90^0 (EMAP)

Iteration	m^0	m_L	$m^0(V_{\mathrm{Re}})$	$m_\alpha^T(V_{\mathrm{Re}})$	m_{non}
1	2.624	0.513	2.622	1.362	
6	2.515	0.588	2.515	1.423	
12	2.383	0.676	2.382	1.461	1.523
18	2.249	0.781	2.249	1.493	
23	2.140	0.881	2.140	1.514	

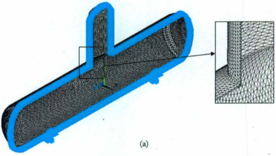

(a)

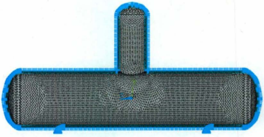

(b)

Figure 4.50 Finite Element Mesh of Oblique Nozzle 90^0 (a) Isometric View b) Front View

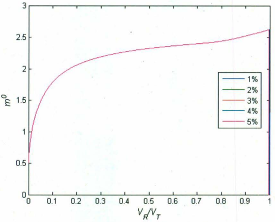

Figure 4.51 Variation of m^0 with various percentages of cut-off stress for Oblique Nozzle 90^0

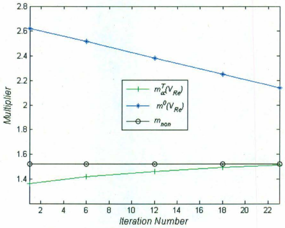

Figure 4.52 Variation of $m^0(V_{Re})$ and $m_\alpha^T(V_{Re})$ with iterations of Oblique Nozzle 90^0

4.7 Discussion of Results

This Elastic Reference Volume method is simple and straightforward as it does not require any sub-classification of the components. After obtaining the stress distribution from the initial elastic analysis, the corrected $m^0(V_{\text{Re}})$ is calculated by cutting down all the elements having stress less than 5 percentage of peak stress as dead volume. The variation of the $m^0(V_{\text{Re}})$ with various percentages of cut-off stress are presented in the results. As seen from the examples using the m^0 vs. $\overline{V}_\eta$ plot, the components which requirement dead volume correction can be identified.

For the well designed components (i.e., Section 4.6.1 to Section 4.6.5) which do not have much dead volume, the correction applied is less as can be seen from their plots, where the variation of $m^0(V_{\text{Re}})$ with various percentages of cut-off stress is very less. For those components which develop flaws during the operation (i.e., Section 4.6.6 to Section 4.6.10), there will be presence of dead volume. Whenever there is a flaw, the peak stresses present in the component are high and the amount of dead volume correction applied is also high. This case is demonstrated using the cracked components. There is no need to catgorize the components for this method as the method will take care of the correction by itself.

A few other models like indeterminate beam and oblique nozzles are also studied to show the method's applicability to the more complicated structures. Using the corrected $m^0(V_{\text{Re}})$ and m_L, $m_\alpha^T(V_{\text{Re}})$ is calculated, which is found to be a lower bounded value of limit load multiplier. The results obtained after the initial linear elastic iteration are a bit conservative in the case of the components with flaws, due to the peak stress effect on the m_L multiplier, but with the EMAP iterations the estimated limit loads reached a good agreement with the non-linear finite element analysis (i.e., <5% error). The time taken for the ERVM is also compared with the nonlinear analysis and it is shown that there is a considerable advantage. It is seen that this advantage increases with the complexity of the problem. In the next chapter another method for reference volume correction, The *Plastic Reference Volume Method* is explained.

CHAPTER 5
PLASTIC REFERENCE VOLUME METHOD

5.1 Introduction

Plastic reference volume method for reference volume correction while finding out limit loads in the components or structures are presented. This reference volume correction concept is used in combination with m_α - Tangent method to obtain the lower bound limit load of general component or structure. The *Plastic Reference Volume Method* for finding out the reference volume of any general component involves integration of the upper bound multiplier vs. sub-volume ratio curve. Reference volume is a sub-volume of the component which will actively participate in plastic action at failure. Finally this method is tested with the help of different components ranging from well designed components to components with highly localized stresses.

5.2 Plastic Reference Volume Method

The proposed method for finding out the *reference volume* of any general component is a new approach which involves integration of the m^0 *vs.* $\overline{V}_\eta$ curve. Reference volume is a sub-volume of the component which will actively participate in plastic action at failure, where as dead volume is the sub-volume that does not participate.

Plastic Reference Volume method is a different approach of calculating the reference volume. In this approach by integrating the m^0 *vs.* $\overline{V}_\eta$ curve the multiplier is been calculated at the reference stress location. In the elastic reference volume method the complete elastic stress distribution is considered and some portion of it is cut down to define the dead volume. where as in plastic reference volume method reference volume multiplier is been calculated at the reference stress state which is the average of the complete stress profile.

After the first linear elastic FEA run, the m^0 vs. $\overline{V}_\eta$ plot will be generated as discussed in Sec. 4.4. A schematic of m^0 vs. $\overline{V}_\eta$ plot is shown in Fig.5.1. As each of the sub-volume had a corresponding m^0 value, the reference volume which is also a sub-volume will have a corresponding m^0 known as reference multiplier, $m^0(V_R)$. As can be seen from Fig. 5.1, when ever the sub-volume ratio is close to zero $m^0 = m_L$ and when the sub-volume ratio reaches one $m^0 = m^0(V_T)$. Integrating the m^0 vs. $\overline{V}_\eta$ curve, is based on the assumption that the maximum stress developed within the component will be sufficient large to correct the dead volume effect in a component. The integration leads to a statically determinate stress field which satisfies the limit state condition of $m^0(V_{Rp}) = m^0 = m_L$. The stress field achieved after the integration is similar to the plastic failure stress field, and will reach the plastic failure stress field with the EMAP iterations. Due to this reason the method is named as the Plastic Reference Volume Method.

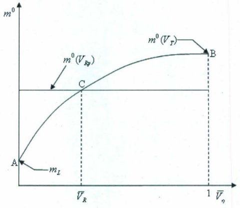

Figure 5.1 Plot of m^0 vs. $\overline{V}_\eta$

The relationship between the upper bound multiplier and the sub volume ratio is given by the Eq. 4.9. The multiplier with plastic reference volume correction $m^0(V_{Rp})$ can be obtained by integrating the m^0 vs. $\overline{V}_\eta$ curve

$$m^0(V_{Rp}) = \int_0^1 m(\overline{V}_\eta)\, d\overline{V}_\eta \tag{5.1}$$

For ease of calculations this value can be numerically obtained as follows:

$$\int_0^1 m(\overline{V}_\eta) d\overline{V}_\eta = m_L + \sum_{k=2}^{N} (\overline{V}_k - \overline{V}_{k-1})(m_k^0 - m_L) \tag{5.2}$$

For the ease of calculation the equation is expressed in terms of m^0 and m_L. The point 'C' which is the point of intersection of the $m^0(V_{Rp})$ line with m^0 vs. $\overline{V}_\eta$ curve will give us the value of reference volume factor $\overline{V}_{Rp}$. This Reference Volume Factor is the measure of the reference volume (or) measure of the dead volume corrected in this particular iteration.

5.2.1 Categorization of Components

For the purpose of this method the general components are categorized into two groups depending on there initial m^0/m_L values. The value of m^0/m_L is used as an indicator for finding the presence of peak stress in a component.

1. If $m^0/m_L < 1+\sqrt{2}$ then the components are well designed, which have negligible peak stress. In these components the correction applied due to the maximum stress is sufficient to correct the dead volume effect completely, which leads to $m^0(V_{Rp})$ being a lower bound values.
2. If $m^0/m_L > 1+\sqrt{2}$ then the components will have peak stress effect. Peak Stresses causes a lower m_L. In this category components are again divided into two groups. First ones that develop flaws or defects during operation (ie, cracked components) and second those which have large dead volumes because of their geometry (i.e., notched components). In both these cases the presence of peak stresses, narrows the amount of correction being applied leading $m^0(V_{Rp})$ to be a upper bound values.

5.3 General Procedure for Finding Lower Bound Limit Loads Using Plastic Reference Volume

In this section a general procedure is being outlined in a step by step manner to find out the lower bound multipliers for general mechanical components and structures using the proposed method.

- The first linear elastic finite element analysis is carried out for the model with the prescribed loading and boundary conditions.
- The elements in the component are sorted in the descending order of the equivalent stress values.
- Then values of m^0 are plotted against $\overline{V}_\eta$ as discussed in Sec. 4.4 and $m^0(V_{Rp})$ will be calculated using the Eq. (5.2).
- Depending on the value of m^0/m_L the components are grouped.
- For the components whose $m^0/m_L < 1+\sqrt{2}$, the value of reference volume corrected multiplier $m^0(V_{Rp})$ is taken as the final value of the multiplier.
- For the components whose $m^0/m_L > 1+\sqrt{2}$, the value of $m_\alpha^T(V_{Rp})$ should be calculated using the corrected multiplier $m^0(V_{Rp})$.
- The above steps are continued using EMAP until the converged or near converged solution are obtained. The results of fifty EMAP iterations and convergence criteria are provided in appendix C.

In the following sections various components are analyzed using the plastic reference volume correction method and the results are been discussed. The examples are chosen in such a way that there will be components from each of the categories explained in Sec. 5.2.1. For the EMAP analysis a fixed 'q' of 0.1 is used. The non-linear analysis results with the perfectly plastic material properties are used as the actual multiplier for the comparison purposes.

5.4 Application to General Components

5.4.1 Thick Walled Cylinder

The geometry, material properties and loading is similar to the example discussed in the section 4.6.1. The reference volume multiplier calculation for first iteration is graphically represented in the Fig. 5.2. From the Fig. 5.3, it can be seen that, as $m^0 / m_L < 1 + \sqrt{2}$ for the thick walled cylinder, $m^0(V_{Rp})$ calculated is always lower bounded. The variation of $m^0(V_{Rp})$ with different iteration for thick walled cylinder is presented in Tab. 5.1 and Fig. 5.3.

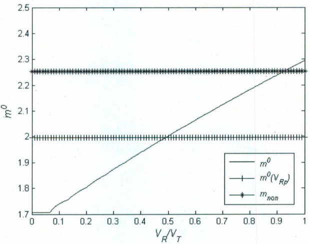

Figure 5.2 $m^0(V_{Rp})$ in first iteration for Thick walled Cylinder

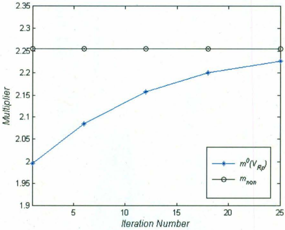

Figure 5.3 Variation of $m^0(V_{Rp})$ with iterations for Thick Walled Cylinder (EMAP)

Table 5.1 Comparison of Various Multipliers for Thick Walled Cylinder (EMAP)

Iteration	m^0	m_L	$m^0(V_{Rp})$	m_{non}
1	2.294	1.706	1.994	
6	2.268	1.901	2.063	
12	2.258	2.053	2.161	2.254
18	2.255	2.142	2.204	
25	2.255	2.199	2.232	

5.4.2 Torispherical Head

The geometry, material properties and loading is similar to the example discussed in the section 4.6.2. The reference volume multiplier calculation for first iteration is graphically represented in the Fig. 5.4. From the Fig. 5.5, it can be seen that, as $m^0 / m_L < 1+\sqrt{2}$ for the torispherical head, $m^0(V_{Rp})$ calculated is always lower bounded. The variation of

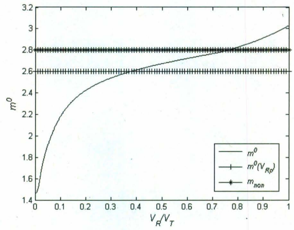

Figure 5.4 $m^0(V_{Rp})$ in first iteration for Torispherical Head

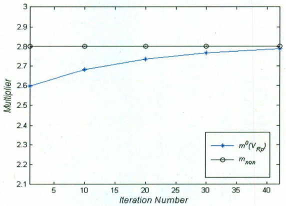

Figure 5.5 Variation of $m^0(V_{Rp})$ with iterations for Torispherical Head (EMAP)

$m^0(V_{Rp})$ with different iteration for torispherical head is presented in Tab. 5.2 and Fig. 5.5.

Table 5.2 Comparison of Various Multipliers for Torispherical Head (EMAP)

Iteration	m^0	m_L	$m^0(V_{Rp})$	m_{non}
1	3.029	1.458	2.592	
10	2.932	1.883	2.684	
20	2.893	2.211	2.743	2.808
30	2.879	2.415	2.772	
42	2.871	2.559	2.791	

5.4.3 Unreinforced Axi-Symmetric Nozzle

The geometry, material properties and loading is similar to the example discussed in the section 4.6.3. The reference volume multiplier calculation for first iteration is graphically represented in the Fig. 5.6. From the Fig. 5.7, it can be seen that, as $m^0 / m_L < 1+\sqrt{2}$ for the unreinforced axi-symmetric nozzle, $m^0(V_{Rp})$ calculated is always lower bounded. Even after the convergence the lower boundedness continues . The variation of $m^0(V_{Rp})$ with different iteration for unreinforced axi-symmetric nozzle is presented in Tab. 5.3 and Fig. 5.7.

Table 5.3 Comparison of Various Multipliers for Unreinforced Axi-symmetric Nozzle (EMAP)

Iteration	m^0	m_L	$m^0(V_{Rp})$	m_{non}
1	3.029	1.458	1.724	
10	2.932	1.883	1.771	
20	2.893	2.211	1.774	1.773
30	2.879	2.415	1.763	
42	2.871	2.559	1.764	

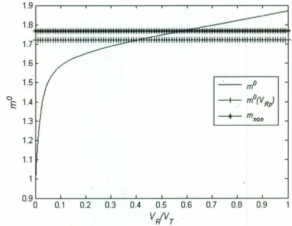

Figure 5.6 $m^0(V_{Rp})$ in first iteration for unreinforced axi-symmetric nozzle

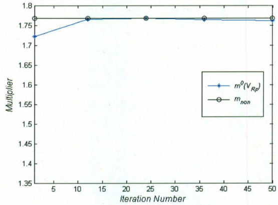

Figure 5.7 Variation of $m^0(V_{Rp})$ for unreinforced axi-symmetric nozzle (EMAP)

5.4.4 Reinforced Axi-symmetric Nozzle

The geometry, material properties and loading is similar to the example discussed in the section 4.6.4. The reference volume multiplier calculation for first iteration is graphically represented in the Fig. 5.8. From the Fig. 5.9, it can be seen that, as $m^0 / m_L < 1+\sqrt{2}$ for the reinforced axi-symmetric nozzle, $m^0(V_{Rp})$ calculated is always lower bounded. The variation of $m^0(V_{Rp})$ with different iteration for reinforced axi-symmetric nozzle is presented in Tab. 5.4 and Fig. 5.9.

Table 5.4 Comparison of Various Multipliers of Reinforced Axi-symmetric Nozzle (EMAP)

Iteration	m^0	m_L	$m^0(V_{Rp})$	m_{non}
1	2.011	1.248	1.852	
3	2.006	1.351	1.863	
6	2.002	1.489	1.884	1.924
9	1.998	1.608	1.892	
14	1.993	1.764	1.903	

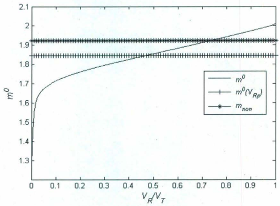

Figure 5.8 $m^0(V_{Rp})$ in first iteration for reinforced axi-symmetric nozzle

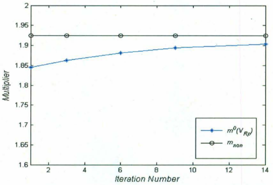

Figure 5.9 Variation of $m^0(V_{Rp})$ with iterations for reinforced axi-symmetric nozzle (EMAP)

5.4.5 Pressure Vessel Support Skirt

The geometry, material properties and loading is similar to the example discussed in the section 4.6.5. The reference volume multiplier calculation for first iteration is graphically represented in the Fig. 5.10. From the Fig. 5.11, it can be seen that, as $m^0 / m_L < 1+\sqrt{2}$ for the reinforced axi-symmetric nozzle, $m^0(V_{Rp})$ calculated is always lower bounded. The variation of $m^0(V_{Rp})$ with different iteration for reinforced axi-symmetric nozzle is presented in Tab. 5.5 and Fig. 5.11.

Table 5.5 Comparison of Various Multipliers of Pressure Vessel Support Skirt (EMAP)

Iteration	m^0	m_L	$m^0(V_{Rp})$	m_{non}
1	3.614	1.523	3.053	
12	3.463	2.064	3.114	
24	3.377	2.427	3.121	3.161
36	3.325	2.640	3.122	
50	3.288	2.800	3.133	

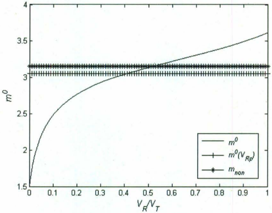

Figure 5.10 $m^0(V_{Rp})$ **in first iteration for Pressure Vessel Support Skirt**

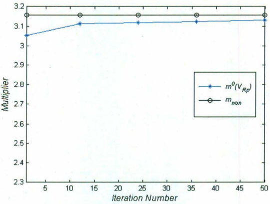

Figure 5.11 Variation of $m^0(V_{Rp})$ **with iterations of Pressure Vessel Support Skirt (EMAP)**

5.4.6 Compact Tension (CT) Specimen

The geometry, material properties and loading is similar to the example discussed in the section 4.6.6. The reference volume multiplier calculation for first iteration is graphically represented in the Fig. 5.12. From the Fig. 5.13, it can be seen that, as $m^0 / m_L > 1+\sqrt{2}$ for the CT Specimen, $m^0(V_{Rp})$ calculated is upper bounded. using the corrected reference volume multiplier $m^0(V_{Rp})$, the $m_\alpha^T(V_{Rp})$ is calculated. The variation of $m^0(V_{Rp})$ and $m_\alpha^T(V_{Rp})$ with different iteration for CT Specimen is presented in Tab. 5.6 and Fig. 5.13.

The presence of the peak stresses in the CT Specimen is causing the lower bound multiplier in the first iteration to be bit conservative, but with the EMAP iterations the results seen to be converging to nonlinear analysis solution. The time taken for the PRVM is 138 CPU units when compared to 186 CPU units for nonlinear analysis.

Table 5.6 Comparison of Various Multipliers of CT Specimen Pressure

Iteration	m^0	m_L	$m^0(V_{Rp})$	$m_\alpha^T(V_{Rp})$	m_{non}
1	1.549	0.108	1.164	0.402	
5	1.395	0.162	1.113	0.504	
10	1.273	0.248	1.071	0.602	0.812
15	1.189	0.346	1.033	0.671	
21	1.115	0.462	0.992	0.743	

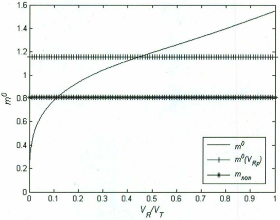

Figure 5.12 $m^0(V_{Rp})$ **in first iteration for CT Specimen**

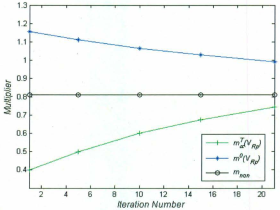

Figure 5.13 Variation of $m^0(V_{Rp})$ **and** $m^T_\alpha(V_{Rp})$ **with iterations for CT Specimen (EMAP)**

5.4.7 Single Edge Notch Bend

The geometry, material properties and loading is similar to the example discussed in the section 4.6.7. The reference volume multiplier calculation for first iteration is graphically represented in the Fig. 5.14. From the Fig. 5.15, it can be seen that, as $m^0 / m_L > 1+\sqrt{2}$ for the single edge notch bend, $m^0(V_{Rp})$ calculated is upper bounded. using the corrected reference volume multiplier $m^0(V_{Rp})$, the $m_\alpha^T(V_{Rp})$ is calculated. The variation of $m^0(V_{Rp})$ and $m_\alpha^T(V_{Rp})$ with different iteration for single edge notch bend is presented in Tab. 5.7 and Fig. 5.15.

The presence of the peak stresses in the Single Edge Notch Bend is causing the lower bound multiplier in the first iteration to be bit conservative, but with the EMAP iterations the results seen to be converging to nonlinear analysis solution. The time taken for the PRVM is 242 CPU units when compared to 556 CPU units for nonlinear analysis.

Table 5.7 Comparison of Various Multipliers for Single Edge Notch Bend (EMAP)

Iteration	m^0	m_L	$m^0(V_{Rp})$	$m_\alpha^T(V_{Rp})$	m_{non}
1	4.759	0.202	3.304	0.854	
5	3.632	0.287	2.752	1.011	
10	2.709	0.417	2.251	1.142	1.353
15	2.159	0.564	1.933	1.194	
20	1..843	0.712	1.724	1.221	

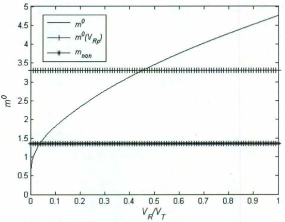

Figure 5.14 $m^0(V_{Rp})$ in first iteration for Single Edge Notch Bend

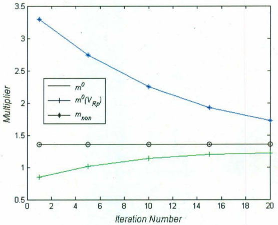

Figure 5.15 Variation of $m^0(V_{Rp})$ and $m_\alpha^T(V_{Rp})$ with iterations for Single Edge Notch Bend (EMAP)

5.4.8. Plate with Multiple Cracks

The geometry, material properties and loading is similar to the example discussed in the section 4.6.8. The reference volume multiplier calculation for first iteration is graphically represented in the Fig. 5.16. From the Fig. 5.17, it can be seen that, as $m^0/m_L > 1+\sqrt{2}$ for the single edge notch bend, $m^0(V_{Rp})$ calculated is upper bounded. using the corrected reference volume multiplier $m^0(V_{Rp})$, the $m_\alpha^T(V_{Rp})$ is calculated. The variation of $m^0(V_{Rp})$ and $m_\alpha^T(V_{Rp})$ with different iteration for single edge notch bend is presented in Tab. 5.8 and Fig. 5.17.

The presence of the peak stresses in the Plate with multiple cracks is causing the lower bound multiplier in the first iteration to be bit conservative, but with the EMAP iterations the results seen to be converging to nonlinear analysis solution. The time taken for the PRVM is 127 CPU units when compared to 175 CPU units for nonlinear analysis.

Table 5.8 Comparison of Various Multipliers for Plate with Multiple (EMAP)

Iteration	m^0	m_L	$m^0(V_{Rp})$	$m_\alpha^T(V_{Rp})$	m_{non}
1	2.359	0.197	2.001	0.712	
7	2.270	0.312	1.943	0.913	
14	2.167	0.484	1.874	1.101	1.362
21	2.059	0.645	1.791	1.204	
29	1.935	0.773	1.712	1.263	

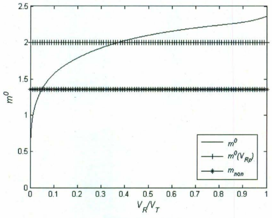

Figure 5.16 $m^0(V_{Rp})$ in first iteration for Plate with Multiple Cracks

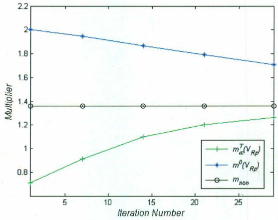

Figure 5.17 Variation of $m^0(V_{Rp})$ and $m_\alpha^T(V_{Rp})$ with iterations for Plate with Multiple Cracks (EMAP)

5.4.9 Plate with a Hole

The geometry, material properties and loading is similar to the example discussed in the section 4.6.9. The reference volume multiplier calculation for first iteration is graphically represented in the Fig. 5.18. From the Fig. 5.19, it can be seen that, as $m^0 / m_L > 1 + \sqrt{2}$ for the plate with a hole, $m^0(V_{Rp})$ calculated is upper bounded. using the corrected reference volume multiplier $m^0(V_{Rp})$, the $m_\alpha^T(V_{Rp})$ is calculated. The variation of $m^0(V_{Rp})$ and $m_\alpha^T(V_{Rp})$ with different iteration for plate with a hole is presented in Tab. 5.9 and Fig. 5.19.

The Plate with a hole is a good example for the notch problems, as this is a notch the result from the initial analysis is much closer to the non linear analysis results when compared to the crack problems. The time taken for the PRVM is 72 CPU units when compared to 191 CPU units for nonlinear analysis.

Table 5.9 Comparison of Various Multipliers of Plate with a Hole (EMAP)

Iteration	m^0	m_L	$m^0(V_{Rp})$	$m_\alpha^T(V_{Rp})$	m_{non}
1	1.221	0.481	1.054	0.781	
2	1.216	0.496	1.053	0.793	
4	1.206	0.526	1.051	0.812	0.922
6	1.197	0.556	1.042	0.834	
8	1.188	0.584	1.040	0.851	

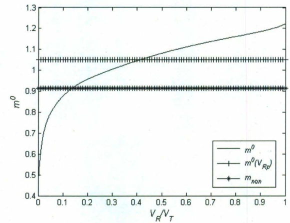

Figure 5.18 $m^0(V_{Rp})$ in first iteration for Plate with a Hole

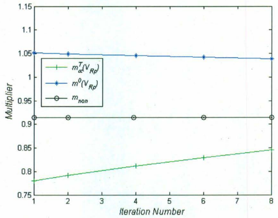

Figure 5.19 Variation of $m^0(V_{Rp})$ and $m_\alpha^T(V_{Rp})$ with iterations for Plate with a Hole (EMAP)

5.4.10 Indeterminate Beam

The geometry, material properties and loading is similar to the example discussed in the section 4.6.10. The reference volume multiplier calculation for first iteration is graphically represented in the Fig. 5.20. From the Fig. 5.21, it can be seen that, as $m^0 / m_L > 1+\sqrt{2}$ for indeterminate beam, $m^0(V_{Rp})$ calculated is upper bounded. using the corrected reference volume multiplier $m^0(V_{Rp})$, the $m_\alpha^T(V_{Rp})$ is calculated. The variation of $m^0(V_{Rp})$ and $m_\alpha^T(V_{Rp})$ with different iteration for Indeterminate beam is presented in Tab. 5.10 and Fig. 5.21.

The Indeterminate beam is a good example for the problems which has the dead volume due to the geometric properties, the result from the initial analysis is much closer to the non linear analysis results when compared to the crack problems. The results in all the examples are chosen at equal interval, for ease of comparison for both the ERVM and PRVM. Due to this reason at times the PRVM results look little conservative. The time taken for the PRVM is 535 CPU units when compared to 583 CPU units for nonlinear analysis.

Table 5.10 Comparison of Various Multipliers for Indeterminate Beam (EMAP)

Iteration	m^0	m_L	$m^0(V_{Rp})$	$m_\alpha^T(V_{Rp})$	m_{non}
1	2.649	0.613	1.913	1.231	
4	2.357	0.711	1.841	1.274	
8	2.124	0.837	1.792	1.343	1.543
12	1.988	0.951	1.744	1.401	
15	1.920	1.027	1.731	1.442	

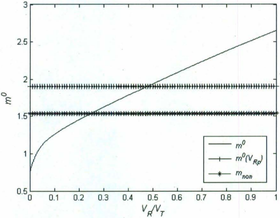

Figure 5.20 $m^0(V_{Rp})$ **in first iteration for Indeterminate Beam**

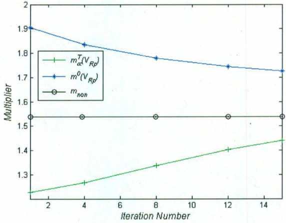

Figure 5.21 Variation of $m^0(V_{Rp})$ **and** $m_\alpha^T(V_{Rp})$ **with iterations of Indeterminate Beam (EMAP)**

5.4.11 Oblique Nozzle

The geometry, material properties and loading is similar to the example discussed in the section 4.6.11. Four different Nozzle angles are been studied (i.e., $\theta = 30^0$, 45^0, 60^0 and 90^0)

5.4.11.1 Nozzle Angle $\theta = 30^0$

The reference volume multiplier calculation for first iteration is graphically represented in the Fig. 5.22. From the Fig. 5.23, it can be seen that, as $m^0 / m_L > 1+\sqrt{2}$ for oblique nozzle 30^0, $m^0(V_{Rp})$ calculated is upper bounded. using the corrected reference volume multiplier $m^0(V_{Rp})$, the $m_\alpha^T(V_{Rp})$ is calculated. The variation of $m^0(V_{Rp})$ and $m_\alpha^T(V_{Rp})$ with different iteration for oblique nozzle 30^0 is presented in Tab. 5.11 and Fig. 5.23. The time taken for the PRVM is 3415 CPU units when compared to 25200 CPU units for nonlinear analysis.

Table 5.11 Comparison of Various Multipliers of Oblique Nozzle 30^0 (EMAP)

Iteration	m^0	m_L	$m^0(V_{Rp})$	$m_\alpha^T(V_{Rp})$	m_{non}
1	1.867	0.127	1.393	0.473	
2	1.811	0.141	1.362	0.504	
4	1.698	0.171	1.291	0.551	0.712
6	1.589	0.201	1.222	0.582	
9	1.432	0.244	1.123	0.614	

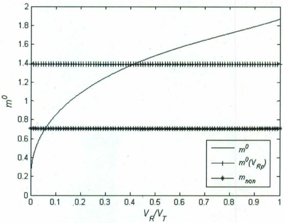

Figure 5.22 $m^0(V_{Rp})$ in first iteration for Oblique Nozzle 30^0

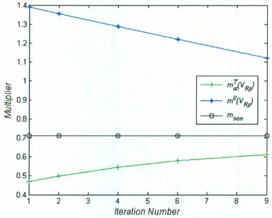

Figure 5.23 Variation of $m^0(V_{Rp})$ and $m_\alpha^T(V_{Rp})$ with iterations of Oblique Nozzle 30^0 (EMAP)

5.4.11.2 Nozzle Angle $\theta = 45^0$

The reference volume multiplier calculation for first iteration is graphically represented in the Fig. 5.24. From the Fig. 5.25, it can be seen that, as $m^0 / m_L > 1 + \sqrt{2}$ for oblique nozzle 45^0, $m^0(V_{Rp})$ calculated is upper bounded. using the corrected reference volume multiplier $m^0(V_{Rp})$, the $m_\alpha^T(V_{Rp})$ is calculated. The variation of $m^0(V_{Rp})$ and $m_\alpha^T(V_{Rp})$ with different iteration for oblique nozzle 45^0 is presented in Tab. 5.12 and Fig. 5.25. The time taken for the ERVM is 3212 CPU units when compared to 24300 CPU units for nonlinear analysis.

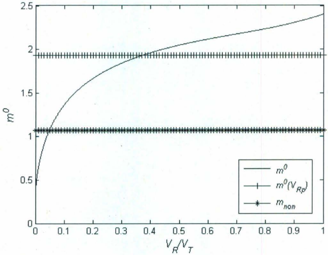

Figure 5.24 $m^0(V_{Rp})$ in first iteration for Oblique Nozzle 45^0

Table 5.12 Comparison of Various Multipliers for Oblique Nozzle 45^0 (EMAP)

Iteration	m^0	m_L	$m^0(V_{Rp})$	$m_\alpha^T(V_{Rp})$	m_{non}
1	2.401	0.242	1.931	0.794	
2	2.364	0.263	1.902	0.822	
4	2.288	0.304	1.843	0.881	1.072
6	2.210	0.343	1.784	0.923	
9	2.083	0.398	1.683	0.952	

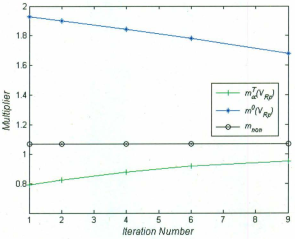

Figure 5.25 Variation of $m^0(V_{Rp})$ and $m_\alpha^T(V_{Rp})$ with iterations for Oblique Nozzle 45^0 (EMAP)

5.4.11.3 Nozzle Angle $\theta = 60^0$

The reference volume multiplier calculation for first iteration is graphically represented in the Fig. 5.26. From the Fig. 5.27, it can be seen that, as $m^0 / m_L > 1 + \sqrt{2}$ for oblique nozzle 60^0, $m^0(V_{Rp})$ calculated is upper bounded. using the corrected reference volume multiplier $m^0(V_{Rp})$, the $m_\alpha^T(V_{Rp})$ is calculated. The variation of $m^0(V_{Rp})$ and $m_\alpha^T(V_{Rp})$ with different iteration for oblique nozzle 60^0 is presented in Tab. 5.13 and Fig. 5.27. The time taken for the ERVM is 3007 CPU units when compared to 23600 CPU units for nonlinear analysis.

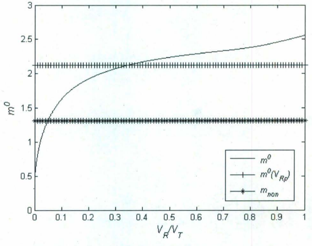

Figure 5.26 $m^0(V_{Rp})$ in first iteration for Oblique Nozzle 60^0

Table 5.13 Comparison of Various Multipliers for Oblique Nozzle 60^0 (EMAP)

Iteration	m^0	m_L	$m^0(V_{Rp})$	$m_\alpha^T(V_{Rp})$	m_{non}
1	2.558	0.351	2.122	1.014	
4	2.476	0.420	2.064	1.093	
8	2.361	0.503	1.971	1.154	1.314
12	2.237	0.552	1.873	1.163	
15	2.141	0.594	1.793	1.172	

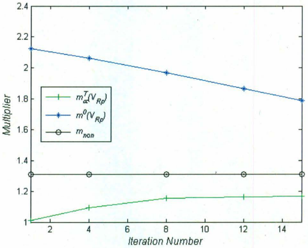

Figure 5.27 Variation of $m^0(V_{Rp})$ and $m_\alpha^T(V_{Rp})$ with iterations for Oblique Nozzle 60^0 (EMAP)

5.4.11.4 Nozzle Angle $\theta = 90^0$

The reference volume multiplier calculation for first iteration is graphically represented in the Fig. 5.28. From the Fig. 5.29, it can be seen that, as $m^0 / m_L > 1+\sqrt{2}$ for oblique nozzle 90^0, $m^0(V_{Rp})$ calculated is upper bounded. using the corrected reference volume multiplier $m^0(V_{Rp})$, the $m_\alpha^T(V_{Rp})$ is calculated. The variation of $m^0(V_{Rp})$ and $m_\alpha^T(V_{Rp})$ with different iteration for oblique nozzle 90^0 is presented in Tab. 5.14 and Fig. 5.29. The time taken for the PRVM is 2895 CPU units when compared to 22400 CPU units for nonlinear analysis.

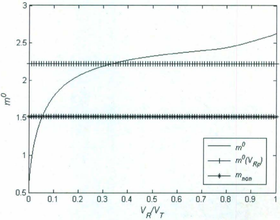

Figure 5.28 $m^0(V_{Rp})$ in first iteration for Oblique Nozzle 90^0

Table 5.14 Comparison of Various Multipliers for Oblique Nozzle 90^0

Iteration	m^0	m_L	$m^0(V_{Rp})$	$m_\alpha^T(V_{Rp})$	m_{non}
1	2.624	0.513	2.223	1.244	
6	2.515	0.588	2.141	1.291	
12	2.383	0.676	2.042	1.334	1.523
18	2.249	0.781	1.934	1.352	
23	2.140	0.881	1.843	1.391	

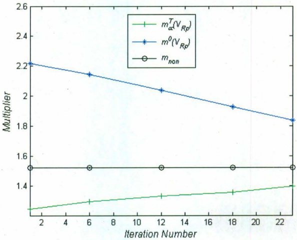

Figure 5.29 Variation of $m^0(V_{Rp})$ and $m_\alpha^T(V_{Rp})$ with iterations for Oblique Nozzle 90^0 (EMAP)

5.5 Discussion of Results

From initial elastic analysis for any general component m^0 / m_L can be calculated; depending on the m^0 / m_L the components are categorized into one of the categories as explained in section (5.2). The examples in this chapter are so chosen that there will be representation from each of these categories. For the components which fall under the first category (i.e., Section 5.6.1 to Section 5.6.5), the peak stress will not be present and the maximum stress present in the component is sufficient to correct the dead volume effect. $m^0(V_{Rp})$ will be the lower bound.

For the components which fall under the second category (i.e., Section 5.6.6 to Section 5.6.12), due to the presence of the peak stress the amount of the correction applied will not be sufficient. The $m_\alpha^T(V_{Rp})$ calculated using the $m^0(V_{Rp})$ and m_L will be lower bound. It can be concluded that if the plastic reference volume correction is employed, the m_α^T multiplier will always be a lower bounded value. The applicability of the proposed procedures is demonstrated through numerical examples (both 2D and 3D models). The estimated limit loads are in good agreement with the ones obtained from nonlinear finite element analysis (i.e,, <7 % error).

The time taken for the PRVM is also compared with the nonlinear analysis and it is shown that there is a considerable advantage. It is seen that this advantage increases with the complexity of the problem. When compared to ERVM there is a slight more advantage of time for PRVM.

The limit load estimates obtained by the plastic reference volume correction are conservative when compared to the ones obtained by elastic reference volume method. The reason for these conservative results is the presence of the peak stresses effect in the second category components. This problem is addressed by a new method in the following chapter.

Chapter-6
LOWER BOUNDEDNESS of m_α TANGENT METHOD

6.1 Introduction

Using the *reference volume methods* as discussed in the previous chapters, the reference volume effect of the components can be taken care-off. The results from the reference volume methods are bit conservative; the reason for these conservative results can be explained as the presence of the peak stresses in the components, which will lower the lower bound multiplier m_L. This kind of behavior can be seen mostly in the second category components (categorization is explained in section 5.2.1), which have some cracks or notches developed during the operation. In the current chapter a new method is presented which will take both the reference volume correction and peak stress correction into consideration and calculate a lower bounded limit load multiplier. The proposed method combines the newly developed reference volume correction with the m_α-tangent method to ensure the lower boundedness of m_α-tangent multiplier. In m_α-tangent method developed by Seshadri and Hossain [4] assumes that the secondary stresses will not get redistributed when the peak stresses are being blunted. This assumption is not always true particularly in cases of components undergoing highly localized plastic flow such as cracked and notched components and structures. Proposed method will address this issue by taking the reference volume of the component into account and calculating m_α-tangent multiplier for only kinematically active areas of the components. Using this method we can obtain the m_α-tangent multiplier which is always lower bounded.

6.2 Theoretical background

A Schematic m^0 vs. $\overline{V}_\eta$ plot for different EMAP iterations is presented in Fig .6.1. From the plot it can be seen that when $\overline{V}_\eta = 0$, value of the multiplier is equal to the lower bound multiplier m_L, and when $\overline{V}_\eta = 1$, the value of the multiplier is equal to the upper bound multiplier m^0. A typical m^0 vs. $\overline{V}_\eta$ curve generated from a linear elastic analysis is been represented as curve ABC in Fig 6.1. When this curve is compared with the actual limit load multiplier, which is represented as the straight line (i.e., m), can be divided into two sections. Section AB, which includes the peak stress effect. Section BC, which includes the dead volume effect. For the curve ABC to reach the straight line we need to correct both ends of the curve. This will be achieved by the following method.

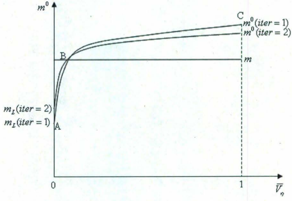

Fig. 6.1 Schematic of m^0 vs. $\overline{V}_\eta$ plot for different EMAP iterations

6.3 Method for Correcting Dead Volume and Peak Stress Effects Simultaneously

This method makes use of both Two-bar method and m_α-tangent method. On a constraint map (i.e., Fig. 6.2) the Two-bar method can be represented by the TBM curve and m_α-tangent method is represented by the $R_\alpha^T = 1$ curve.

6.3.1 Dead Volume Correction

The Point B' on TBM represents a combined primary, secondary and peak stresses and will be denoted as $R_{B'}^0$. The point B on $R_\alpha^T = 1$ curve represents a combined primary and secondary stress state and will be denoted as R_B^0.

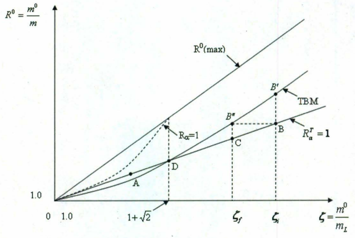

Fig. 6.2 Constraint Map [4]

From the linear elastic analysis the m^0 calculated will have contributions from the dead volume as well as the reference volume.

The dead volume contribution (DVC) in the m^0 can be calculated using the following equation

$$DVC = \frac{\left(R_{B'}^0 - R_B^0\right)}{R_{B'}^0} \tag{6.1}$$

Therefore, the reference volume contribution (RVC) in m^0 can be calculated using the following equation

$$RVC = 1 - DVC$$

$$RVC = 1 - \frac{\left(R_{B'}^0 - R_B^0\right)}{R_{B'}^0} = \left(\frac{R_B^0}{R_{B'}^0}\right) \tag{6.2}$$

Using the reference volume contribution from Eq. 6.2, m^0 due to the reference volume contribution is calculated as follows

$$m^0_{B,ref} = m^0 (RVC)$$

$$m^0_{B,ref} = m^0 \left(\frac{R^0_B}{R^0_{B'}} \right) \tag{6.3}$$

The $m^0_{B,ref}$ calculated using Eq. 6.3 will be free from the dead volume effect.

6.3.2 Peak Stress Correction

As the point B on $R^T_\alpha = 1$ curve represents a combined primary and secondary stress state, its corresponding point on the TBM curve (i.e., Point B'') will give us the ζ_f which will be independent of peak stresses. ζ_f will be evaluated by solving the following equation:

$$\frac{m^0}{m} = 1 + 0.2929(\zeta_i - 1) = \frac{\zeta_f^2 + 1}{2\zeta_f} \tag{6.4}$$

The roots of Eq. (6.4) are

$$\zeta_f = (1 + C_e) \pm \sqrt{(1 + C_e)^2 - 1} \tag{6.5}$$

where $C_e = 0.2929(\zeta_i - 1)$.

The ζ_f calculated using the Eq. 6.5, will be free from the peak stress effect for that particular iteration. Once the $m^0_{B,ref}$ and ζ_f are established, the new lower bounded limit load multiplier can be calculated using the following equation

$$m^T_\alpha = \frac{m^0_{B,ref}}{1 + 0.2929(\zeta_f - 1)} \tag{6.6}$$

The m^T_α calculated using the Eq. 6.6 will be free from both dead volume and peak stress effects for that particular stress distribution. This procedure need to be continued with the help of EMAP until we reach the point 'D' on the constraint plot. At this point the m^T_α calculated will be completely independent of dead volume and peak stress effects of the component. According to Reinhardt [20] within the m_α triangle any point that lies below the $R_\alpha = 1$ curve represents a lower bounded multiplier. In the current method as we always travel along the $R_\alpha^T = 1$ and reach the m_α triangle below the $R_\alpha = 1$ curve we can theoretically say that the multiplier obtained by this method is always lower bounded.

6.4 General Procedure

In this section a general procedure is being outlined in a step by step manner to find out lower bounded m_α-tangent multiplier by applying the reference volume and peak stress corrections.

- For any given component, initially a linear elastic analysis is performed.
- The m^0 and m_L values are calculated using Eq. (3.10) and Eq. (3.11) respectively.
- The value of m^0 / m_L computed.
- If $m^0 / m_L < 1+\sqrt{2}$, the value of limit load multiplier can be calculated using the regular m_α^T formula.
- If $m^0 / m_L > 1+\sqrt{2}$ then the following steps are continued.
- Using Eq. (6.3) the m^0 value is corrected for reference volume effect.
- Using Eq. (6.5) the ζ value is corrected for peak stress effect.
- Once $m_{B,ref}^0$ and ζ_f are achieved, the lower bounded m_α^T is computed using Eq. (6.6).
- These steps are repeated using the EMAP iterations until the converged or near converged solution are obtained. The results of fifty EMAP iterations and convergence criteria are provided in appendix C.

For non-linear analysis elastic perfectly plastic material model is assumed, the results from this analysis is taken as the actual multiplier. These results are used for the comparison with the linear elastic results obtained through above mentioned method. In the following section, different components whose $m^0 / m_L > 1+\sqrt{2}$ are analyzed using the above method and the results are compared with the results from non linear analysis.

6.5 Numerical Examples

6.5.1 Compact Tension (CT) Specimen

The geometry, material properties and loading is similar to the example discussed in the section 4.6.6. Variations of different multipliers with different iteration for CT Specimen are presented in Tab. 6.1 and Fig. 6.3.

Table 6.1 Comparison of Various Multipliers for CT Specimen (EMAP)

Iteration	m^0	m_L	$m^0_{B,ref}$	ζ_f	m^T_α	m_{non}
1	1.549	0.108	1.061	9.692	0.444	
5	1.395	0.162	1.035	6.294	0.553	
10	1.273	0.248	1.064	4.182	0.663	0.812
15	1.189	0.346	1.093	3.101	0.742	
21	1.115	0.462	1.122	2.423	0.791	

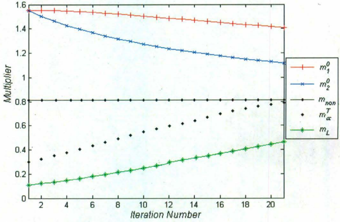

Figure 6.3 Variation of multipliers with iterations for CT Specimen

6.5.2 Single Edge Notch Bend

The geometry, material properties and loading is similar to the example discussed in the section 4.6.7. Variations of different multipliers with different iteration for Single Edge Notch Bend are presented in Tab. 6.2 and Fig. 6.4.

Table 6.2 Comparison of Various Multipliers for Single Edge Notch Bend (EMAP)

Iteration	m^0	m_L	$m^0_{B,ref}$	ζ_f	m^T_α	m_{non}
1	4.759	0.202	3.071	15.181	0.601	
5	3.632	0.287	2.524	8.724	0.773	
10	2.709	0.417	2.133	5.023	0.982	1.353
15	2.159	0.564	1.932	3.361	1.144	
20	1.843	0.712	1.801	2.422	1.273	

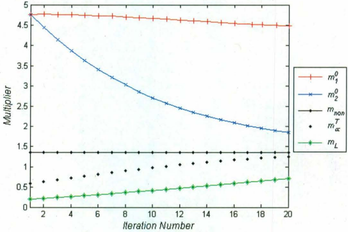

Figure 6.4 Variation of multipliers with iterations for Single Edge Notch Bend

6.5.3. Plate with Multiple Cracks

The geometry, material properties and loading is similar to the example discussed in the section 4.6.8. Variations of different multipliers with different iteration for Plate with Multiple Cracks are presented in Tab. 6.3 and Fig. 6.5.

Table 6.3 Comparison of Various Multipliers for Plate with Multiple Cracks (EMAP)

Iteration	m^0	m_L	$m^0_{B,ref}$	ζ_f	m^T_α	m_{non}
1	2.359	0.197	1.654	8.292	0.533	
7	2.270	0.312	1.744	5.494	0.754	
14	2.167	0.484	1.862	3.773	1.024	1.362
21	2.059	0.645	1.933	2.951	1.232	
29	1.935	0.773	1.922	2.422	1.353	

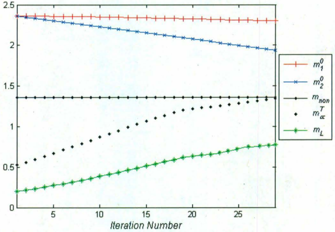

Figure 6.5 Variation of multipliers with iterations for Plate with Multiple Cracks

6.5.4 Plate with a Hole

The geometry, material properties and loading is similar to the example discussed in the section 4.6.10. Variations of different multipliers with different iteration for Plate with a Hole are presented in Tab. 6.5 and Fig. 6.7.

Table 6.4 Comparison of Various Multipliers for Plate with a Hole (EMAP)

Iteration	m^0	m_L	$m^0_{B,ref}$	ζ_f	m^T_α	m_{non}
1	1.221	0.481	1.214	2.503	0.844	
2	1.216	0.496	1.213	2.441	0.852	
4	1.206	0.526	1.205	2.291	0.881	0.922
6	1.197	0.556	1.196	2.154	0.904	
8	1.188	0.584	1.186	2.032	0.913	

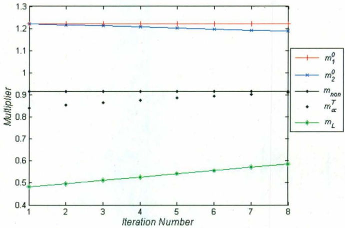

Figure 6.6 Variation of multipliers with iterations for Plate with a Hole

6.5.5 Indeterminate Beam

The geometry, material properties and loading is similar to the example discussed in the section 4.6.11. Variations of different multipliers with different iteration for indeterminate beam are presented in Tab. 6.6 and Fig. 6.8.

Table 6.5 Comparison of Various Multipliers for Indeterminate Beam (EMAP)

Iteration	m^0	m_L	$m^0_{B,ref}$	ζ_f	m^T_α	m_{non}
1	2.649	0.613	2.304	3.673	1.294	
4	2.357	0.711	2.193	3.034	1.371	
8	2.124	0.837	2.104	2.502	1.464	1.543
12	1.988	0.951	1.986	2.092	1.512	
15	1.920	1.027	1.919	1.811	1.533	

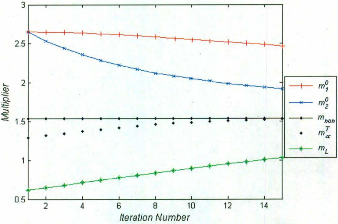

Figure 6.7 Variation of multipliers with iterations for Indeterminate Beam

6.5.6 Oblique Nozzle

The geometry, material properties and loading is similar to the example discussed in the section 4.6.12.

6.5.6.1 Nozzle Angle $\theta = 30^0$

Variations of different multipliers with different iteration for Oblique Nozzle 30^0 are presented in Tab. 6.7 and Fig. 6.9.

Table 6.6 Comparison of Various Multipliers for Oblique Nozzle 30^0 (EMAP)

Iteration	m^0	m_L	$m^0_{B,ref}$	ζ_f	m^T_α	m_{non}
1	1.867	0.127	1.271	9.964	0.354	
6	1.589	0.201	1.204	5.871	0.493	
12	1.288	0.283	1.103	3.813	0.604	0.712
18	1.053	0.352	1.002	2.812	0.661	
24	0.900	0.407	0.886	2.214	0.674	

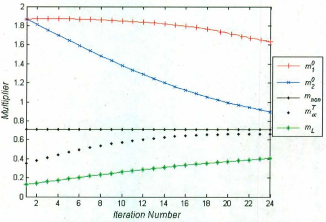

Figure 6.8 Variation of multipliers with iterations for Oblique Nozzle 30^0

6.5.6.2 Nozzle Angle $\theta = 45^0$

Variations of different multipliers with different iteration for Oblique Nozzle 45^0 are presented in Tab. 6.8 and Fig. 6.10.

Table 6.7 Comparison of Various Multipliers for Oblique Nozzle 45^0 (EMAP)

Iteration	m^0	m_L	$m^0_{B,ref}$	ζ_f	m^T_α	m_{non}
1	2.400	0.242	1.732	7.084	0.622	
6	2.209	0.343	1.744	4.992	0.804	
12	1.951	0.429	1.673	3.824	0.911	1.072
18	1.687	0.501	1.564	3.063	0.974	
25	1.429	0.605	1.425	2.363	1.024	

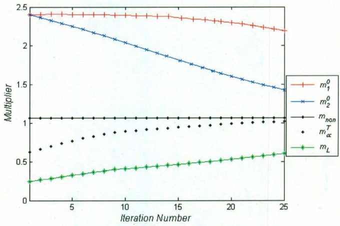

Figure 6.9 Variation of multipliers with iterations for Oblique Nozzle 45^0

6.5.6.3 Nozzle Angle $\theta = 60^0$

Variations of different multipliers with different iteration for Oblique Nozzle 60^0 are presented in Tab. 6.9 and Fig. 6.11.

Table 6.8 Comparison of Various Multipliers for Oblique Nozzle 60^0 (EMAP)

Iteration	m^0	m_L	$m^0_{B,ref}$	ζ_f	m^T_α	m_{non}
1	2.558	0.351	1.963	5.502	0.843	
6	2.420	0.464	2.004	4.241	1.032	
12	2.237	0.552	1.968	4.052	1.144	1.314
18	2.044	0.641	1.918	3.194	1.222	
25	1.829	0.764	1.825	2.391	1.301	

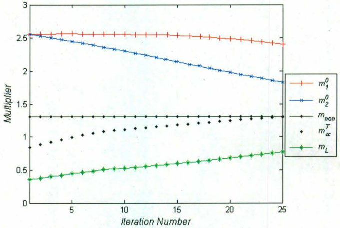

Figure 6.10 Variation of multipliers with iterations for Oblique Nozzle 60^0

6.5.6.4 Nozzle Angle $\theta = 90^0$

Variations of different multipliers with different iteration for Oblique Nozzle 90^0 are presented in Tab. 6.10 and Fig. 6.12.

Table 6.9 Comparison of Various Multipliers for Oblique Nozzle 90^0 (EMAP)

Iteration	m^0	m_L	$m^0_{B,ref}$	ζ_f	m^T_α	m_{non}
1	2.624	0.513	2.184	4.172	1.133	
6	2.515	0.588	2.194	3.651	1.231	
12	2.383	0.676	2.183	3.161	1.332	1.523
18	2.249	0.781	2.149	2.743	1.432	
24	2.119	0.902	2.117	2.354	1.513	

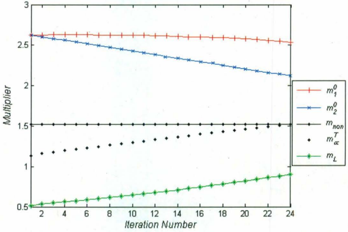

Figure 6.11 Variation of multipliers with iterations for Oblique Nozzle 90^0

6.6 Discussion of the Results

The objective of the proposed method is to obtain the lower bounded m_α-tangent limit load multiplier by simultaneously correcting the peak stress effect and the reference volume effect. This method is particularly helpful in the components in which peak stresses are present, like the components that develop notches and cracks during their operation.

Different cracked components (Section 6.5.1 to Section 6.5.3), notched components (Section 6.5.4) and complex components (Section 6.5.5 and 6.5.6) are examined in the chapter and the results are presented in tables and plots. The examples covered both 2D and 3D models, which demonstrate the robustness of the method.

From the results it can be seen that m_α^T calculated using the dead volume corrected upper bound multiplier ($m_{B,ref}^0$) and peak stress corrected m^0 / m_L ratio (ζ_f) will always be a lower bound multiplier. This gives support to the theoretical assumption of always lower boundedness of m_α^T multiplier due to the incorporation of both corrections. Using the EMAP this lower bound multiplier will converge very well onto the non-linear limit load multiplier (< 2% error). The other benefit of this method is that the formulas are so simple that they can be readily added onto the APDL macro and we can obtain the lower bounded limit load multiplier directly from the FE commercial code.

Chapter-7
REFERENCE VOLUME FOR ORTHOTROPIC MATERIAL

7.1 Introduction

In the modern world, components made of anisotropic material, for which the material properties show appreciable differences in different directions. The anisotropic material used in the current proposed research is specified as orthotropic, which means it has three orthogonal planes of material property symmetry. The material is assumed to be homogeneous. The knowledge of the limit load is useful in the design and sizing of components and structures made from these materials. Finding out the limit loads of components made of orthotropic material, involves predicting kinematically active volume (reference volumes) at the plastic collapse. The proposed method uses the reference volume approach for anisotropic material and m_α tangent method together to obtain the lower bound limit loads for components made of anisotropic materials.

7.2 Constitutive Relationships of Orthotropic Material

The constitutive relations ships of orthotropic materials are been discussed by Pan and Seshadri [8]. The deformation of an isotropic material can be characterized by two parameters, the stiffness modulus, E, and the Poisson's ratio, ν. In most cases, the change in the effective stiffness, E, dominates over the change in ν in going from the purely elastic to the elastic-plastic structure. Therefore, a good estimate of the collapse load can usually be obtained by adjusting E and choosing a constant ν. The starting value of E is chosen as the elastic value.

In an orthotropic structure, on the other hand, the deformation is controlled by nine parameters. Which of these dominates the collapse depends on both mechanical properties and loading [48]. If one parameter is used to characterize plastic flow (i.e., an equivalent stress defined in terms of the stress components), only one parameter is adjusted during the softening procedure, and the others must be chosen such that they can become compatible with the plastic limit state. At collapse, it is expected that the stress and strain states in the significant regions of the structure are determined by the plastic flow rule. During moduli modification, all material parameters change in fixed proportion to each other, and a realistic stress distribution at collapse should be obtained if the initial elastic parameters are chosen in such a proportion to each other as the plastic flow rule suggests. The objective is to allow, as much as possible, for the stress fields to follow the orthotropic yield surface. Hill's yield criterion for characterizing an orthotropic material is given by [13];

$$f(s_{ij}) = F(\sigma_y - \sigma_z)^2 + G(\sigma_z - \sigma_x)^2 + H(\sigma_x - \sigma_y)^2 + 2L\tau_{yz}^2 + 2M\tau_{xz}^2 + 2N\tau_{xy}^2 = 1 \quad (7.1)$$

where F, G, H, L, M, N are parameters characteristic of the current state of orthotropic. If X, Y, Z are the tensile yield stresses in the principal directions of orthotropy, the following relationships are valid [49]:

$$\begin{aligned} \frac{1}{X^2} &= G + H \,,\ 2F = \frac{1}{Y^2} + \frac{1}{Z^2} - \frac{1}{X^2} \\ \frac{1}{Y^2} &= H + F \,,\ 2G = \frac{1}{Z^2} + \frac{1}{X^2} - \frac{1}{Y^2} \\ \frac{1}{Z^2} &= F + G \,,\ 2H = \frac{1}{X^2} + \frac{1}{Y^2} - \frac{1}{Z^2} \end{aligned} \quad (7.2)$$

If R, S, T are the yield stresses in shear with respect to the principal axes of orthotropy, then:

$$2L = \frac{1}{R^2}, 2M = \frac{1}{S^2}, 2N = \frac{1}{T^2} \quad (7.3)$$

The elastic moduli are modified on the directional basis as follows:

$$\left(E_{sij}\right)_n = \left[\frac{\sigma_{arb}}{\bar{\sigma}_{s(n-1)}}\right]^q \left(E_{sij}\right)_{n-1} \quad (7.4)$$

In the above equation, the subscript s refers to the element number, while i, j can be any combination of x, y and z. n refers to the iteration number. In order to ensure that plastic flow type deformations are favored, the initial elastic moduli and Poisson's ratio are determined by comparing elastic and plastic strains. The elastic stress strain relations are given by [50]:

$$\varepsilon_x = \frac{\sigma_x}{E_x} - \frac{\nu_{xy}}{E_y}\sigma_y - \frac{\nu_{xz}}{E_z}\sigma_z$$

$$\varepsilon_y = \frac{-\nu_{xy}}{E_x}\sigma_x + \frac{\sigma_y}{E_y} - \frac{\nu_{xz}}{E_z}\sigma_z \tag{7.5}$$

$$\varepsilon_z = \frac{-\nu_{xz}}{E_x}\sigma_x - \frac{\nu_{yz}}{E_y}\sigma_y + \frac{\sigma_z}{E_z}$$

$$\tau_{xy} = \frac{\gamma_{xy}}{G_{xy}}, \tau_{yz} = \frac{\gamma_{yz}}{G_{yz}}, \tau_{xz} = \frac{\gamma_{xz}}{G_{xz}} \tag{7.6}$$

The plastic component of the flow rule can be expressed as:

$$d\varepsilon_x = d\lambda\ [H(\sigma_x - \sigma_y) + G(\sigma_x - \sigma_z)]$$

$$d\varepsilon_y = d\lambda\ [H(\sigma_y - \sigma_z) + G(\sigma_y - \sigma_x)] \tag{7.7}$$

$$d\varepsilon_z = d\lambda\ [H(\sigma_z - \sigma_x) + G(\sigma_z - \sigma_y)]$$

$$d\gamma_{xy} = 2d\,\lambda\, N\,\tau_{xy}$$

$$d\gamma_{yz} = 2d\,\lambda\, N\,\tau_{yz} \tag{7.8}$$

$$d\gamma_{xz} = 2d\,\lambda\, N\,\tau_{xz}$$

By relating Eq. 7.5 and Eq. 7.6 with Eq. 7.7 and Eq.7.8 the expressions for the elastic properties can be obtained as [51 & 52]:

$$E_x = C\sigma_{ox}^2, E_y = C\sigma_{oy}^2, E_z = C\sigma_{oz}^2 \tag{7.9}$$

$$G_{xy} = C\tau_{oxy}^2, G_{yz} = C\tau_{oyz}^2, G_{zx} = C\tau_{ozx}^2$$

$$\nu_{yx} = \frac{\sigma_{oy}^2}{2}\left[\frac{1}{\sigma_{ox}^2} + \frac{1}{\sigma_{oy}^2} - \frac{1}{\sigma_{oz}^2}\right] \tag{7.10}$$

$$\nu_{zy} = \frac{\sigma_{oz}^2}{2}\left[\frac{1}{\sigma_{oz}^2} + \frac{1}{\sigma_{oy}^2} - \frac{1}{\sigma_{ox}^2}\right] \tag{7.10}$$

$$\nu_{zx} = \frac{\sigma_{ox}^2}{2}\left[\frac{1}{\sigma_{ox}^2} + \frac{1}{\sigma_{oz}^2} - \frac{1}{\sigma_{oy}^2}\right]$$

where, the variable $C = 3/(2\mu\bar{\sigma}_o^2)$, and has a dimension of Pa^{-1}. Since the value of C would not affect the stress distribution of the component, it can take values such as 1 Pa^{-1}. The elastic properties given in Eq. (7.9) and Eq. (7.10) are used as the initial elastic properties for the repeated elastic analysis, and are modified using Eq. (7.4) for each iteration. The Poisson's ratio values in Eq. (7.10) are kept unchanged during the iterations. To ensure the positive definiteness of the elastic matrix, the denominator 2 in the Poisson ratios expressions is replaced by 3.33 in the current investigation it is similar adjustment as used by Pan and Seshadri [8]

7.3 Multipliers for Orthotropic Material

According to the Li pan and Seshadri [8], the upper bound multiplier for an Orthotropic material can be calculated using the following equation.

$$m^0 = \sigma_{0x}\left[\frac{\sum_{k=1}^{N}(\Delta V_k / E_{Sxk})}{\sum_{k=1}^{N}(\bar{\sigma}_k^2 \Delta V_k / E_{Sxk})}\right]^{1/2} \tag{7.11}$$

where N is the total number of finite elements of the structure; $\bar{\sigma}_k$, ΔV_k, E_{Sxk} are the effective stress, element volume and secant modulus in x direction of element k, respectively. σ_{0x} is the yield stress in the reference direction x. The reference direction is chosen in the direction where the yield strength is minimum. The lower bound multiplier can be given by the following expression:

$$m_L = \frac{\sigma_{ox}}{\bar{\sigma}_{\max}^0} \tag{7.12}$$

where $\bar{\sigma}^0_{\max}$ is the maximum effective stress in the finite element model. Indermohan *et. al* [53] used the m_β multiplier Method to finding out the limit load multipliers which is bit complicated due to the β calculation [54].

7.4 General Procedure

The following is the procedure for finding out the reference volume and lower bound limit loads of a general component with orthotropic material properties.

- Modify initial elastic properties derived from Eq. (7.9) and Eq. (7.10) are used as material input.
- The first linear elastic finite element analysis is carried out for the model with the prescribed loading and boundary conditions.
- The elements in the component are sorted in the descending order of the equivalent stress values (directly available from FEA run).
- The m^0 value will be calculated using Eq. (7.11) for the component in steps of each sub-volume and m_L is calculated using Eq. (7.12).
- Then these values of m^0 are plotted against $\bar{V}_\eta$.
- Either the Elastic Reference Volume Method (ERVM) (i.e., Chapter 4) or the Plastic Reference Volume Method (PRVM) (i.e., Chapter 5) can be employed for the dead volume correction.
- The above steps are continued using the EMAP iterations until the converged or near converged solution are obtained.

In the following section different components are examined to demonstrate the method's robustness and validity. In this chapter both ERVM and PRVM are employed for the dead volume correction.

7.5 Application to General Components

7.5.1 Orthotropic Thick Cylinder

A cylinder under internal pressure (Fig.7.1) is analyzed using plane strain considerations. The inner radius of the cylinder is 30 mm, and the outer radius is 40 mm. An internal pressure of 250 MPa is applied. The cylinder is made of Zircalloy. The alloy is assumed to be perfectly-plastic and possesses orthotropic symmetry. A general three dimensional orthotropic material has nine independent elastic constants and six plastic constants. For two-dimensional problems, the number of independent elastic and plastic constants required is seven and four, respectively.

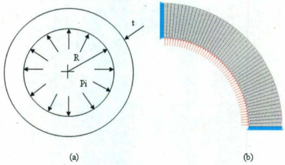

Figure 7.1 Orthotrpic thick walled cylinder (a) Geometry and dimensions (b) Typical finite element mesh with loading

In the present investigation, the following material properties are specified:

1. Original elastic properties are (for nonlinear finite element analysis)

   $E_x = 95.79$ GPa; $E_y = 100.59$ GPa; $E_z = 100.99$ GPa;

   $G_{xy} = 36.15$ GPa; $\nu_{xy} = 0.361$; $\nu_{zy} = 0.345$; $\nu_{zx} = 0.341$;

2. Yield stresses in the respective directions are given by

   $\sigma_{0x} = 472.3$ MPa; $\sigma_{0y} = 579.2$ MPa; $\sigma_{0z} = 630.9$ MPa;

$\tau_{0xy} = 366.6$ MPa; $\tau_{0yz} = 262.9$ MPa; $\tau_{0xz} = 262.9$ MPa;

3. Modified initial elastic properties based on Eq. (7.9) and Eq. (7.10) are as follows:

$E_x = 223.07$ GPa; $E_y = 335.47$ GPa; $E_z = 398.03$ GPa;

$G_{xy} = 134.39$ GPa; $G_{yz} = 69.12$ GPa; $G_{xz} = 69.12$ GPa;

$\nu_{xy} = 0.498$; $\nu_{zy} = 0.121$; $\nu_{zx} = 0.479$.

7.5.1.1 Elastic Reference Volume Method (ERVM)

From the initial elastic analysis the upper bound multiplier m^0 is 0.779 and m_L is 0.557. The m^0 / m_L ratio 1.3986 is less than $1+\sqrt{2}$ limit, the $m_\alpha^T(V_{\text{Re}})$ calculated using ERVM is 0.70 which is lower bounded. Variation of $m^0(V_{\text{Re}})$ and $m_\alpha^T(V_{\text{Re}})$ with different iteration for anisotropic thick cylinder are presented in Tab. 7.1 and Fig. 7.2. m^0 and $m^0(V_{\text{Re}})$ columns of the Tab. 7.1. are equal which shows that this component is independent of dead volume effect.

Table 7.1 Comparison of Various Multipliers of anisotropic thick cylinder for Elastic Reference Volume Correction (EMAP)

Iteration	m^0	m_L	$m^0(V_{\text{Re}})$	$m_\alpha^T(V_{\text{Re}})$	m_{non}
1	0.779	0.557	0.779	0.704	
6	0.772	0.613	0.772	0.713	
12	0.769	0.655	0.769	0.731	0.744
18	0.767	0.681	0.767	0.741	
22	0.766	0.691	0.766	0.742	

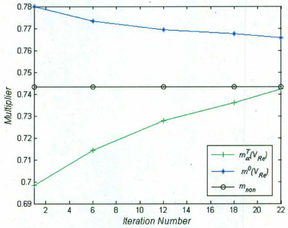

Figure 7.2 Variation of $m^0(V_{\mathrm{Re}})$ and $m_\alpha^T(V_{\mathrm{Re}})$ with iterations for anisotropic thick cylinder

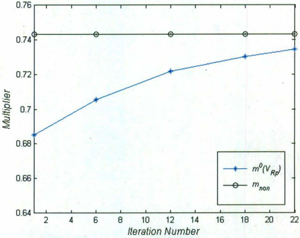

Figure 7.3 Variation of $m^0(V_{Rp})$ with iterations for anisotropic thick cylinder

7.5.1.2 Plastic Reference Volume Method (PRVM)

From the initial elastic analysis the upper bound multiplier m^0 is 0.779 and m_L is 0.557. The m^0/m_L ratio 1.3986 is less than $1+\sqrt{2}$ limit, the plastically reference volume corrected multiplier $m^0(V_{Rp})$ calculated using PRVM is 0.69 which is lower bounded. Variation of $m^0(V_{Rp})$ with different iteration for anisotropic thick cylinder are presented are presented in Tab. 7.2 and Fig.7.3.

Table 7.2 Comparison of Various Multipliers of anisotropic thick cylinder for Plastic Reference Volume Correction (EMAP)

Iteration	m^0	m_L	$m^0(V_{Rp})$	m_{non}
1	0.779	0.557	0.694	
6	0.772	0.603	0.713	
12	0.769	0.644	0.724	0.744
18	0.767	0.670	0.731	
22	0.766	0.691	0.738	

7.5.2 Transversely Isotropic Bridgman Notch Bar

A Bridgman notch subjected to remote tensile load is modeled and analyzed axi symmetrically (Fig. 7.4). The notch bar has a maximum diameter of 26.416 mm, minimum diameter of 21.082 mm and notch radius of 6.858 mm. the remote tensile load is 500 MPa. The Notch bar is made of Zircalloy. The alloy is assumed to be perfectly-plastic and transversely isotropic, which means the material is isotropic in the *y-z* plane. Due to symmetry in geometry and loading, only a quarter slice of notch is modeled using Plane82 elements with axi-symmetric consideration.

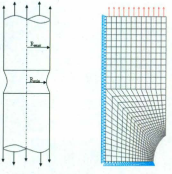

(a) (b)

Figure 7.4 A Transversely Isotropic Bridgman Notch bar (a) Geometry and dimensions (b) Typical finite element mesh with loading

2. Yield stresses in the respective directions are given by

$\sigma_{0x} = 472.3$ MPa ; $\sigma_{0y} = 579.2$ MPa ; $\sigma_{0z} = 579.2$ MPa ;

$\tau_{0xy} = 262.9$ MPa ; $\tau_{0yz} = 262.9$ MPa ; $\tau_{0xz} = 366.6$ MPa ;

3. Modified initial elastic properties based on Eq. (7.9) and Eq. (7.10) are as follows:

$E_x = 223.06$ GPa; $E_y = 335.47$ GPa; $E_z = 335.47$ GPa;

$G_{xy} = 69.12$ GPa; $G_{yz} = 69.12$ GPa; $G_{xz} = 134.39$ GPa;

$\nu_{xy} = 0.451$; $\nu_{yz} = 0.149$; $\nu_{xz} = 0.451$.

7.5.2.1 Elastic Reference Volume Method (ERVM)

From the initial elastic analysis the upper bound multiplier m^0 is 1.111 and m_L is 0.477. The m^0 / m_L ratio 2.3291 is less than $1+\sqrt{2}$ limit, the $m_\alpha^T(V_{\mathrm{Re}})$ calculated using ERVM is 0.80 which is lower bounded. Variation of $m^0(V_{\mathrm{Re}})$ and $m_\alpha^T(V_{\mathrm{Re}})$ with different iteration for anisotropic thick cylinder are presented in Tab. 7.3 and Fig. 7.5. m^0 and $m^0(V_{\mathrm{Re}})$ columns of the Tab. 7.3. are equal which shows that this component is independent of dead volume effect.

Table 7.3 Comparison of Various Multipliers of Transversely Isotropic Bridgman notch bar for Elastic Reference Volume Correction (EMAP)

Iteration	m^0	m_L	$m^0(V_{\mathrm{Re}})$	$m_\alpha^T(V_{\mathrm{Re}})$	m_{non}
1	1.111	0.477	1.111	0.803	
8	1.096	0.611	1.096	0.889	
16	1.084	0.724	1.084	0.952	1.004
24	1.074	0.801	1.074	0.984	
32	1.065	0.851	1.065	0.989	

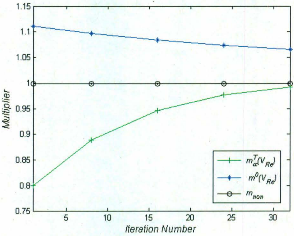

Figure 7.5 Variation of $m^0(V_{\mathrm{Re}})$ and $m_\alpha^T(V_{\mathrm{Re}})$ with iterations for Transversely Isotropic Bridgman notch bar

7.5.2.2 Plastic Reference Volume Method (PRVM)

From the initial elastic analysis the upper bound multiplier m^0 is 1.111 and m_L is 0.477.The m^0/m_L ratio 2.3291 is less than $1+\sqrt{2}$ limit, the $m^0(V_{Rp})$ calculated using

PRVM is 0.75 which is lower bounded. The comparisons of various multipliers for Plastic reference volume correction for first iterations are presented in Tab 7.4. Variation of $m^0(V_{Rp})$ with different iteration for Transversely Isotropic Bridgman notch bar are presented are presented in Tab.7.4 and Fig.7.6.

Table 7.4 Comparison of Various Multipliers of Transversely Isotropic Bridgman notch bar for Plastic Reference Volume Correction (EMAP)

Iteration	m^0	m_L	$m^0(V_{Rp})$	m_{non}
1	1.111	0.477	0.984	
8	1.096	0.611	0.993	
16	1.084	0.724	0.994	1.004
24	1.074	0.801	1.001	
32	1.065	0.851	1.002	

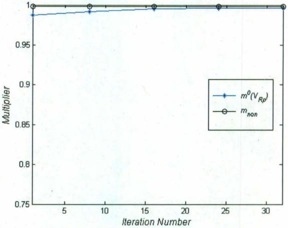

Figure 7.6 Variation of $m^0(V_{Rp})$ with iterations for Transversely Isotropic Bridgman notch bar

7.5.3 Transversely Isotropic Plate with a Hole

A Plate With a hole (Fig.7.7) with the following dimensions are considered: Plate width $2W = 150\,\text{mm}$; length $2L = 300\,\text{mm}$; hole radius $r = 23\,\text{mm}$. It is subjected to a tensile load of $P = 100\,\text{MPa}$. The Notch bar is made of Zircalloy. The alloy is assumed to be perfectly-plastic and transversely isotropic, which means the material is isotropic in the x-y plane. Due to symmetry in geometry and loading, only a quarter of the plate is modeled using Plane82 elements with plane stress consideration.

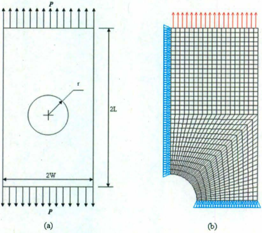

Figure 7.7 Transversely Isotropic Plate with a Hole (a) Geometry and dimensions (b) Typical finite element mesh with loading.

In the present investigation, the following material properties are specified:

1. Original elastic properties are (for nonlinear finite element analysis)

$E_x = 95.79$ GPa; $E_y = 95.79$ GPa; $E_z = 100.99$ GPa;

$G_{xy} = 36.15$ GPa; $\nu_{xz} = \nu_{yz} = 0.361$; $\nu_{xy} = 0.341$;

2. Yield stresses in the respective directions are given by

$\sigma_{0x} = 472.3$ MPa; $\sigma_{0y} = 472.3$ MPa; $\sigma_{0z} = 579.2$ MPa;

$\tau_{0xy} = 262.9$ MPa; $\tau_{0yz} = 262.9$ MPa; $\tau_{0xz} = 366.6$ MPa;

3. Modified initial elastic properties based on Eq. (7.9) and Eq. (7.10) are as follows:

$E_x = 223.06$ GPa; $E_y = 223.06$ GPa; $E_z = 335.47$ GPa;

$G_{xy} = 69.12$ GPa; $G_{yz} = 69.12$ GPa; $G_{xz} = 134.39$ GPa;

$\nu_{xy} = 0.149$; $\nu_{yz} = 0.451$; $\nu_{xz} = 0.451$.

7.5.3.1 Elastic Reference Volume Method (ERVM)

From the initial elastic analysis the upper bound multiplier m^0 is 5.317 and m_L is 1.985. The m^0/m_L ratio 2.6786 is greater than $1+\sqrt{2}$ limit, the $m_\alpha^T(V_{\text{Re}})$ calculated using ERVM is 3.62 which is lower bounded. Variation of $m^0(V_{\text{Re}})$ and $m_\alpha^T(V_{\text{Re}})$ with different iteration for Transversely Isotropic Plate with a Hole are presented in Tab. 7.5 and Fig. 7.8. m^0 and $m^0(V_{\text{Re}})$ columns of the Tab. 7.3. are not equal which shows that this component is having some dead volume effect, but the correction applied is small as the m^0/m_L is close to $1+\sqrt{2}$ limit.

Table 7.5 Comparison of Various Multipliers of Transversely Isotropic Plate with a Hole for Elastic Reference Volume Correction (EMAP)

Iteration	m^0	m_L	$m^0(V_{\text{Re}})$	$m_\alpha^T(V_{\text{Re}})$	m_{non}
1	5.317	1.985	5.314	3.622	
2	5.291	2.053	5.288	3.664	
4	5.243	2.189	5.240	3.723	3.994
6	5.198	2.323	5.195	3.824	
10	5.114	2.579	5.112	3.969	

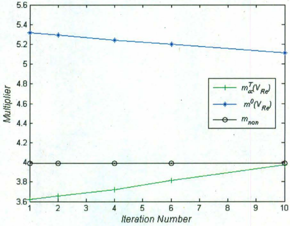

Figure 7.8 Variation of $m^0(V_{\text{Re}})$ and $m_\alpha^T(V_{\text{Re}})$ with iterations for Transversely Isotropic Plate with a Hole

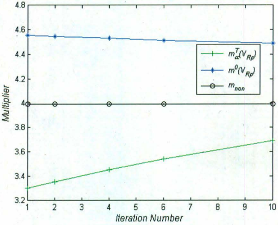

Figure 7.9 Variation of $m^0(V_{Rp})$ and $m_\alpha^T(V_{Rp})$ with iterations for Transversely Isotropic Plate with a Hole

7.5.2.2 Plastic Reference Volume Method (PRVM)

From the initial elastic analysis the upper bound multiplier m^0 is 5.317 and m_L is 1.985.As, the m^0 / m_L ratio 2.6786 is greater than $1+\sqrt{2}$ limit, the $m_\alpha^T(V_{Rp})$ calculated using PRVM is 3.30 which is lower bounded. Variation of $m^0(V_{Rp})$ and $m_\alpha^T(V_{Rp})$ with different iteration for Transversely Isotropic Plate with a Hole are presented in Tab. 7.6 and Fig. 7.9.

Table 7.6 Comparison of Various Multipliers of Transversely Isotropic Plate with a Hole for Plastic Reference Volume Correction (EMAP)

Iteration	m^0	m_L	$m^0(V_{Rp})$	$m_\alpha^T(V_{Rp})$	m_{non}
1	5.317	1.985	4.551	3.304	
2	5.291	2.053	4.544	3.352	
4	5.243	2.189	4.532	3.453	3.994
6	5.198	2.323	4.514	3.544	
10	5.114	2.579	4.493	3.694	

7.6 Discussion of the Results

The objective of the proposed method is to ensure the lower boundedness of the m_α tangent multiplier for components made of orthotropic materials by combining the newly developed reference volume concept with m_α tangent method. The secant modulus in the reference direction in the elastic analysis is used to estimate the plastic flow parameter for the orthotropic components. Modified initial elastic properties are adopted to ensure the elastic stress field follows the anisotropic yield surface.

From initial elastic analysis for any component we can calculate the value of m^o / m_L. Depending on the m^0 / m_L the components are classified into two categories as explained previously. In this chapter the examples are so chosen that there will be representation from both the categories. For these examples, both the elastic reference volume correction as well as the plastic reference volume correction has been applied.

For the components which fall under the first category (Section 7.5.1 and Section 7.5.2), the upper bound multiplier with plastic reference volume correction $m^0(V_{Rp})$ gives the lower bound value, and for the components which fall under the second category (Section 7.5.3), m_α tangent multiplier with plastic reference volume correction $m_\alpha^T(V_{Rp})$ gives the lower bound value. The method is demonstrated using the examples and results are found to be in good agreement with the non-linear finite element solution. When the elastic reference volume is applied m_α tangent multiplier with elastic reference volume correction $m_\alpha^T(V_{\mathrm{Re}})$ gives the lower bound value in both the categories.

From the comparison of the results, it can be concluded that the lower bound multiplier obtained by plastic reference volume correction is a bit conservative, when compared to the one obtained using elastic reference volume correction method, as the presence of peak stress in the second category components are delaying the convergence of plastic reference volume method.

Chapter-8

INCORPORATION OF STRAIN HARDENING EFFECT INTO LIMIT ANALYSIS

8.1 Introduction

In an actual component or structure when the stresses exceed the yield strength of the material, the component starts to experience strain hardening. Due to strain hardening the component or structure can withstand more loads [10]. In the traditional way of limit load calculations, the material models are assumed to be elastic perfectly plastic (EPP) [30]-[36]. However, this will lead to a very conservative estimate of limit load for a material that has a significant stain hardening. Therefore, by considering the effect of strain hardening while estimating the limit load more realistic limit load can be obtained. This novel method addresses the effect of material strain hardening on limit load estimation. The commonly used material models including Bilinear Hardening (BH) and Ramberg-Osgood (RO) models are investigated. Bilinear hardening material model, which the elastic modulus and tangent modulus, is the simplest representation of the strain hardened material properties. Ramberg-Osgood material model is more complicated and closer to the actual material properties of a component [55]. In the stress-strain curve once the yield strength point is exceeded then plasticity occurs. In the initial portion of the plastic region, the rise in the curve is due to the presence of the strain hardening in the material. The hidden strength due to strain hardening can be utilized if yield strength of an equivalent elastic perfectly plastic material model is obtained by integrating this portion of the curve. By integrating the equation for the material models, the expressions for equivalent yield strength is obtained. In these expressions all the other variables are known material properties, so these equations are readily solved to obtain the values of the yield strength of equivalent elastic perfectly plastic model. The estimated equivalent yield strength value is used instead of the regular yield strength, and limit analysis is carried out.

8.2 Theoretical background

Generally one of the basic assumption in calculating the limit load values of any general component is, that the material behavior is elastic perfectly plastic (EPP). However, if the material behavior is elastic-plastic hardening then the approach needs to be modified. Assuming a hardening material model:

$$\varepsilon = f(\sigma_0, \sigma) \tag{8.1}$$

where σ_0 is a reference value of stress that is usually taken as the yield strength, and σ is the applied stress [56].

By equating the strain energy densities shown in Fig. 8.1, the strain hardening curve can be represented by an equivalent elastic-perfectly plastic curve in which σ_y^* is the assumed yield strength, i.e., area A_1 should be equal to area A_2. Therefore, σ_y^* can be determined by following equation:

$$\int_{\sigma_0}^{\sigma_y^*} \varepsilon\, d\sigma - \varepsilon_0\left(\sigma_y^* - \sigma_0\right) - \frac{1}{2}\left(\sigma_y^* - \sigma_0\right)\left(\varepsilon_1 - \varepsilon_0\right) = \varepsilon_f\left(\sigma_f - \sigma_y^*\right) - \int_{\sigma_y^*}^{\sigma_f} \varepsilon\, d\sigma \tag{8.2}$$

where $\left(\sigma_y^*, \varepsilon_y^*\right)$ is equivalent yield strength point and (σ, ε) is an arbitrary point on a strain hardening curve, and σ_f related stress to the fracture strain, ε_f. ε_1 can be calculated using the linear relation $\varepsilon_1 = \sigma_y^* / E_0$.

Different material models such as the BH material and RO relationship have been studied here in. These material models can represent true stress strain material curves with in the small strain regions [57-59]. Therefore, the portion of the curve which is used for finding out the equivalent yield stress of equivalent elastic perfectly plastic material model is limited to these regions only, by choosing the cut-off strain, ε_f to be at 0.05. In this way this equivalent yield stress is different from the flow stress normally used in the industry, as flow stress is the average of yield to ulitmate strength of the material.

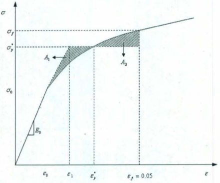

Figure 8.1 Illustrative determination of σ_y^*

8.2.1 Bilinear Hardening Material Model

The stress strain relation ship of a bilinear hardening material model is given by:

$$\varepsilon = \frac{\sigma_0}{E_0} + \frac{(\sigma - \sigma_0)}{E_t} \tag{8.3}$$

A Bilinear material model is presented in Fig. 8.2.

For a bilinear material model the Eq. (8.2) can be rewritten as:

$$LHS = \int_{\sigma_0}^{\sigma_y^*} \left(\frac{\sigma_0}{E_0} + \frac{(\sigma - \sigma_0)}{E_t} \right) d\sigma - \varepsilon_0 (\sigma_y^* - \sigma_0) - \frac{1}{2}(\sigma_y^* - \sigma_0)(\varepsilon_1 - \varepsilon_0)$$

$$RHS = \left(\frac{\sigma_0}{E_0} + \frac{(\sigma_f - \sigma_0)}{E_t} \right)(\sigma_f - \sigma_y^*) - \int_{\sigma_y^*}^{\sigma_f} \left(\frac{\sigma_0}{E_0} + \frac{(\sigma - \sigma_0)}{E_t} \right) d\sigma$$

$LHS = RHS$

$$\sigma_y^* = (1 - \beta)\sigma_0 + \beta \sigma_f \pm \sqrt{\beta(\beta - 1)}(\sigma_f - \sigma_0) \tag{8.4}$$

Using Eq. (8.4) the equivalent yield strength for bilinear hardening material can be obtained.

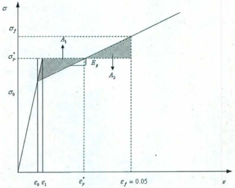

Figure 8.2 Bilinear Hardening Material Model

8.2.2 Ramberg-Osgood Hardening Material Model

The Ramberg-Osgood material model can be written as

$$\varepsilon = \frac{\sigma}{E_0} + \frac{\alpha \sigma_0}{E_0}\left(\frac{\sigma}{\sigma_0}\right)^n \tag{8.5}$$

where α is dimensionless material constant, usually chosen to be equal to 3/7, and n is the strain hardening exponent.

Simplifying Eq. (8.2) using Eq.(8.5), we get an expression that leads to the equivalent yield strength, σ_y^*

$$A\sigma_y^{*2} - B\sigma_y^* + C = 0 \tag{8.6}$$

where A, B and C are expressed in terms of material properties

$$A = 1$$

$$B = 2\left(\sigma_f + \frac{\alpha \sigma_f^n}{\sigma_0^{n-1}}\right)$$

$$C = \frac{2\alpha\, n \sigma_f^{n+1}}{(n+1)(\sigma_0^{n-1})} + \sigma_f^2$$

Usually, the value of fracture strain, ε_f, is available as a material parameter. Therefore, in order to calculate σ_f the following equation need to be solved [56].

$$\sigma_f^n + \frac{\sigma_0^{n-1}}{\alpha}\sigma_f - \frac{E_0\,\sigma_0^{n-1}\,\varepsilon_f}{\alpha} = 0 \tag{8.7}$$

Once σ_f is known Using Eq. (8.6) equivalent yield strength of the Ramberg-Osgood Material model can be calculated.

8.3 General Procedure

In this section a general procedure is being outlined in a step by step manner to find out the lower bound multipliers for components undergoing hardening material model using the proposed method.

- Initially equivalent yield strength is calculated for the given hardened material. For bilinear hardened material Eq (8.4) is used and if it's a Ramberg-Osgood one then Eq (8.6) is used.
- The first linear elastic finite element analysis is carried out for the model with the prescribed loading and boundary conditions.
- The elements in the component are sorted in the descending order of the equivalent stress values.
- The m^0 value will be calculated using Eq. (5.1) for the component in steps of each sub-volume as being discussed in Sec. (5.2) and m_L is calculated using Eq. (3.11).
- Then these values of m^0 are plotted against $\overline{V}_\eta$ and $m^o(V_{Rp})$ will be calculated using the Eq. (5.7).

- Depending on the value of m^0 / m_L the components are grouped as discussed in the section 5.2.1.
- For the components whose $m^0 / m_L < 1+\sqrt{2}$, the value of $m^0(V_{Rp})$ is taken as the final value of the multiplier.
- For the components whose $m^0 / m_L > 1+\sqrt{2}$, the value of $m_\alpha^T(V_{Rp})$ should be calculated as explained in Sec. (5.3)
- The above steps are continued using the EMAP iterations until the converged or near converged solution are obtained. The results of fifty EMAP iterations and convergence criteria are provided in appendix C

In the following section, the method is applied to several component configurations, and the results are compared with the limit load using nonlinear analysis. The elastic-perfectly plastic material is employed to estimate the limit loads using nonlinear finite element analysis. In the plastic limit state the body fully or partially undergoes unrestricted plastic deformation under constant external load. Therefore, the limit load using numerical approach is estimated when the magnitude of strains goes very high and the convergence cannot be achieved any more by further increase in the load. In the following section couples of components are examined to verify the method's robustness and validity.

8.4 Application to General Components

8.4.1 Thick Cylinder

A cylinder under internal pressure (Fig.4.11) with geometric dimensions as described in Section (4.6.1) is examined here. Two different kinds of strain hardening material properties are considered for examination.

- Bilinear Hardening Material Model:

  $E_0 = 200\,\text{GPa}$; $\sigma_0 = 300$ MPa; $E_T = 0.02 \times E_0$; $\varepsilon_f = 0.05$;

  The equivalent yield strength calculated using Eq. (8.4) is $\sigma_y^* = 397.50$ MPa;

- Ramberg-Osgood Material Model:

  $E_0 = 200$ GPa; $\sigma_0 = 300$ MPa; $\alpha = 1.34$; $n = 8.60$;

The stress at the cut-off strain calculated using Eq. (8.7) is $\sigma_f = 433.69$ MPa;

Various coefficients of Eq. (8.6) is calculated and given below:

$A = 1$; $B = 1999.19$; $C = 7.62E6$;

The equivalent yield strength calculated using Eq. (8.6) is $\sigma_y^* = 388.62$ MPa;

The comparisons of various multipliers with different material hardening models for first iterations are presented in Table 8.1. As $m^0 / m_L < 1+\sqrt{2}$ this component fall under first category, so $m^0(V_{Rp})$ is lower bounded. Variation of $m^0(V_{Rp})$ with different iteration for bilinear hardening material model is presented in Table 8.2. Variation of $m^0(V_{Rp})$ with different iteration for Ramberg-Osgood hardening material model is presented in Table 8.3. The variation plots are given in Fig. 8.3 and Fig. 8.4.

Table 8.1 Comparison of various multipliers for different material hardening models (LEFEA)

Problem	m^0	m_L	m^0 / m_L	$m^0(V_{Rp})$	m_{non}
With out Stain hardening	2.294	1.683	1.36	1.992	2.264
Bilinear	3.039	2.212	1.37	2.653	2.981
Ramberg-Osgood	2.972	2.163	1.37	2.592	2.913

Table 8.2 Comparison of various multipliers of thick walled cylinder for bilinear material hardening model (EMAP)

Iteration	m^0	m_L	$m^0(V_{Rp})$	m_{non}
1	3.039	2.212	2.653	
5	3.009	2.439	2.754	
10	2.994	2.641	2.833	2.981
15	2.989	2.772	2.893	
20	2.987	2.856	2.934	

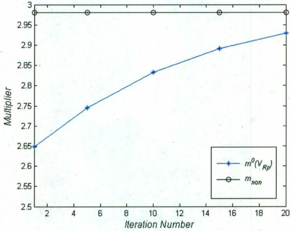

Figure 8.3 Variation of $m^0(V_{Rp})$ with iterations for bilinear hardening thick cylinder

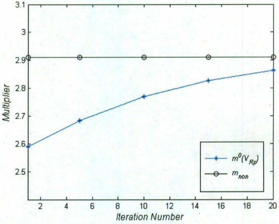

Figure 8.4 Variation of $m^0(V_{Rp})$ and $m_\alpha^T(V_{Rp})$ with iterations for Ramberg-Osgood hardening thick cylinder

Table 8.3 Comparison of various multipliers of thick walled cylinder for Ramberg-Osgood material hardening model (EMAP)

Iteration	m^0	m_L	$m^0(V_{Rp})$	m_{non}
1	2.972	2.163	2.592	
5	2.942	2.384	2.682	
10	2.927	2.582	2.774	2.91
15	2.922	2.710	2.832	
20	2.921	2.792	2.861	

8.4.2 Compact Tension (CT) Specimen

A CT Specimen (Fig.4.26) with geometric dimensions as described in Section (4.6.6) is examined here [60]. Two different kinds of strain hardening material properties are considered for examination.

- Bilinear Hardening Material Model:

  $E_0 = 211\,\text{GPa}; \sigma_0 = 250\,\text{MPa};\ E_T = 0.015 \times E_0;\ \varepsilon_f = 0.05;$

  The equivalent yield strength calculated using Eq. (8.4) is $\sigma_y^* = 327.54$ MPa;

- Ramberg-Osgood Material Model:

  $E_0 = 211$ GPa; $\sigma_0 = 250$ MPa; $\alpha = 1.69$; $n = 8.60$;

  The stress at the cut-off strain calculated using Eq. (8.7) is $\sigma_f = 361.97$ MPa;

  Various coefficients of Eq. (8.6) is calculated and given below:

  $A = 1$; $B = 21101.72$; $C = 6.74E6$;

  The equivalent yield strength calculated using Eq. (8.6) is $\sigma_y^* = 324.33$ MPa;

The comparisons of various multipliers with different material hardening models for first iterations are presented in Table 8.4. As $m^0 / m_L > 1 + \sqrt{2}$ this component fall under second category, so $m_\alpha^T(V_{Rp})$ is calculated.

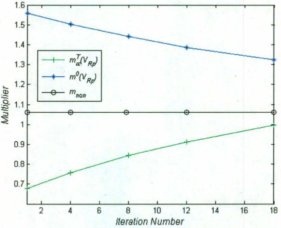

Figure 8.5 Variation of $m^0(V_{Rp})$ and $m_\alpha^T(V_{Rp})$ with iterations for bilinear hardening CT Specimen

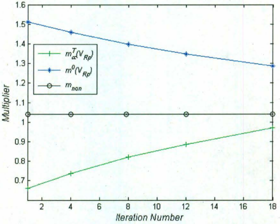

Figure 8.6 Variation of $m^0(V_{Rp})$ and $m_\alpha^T(V_{Rp})$ with iterations for Ramberg-Osgood hardening CT Specimen

Variation of $m^0(V_{Rp})$ and $m_\alpha^T(V_{Rp})$ with different iteration for bilinear hardening material model is presented in Table 8.5. Variation of $m^0(V_{Rp})$ and $m_\alpha^T(V_{Rp})$ with different iteration for Ramberg-Osgood hardening material model is presented in Table 8.6. The variation plots are given in Fig. 8.5 and Fig. 8.6.

Table 8.4 Comparison of various multipliers of CT Specimen for different material hardening models (LEFEA)

Problem	m^0	m_L	m^0/m_L	$m_\alpha^T(V_R)$	m_{non}
With out Stain hardening	1.590	0.167	9.52	0.468	0.809
Bilinear	2.084	0.218	9.53	0.684	1.059
Ramberg-Osgood	2.023	0.212	9.54	0.662	1.044

Table 8.5 Comparison of various multipliers of CT Specimen for bilinear material hardening model (EMAP)

Iteration	m^0	m_L	$m^0(V_{Rp})$	$m_\alpha^T(V_{Rp})$	m_{non}
1	2.084	0.218	1.56	0.684	
4	1.918	0.277	1.50	0.763	
8	1.761	0.369	1.44	0.844	1.059
12	1.644	0.470	1.39	0.912	
18	1.514	0.626	1.32	1.004	

Table 8.6 Comparison of various multipliers of CT Specimen for Ramberg-Osgood material hardening model (EMAP)

Iteration	m^0	m_L	$m^0(V_{Rp})$	$m_\alpha^T(V_{Rp})$	m_{non}
1	2.023	0.212	1.51	0.662	
4	1.863	0.269	1.46	0.742	
8	1.710	0.358	1.40	0.823	1.044
12	1.597	0.456	1.35	0.884	
18	1.471	0.608	1.28	0.973	

8.4.3 Indeterminate Beam

An Indeterminate Beam (Fig.4.41) with geometric dimensions as described in Section (4.6.11) is examined here. Two different kinds of strain hardening material properties are considered for examination.

- Bilinear Hardening Material Model:

  $E_0 = 206.85$ GPa; $\sigma_0 = 206.85$ MPa; $E_T = 0.01 \times E_0$; $\varepsilon_f = 0.05$;

  The equivalent yield strength calculated using Eq. (8.4) is $\sigma_y^* = 257.66$ MPa;

- Ramberg-Osgood Material Model:

  $E_0 = 206.85$ GPa; $\sigma_0 = 206.85$ MPa; $\alpha = 2$; $n = 8.47$;

  The stress at the failure calculated using Eq. (8.7) is $\sigma_f = 301.43$ MPa;

  Various coefficients of Eq. (8.6) are calculated and given below:

  $A = 1$; $B = 20685.59$; $C = 5.50E6$;

  The equivalent yield strength calculated using Eq. (8.6) is $\sigma_y^* = 269.65$ MPa;

The comparisons of various multipliers with different material hardening models for first iterations are presented in Table 8.7. As $m^0 / m_L > 1 + \sqrt{2}$ this component fall under second category, so $m_\alpha^T(V_{Rp})$ is calculated. Variation of $m^0(V_{Rp})$ and $m_\alpha^T(V_{Rp})$ with different iteration for bilinear hardening material model is presented in Table 8.8.

Table 8.7 Comparison of various multipliers of Indeterminate Beam for different material hardening models (LEFEA)

Problem	m^0	m_L	m^0 / m_L	$m_\alpha^T(V_{Rp})$	m_{non}
With out Strain hardening	2.649	0.613	4.32	1.231	1.543
Bilinear	3.300	0.763	4.33	1.529	1.924
Ramberg-Osgood	3.453	0.799	4.32	1.603	2.013

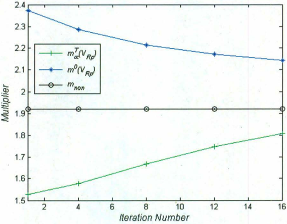

Figure 8.7 Variation of $m^0(V_{Rp})$ and $m_{\alpha}^{T}(V_{Rp})$ with iterations for bilinear hardening indeterminate beam.

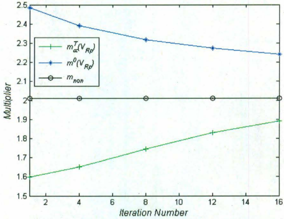

Figure 8.8 Variation of $m^0(V_{Rp})$ and $m_{\alpha}^{T}(V_{Rp})$ with iterations for Ramberg-Osgood hardening indeterminate beam.

Variation of $m^0(V_{Rp})$ and $m_\alpha^T(V_{Rp})$ with different iteration for Ramberg-Osgood hardening material model is presented in Table 8.9.The variation plots are given in Fig.8.7 and Fig. 8.8.

Table 8.8 Comparison of various multipliers of Indeterminate Beam for bilinear material hardening model (EMAP)

Iteration	m^0	m_L	$m^0(V_{Rp})$	$m_\alpha^T(V_{Rp})$	m_{non}
1	3.300	0.763	2.37	1.529	
4	2.935	0.885	2.29	1.584	
8	2.645	1.042	2.22	1.673	1.924
12	2.476	1.185	2.17	1.754	
16	2.369	1.309	2.14	1.809	

Table 8.9 Comparison of various multipliers of Indeterminate Beam for Ramberg-Osgood material hardening model (EMAP)

Iteration	m^0	m_L	$m^0(V_{Rp})$	$m_\alpha^T(V_{Rp})$	m_{non}
1	3.453	0.799	2.48	1.603	
4	3.072	0.926	2.39	1.649	
8	2.768	1.091	2.32	1.744	2.013
12	2.591	1.240	2.27	1.828	
16	2.480	1.370	2.24	1.894	

8.5 Discussion of Results

A simple approach is discussed in this chapter to determine equivalent yield strength of a material model with strain hardening. Two different strain hardening material models, namely the Bilinear Hardening and Ramberg-Osgood models, are specifically investigated. The estimated yield strength along with limit load multipliers (using the reference volume approach) are used to estimate a more appropriate limit load of a component with strain hardening material.

Once the components material properties are know, by using the Eq. (8.4) and Eq. (8.6) its equivalent yield strengths for bilinear material model and Ramberg Osgood material model are calculated respectively. This yield strength is used to perform the elastic finite element analysis. In this research both the material models are studied and the user can choose which ever model they are more comfortable with.

From Initial elastic analysis of any component m^0 / m_L is calculated. Depending on the m^0 / m_L the components are classified into two categories as explained previously. For the components which fall under the first category, $m^0(V_{Rp})$ gives the lower bound value, and for the components which fall under the second category, $m_\alpha^T(V_{Rp})$ gives the lower bound value. The results obtained are lower bounded in all the cases.

The applicability of the proposed procedure is demonstrated through numerical examples (section 8.4.1 to section 8.4.2). The estimated limit loads are in good agreement with the ones obtained using nonlinear finite element analysis.

CHAPTER 9
CONCLUSIONS, CONTRIBUTIONS AND FUTURE RESEARCH

9.1 Conclusions

The newly developed reference volume approaches are found to be very useful in determining the lower bound limit loads of mechanical components and structures. These methods are easy to implement in practice. When compared to the non linear analysis they demand little skill sets, so it can be readily used by any engineer. The other advantage of this method is it takes less computational time as demonstrated by the examples. In this research it is observed that the time advantage increases with the complexity of the problem. When compared to the regular EMAP method, the methods praposed in this thesis are found converging faster.

The *Elastic Reference Volume Method* derived its roots from the pressure bulb concepts of soil mechanics. In this method reference volume effect is corrected based upon the maximum stress developed in the component. The Elastic Reference Volume method is simple and straight forward. After obtaining the stress distribution from the initial elastic analysis, the m^0 vs. $\overline{V}_\eta$ curve is plotted. All the elements having stress less than five percentage of peak stress are considered as dead volume. Using this m^0 vs. $\overline{V}_\eta$ curve we can easily identify the components which need dead volume correction. From the research it's found that all the components whose $m^0/m_L \leq 1+\sqrt{2}$ needs either no or less correction. For those components whose $m^0/m_L > 1+\sqrt{2}$ the corrected $m^0(V_{\mathrm{Re}})$ and m_L are used to calculate $m_\alpha^T(V_{\mathrm{Re}})$, which is found to be lower bounded limit load multiplier for all the examples considered in this research.

The *Plastic Reference Volume Method* for finding out the reference volume of any general component involves integration of the upper bound multiplier vs. sub-volume ratio curve. From initial elastic analysis for any general component m^0/m_L can be calculated, depending on the m^0/m_L the component will fall into one of the categories as explained in section (5.2). For the components which fall under first category, $m^0(V_{Rp})$

will be the lower bound multiplier and for the components which fall under second category, $m_{\alpha}^{T}(V_{Rp})$ will be the lower bound multiplier. From the results it can be concluded that if plastic reference volume correction is employed m_{α}^{T} multiplier will always be a lower bounded value. The elastic reference volume method is found to be effective for both category of components, where as the plastic reference volume is more effective in first category components and conservative when compared to elastic reference volume method in second category components.

The reason for these conservative results can be explained as the presence of the peak stresses in the components, which will lower the lower bound multiplier m_L. This kind of behavior can be seen mostly in the second category components (categorization is explained in section 5.2.1), which have some cracks or notches developed during the operation. A new method is developed which will take both the reference volume correction and peak stress correction into consideration and calculate a lower bounded limit load multiplier. The proposed method combines the newly developed reference volume concept with the m_{α} tangent method to ensure the lower boundedness of m_{α} tangent multiplier.

Taking the practicality of the material usage into consideration a methods is developed to find out limit loads of orthotropic materials. As the usage of orthrotropic materials in industries is increasing day by day, so is the need for finding out limit loads for components made of such material is vary important. . Finding out the limit loads of components made of orthotropic material, involves predicting kinematically active volume (reference volumes) at the plastic collapse. The method uses the reference volume approach for orthrotropic material and m_{α} tangent method together to obtain the lower bound limit loads for components made of anisotropic materials. The secant modulus in the reference direction in the elastic analysis is used to estimate the plastic flow parameter for the anisotropic components. Modified initial elastic properties are adopted to ensure the elastic stress field follows the anisotropic yield surface. From Initial elastic analysis for any component we can calculate the value of m^{0}/m_{L}. Depending on the m^0 / m_L the components are classified into two categories as explained previously. For the components which fall under first category, $m^0(V_{Rp})$ gives the lower bound value and for the components which fall under second category, $m_\alpha^T(V_{Rp})$ gives the lower bound value.

In an actual component or structure when the stresses exceed the yield strength of the material, the component starts to experience strain hardening. Due to strain hardening the component or structure can withstand more loads. In the traditional way of limit load calculations, the material models are assumed to be elastic perfectly plastic (EPP). However, this will lead to a very conservative estimate of limit load for a material that has a significant stain hardening. Therefore, by considering the effect of strain hardening while estimating the limit load more realistic limit load can be obtained. The hidden strength due to strain hardening can be utilized if yield strength of an equivalent elastic perfectly plastic material model is obtained by integrating this portion of the curve. By integrating the equation for the material models, the expressions for equivalent yield strength is obtained. In these expressions all the other variables are known material properties, so these equations are readily solved to obtain the values of the yield strength of equivalent elastic perfectly plastic model. The estimated equivalent yield strength value is used instead of the regular yield strength, and limit analysis is carried out. Two different strain hardening material models namely the Bilinear hardening and Ramberg-Osgood models are in particular investigated. The estimated yield strength along with limit load multipliers (using the reference volume approach) are used to estimate more appropriate limit load of a component with strain hardening material. From Initial elastic analysis for any component we can calculate the value of m^0 / m_L. Depending on the m^0 / m_L the components are classified into two categories as explained previously. For the components which fall under first category, $m^0(V_{Rp})$ gives the lower bound value and for the components which fall under second category, $m_\alpha^T(V_{Rp})$ gives the lower bound value. The results obtained are lower bounded in all the cases. ANSYS [50] software is used for doing all the analysis in this thesis.

9.2 Original Contributions

The following are the original contributions from the current research work:

- The two-bar method is generalized, and the previous assumption of taking equal areas of two bars is proved as an accurate assumption.
- The Elastic reference volume method has been developed, which by correcting the reference volume effect elastically gives the lower bound limit load multiplier.
- The Plastic reference volume method has been developed, which by correcting the reference volume effect plastically and gives the lower bound limit load multiplier. The multipliers obtained from this method are bit conservative when compared to elastic reference volume method.
- A new method which corrects both the dead volume effect and the peak stress effect and always maintain a lower bounded m_α method has been developed.
- The Elastic and Plastic reference volume methods are extended to the anisotropic materials.
- Using the Integration of true stress strain plots, the strain hardening effect is incorporated into the limit analysis.

9.3 Future Research

Using the results from Elastic Reference Volume method, a simplified method can be developed in future. This method can be developed by generating the relationship between the reference volumes of different components and there corresponding multipliers. These relations ships can be shown in the graphical forms and there after, by using a single linear elastic iteration, the reference volume of the multiplier can be predicted. Using the so obtained reference volume the lower bounded limit load multipliers can be estimated.

All the reference volume methods developed in this thesis can be extended to different fields like ship structure design, complex pressure vessel design and complex mechanical components in future.

Currently all the methods proposed are developed and tested using the fixed 'q' EMAP, which is one of the reasons for the slow convergence. In future these methods can be extended and studied using the variable 'q' EMAP. While using the variable 'q' EMAP we may need to address the issue of sudden change in the multipliers in the second iteration and fluctuation in the lower bound multiplier with iterations.

The new method proposed with the simultaneous correction of dead volume and peak stress effects is using the EMAP iterations, which can further be developed for a single elastic analysis. The multipliers obtained from this method are giving closer approximates of limit load multipliers, so these can be further used in fitness for service (FFS) and Integrity assessment of in-service components.

The reference volume method developed for the anisotropic material in this thesis limited itself to the study of the orthotropic materials. In future it can be further extended to the study of completely anisotropic materials.

The inclusion of the strain hardening into the limit analysis proposed in the current research used the actual stress strain plots as it's their basis of development. In future, this method can also be developed for engineering stress strain plots which is more generally used material stress-strain plot. The cutoff-strain limit can be further studied and a direct relationship can be developed between cutoff-strain and the equivalent yield stress.

Publications and Presentations during the Ph.D Program

1. P. S. Reddy, Gudimetla., R. Adibi-Asl and R. Seshadri., 2010, "Incorporation of Strain Hardening Effect into Limit Load Analysis", J. Pressure Vessel Technology, Accepted.
2. P. S. Reddy, Gudimetla., R. Seshadri and Munaswami Katna., July 2010, "Limit Load Estimate Using Reference Volume Approach", Proceedings of the ASME PVP Conference, Bellevue, Washington, USA.
3. P. S. Reddy, Gudimetla., R. Adibi-Asl and R. Seshadri., July 2010, "Incorporation of Strain Hardening Effect into Limit Load Analysis", Proceedings of the ASME PVP Conference, Bellevue, Washington, USA.
4. P. S. Reddy, Gudimetla., March 2010, "Reference Volume for Anisotropic Material Components", presented at Aldrich Conference, St. John's, Canada.
5. P. S. Reddy, Gudimetla., March 2009, "Recent Developments in Limit Load Analysis", presented at Aldrich Conference, St. John's, Canada.

REFERENCES

1. ASME Boiler and Pressure Vessel Code, 2001, American Society of Mechanical Engineers, New York.
2. Mahmood, S. L., Haddara, M. R. and Seshadri, R, 2010, "Limit Loads of Ship Components using the Elastic Modulus Adjustment Procedure (EMAP)", Int. J. Ocean Engineering, Vol. 37, pp. 1452-1463.
3. Seshadri, R. and Mangalaramanan, S. P., 1997, "Lower Bound Limit Loads Using Variational Concepts: The m_α -method", Int. J. Pressure Vessel & Piping, Vol. 71, pp. 93-106.
4. Seshadri, R. and Hossain, M. M., 2009, "Simplified Limit Load Determination Using the m_α^T -method", ASME J. Pressure Vessel Technology, Vol. 131, pp.1-7.
5. Tantichattanont, P., Adluri, S., and Seshadri, R., 2007, "Fitness-for-Service Assessment of Spherical Pressure Vessels with Hot Spots", Int. J. Pressure Vessels Piping, Vol. 84, pp. 762-772
6. Tantichattanont, P., Adluri, S., and Seshadri, R., 2009, "Fitness-for-Service Evaluation of Thermal Hot Spots and Corrosion Damage in Cylindrical Pressure Components", ASME J. Pressure Vessel Technology, Vol. 131.
7. Ahmad, F., Hossain, M. M., and Seshadri, R., 2010, "Fitness-for-Service Assessment of Hydrocarbon Storage Tanks", ASME J. Pressure Vessel Technology, Vol. 132.
8. Pan, L. and Seshadri, R., 2002, "Limit Analysis for Anisotropic Solids Using Variational Principle and Repeated Elastic Finite Element Analysis", Proceedings of ASME Pressure Vessels and Piping Conference, Vol. 442, pp.149-155.
9. Timoshenko, S. P. and Gere, J. M., 1961, *Theory of Elastic Stability*, McGraw-Hill, New York.
10. Shames, I. H. and Cozzarelli, F. A., 1992, *Elastic and Inelastic Stress Analysis*, Prentice-Hall, New Jersey.
11. Mendelson, A., 1968, *Plasticity: Theory and Application*, Macmillan, New York.
12. Calladine, C. R., 2000, *Plasticity for Engineers: Theory and Application*, West Sussex, England.

13. Hill, R., 1950, *The Mathematical Theory of Plasticity*, Oxford University Press, London.
14. Kachanov, L.M., 1971, *Foundations of the Theory of Plasticity*, North-Holland, Amsterdam.
15. Mura, T., Rimawi, W. H. and Lee, S. L., 1965, "Extended Theorems of Limit Analysis", Quarterly of Applied Mathematics, Vol. 23, pp. 171-179.
16. Mura, T. and Lee, S. L., 1963, "Application of Variational Principles to Limit Analysis", Quarterly of Applied Mathematics, Vol. 21, pp. 243-348.
17. Pan, L. and Seshadri, R., 2001, "Limit Load Estimation Using Plastic Flow Parameter in Repeated Elastic Finite Element Analysis", ASME J. Pressure Vessel Technology, Vol. 124, pp. 433-439.
18. Seshadri, R. and Fernando, C. P. D., 1992, "Limit Loads of Mechanical Components and Structures Using the GLOSS R-Node Method", ASME J. Pressure Vessel Technology, Vol. 114, pp. 201-208.
19. Mangalaramanan S. P., 1997, *Robust Limit Loads Using Elastic Modulus Adjustment Technique*, Ph.D. Thesis, Faculty of Engineering and Applied Sciences, Memorial University of Newfoundland.
20. Reinhardt, W. D. and Seshadri, R., 2003, "Limit Load Bounds for the m_α Multiplier", ASME J. Pressure Vessel Technology, Vol. 125, pp.1-8.
21. Pan, L. and Seshadri, R., 2002, "Limit Loads for Layered Structures Using Extended Variational Principles and Repeated Elastic Finite Element Analysis," ASME J. Pressure Vessel Technology, Vol. 124, pp. 425-432.
22. Adibi-Asl, R. and Seshadri, R., 2007, "Simplified Limit Load Determination of Cracked Components Using the Reference Two-Bar Structure", ASME J. Pressure Vessels Technology, Vol. 129, pp. 280-286.
23. ASME Boiler and Pressure Vessel Code, 2007, Section III, New York.
24. ASME Boiler and Pressure Vessel Code, 2007, Section VIII, Division 2, New York.
25. Adibi-Asl, R., Fanous, I. F. Z. and Seshadri, R., 2006, "Elastic Modulus Adjustment Procedures- Improved Convergence Scheme", Int. J. Pressure Vessel and Piping, Vol. 83, pp.154-160.

26. Jones, G. L., and Dhalla, A. K., 1981, "Classification of Clamp Induced Stresses in thin Walled pipe", ASME PVP, Vol.81, pp. 17-23.

27. Marriott, D. L., 1988, "Evaluation of Deformation or Load Control of Stress under Inelastic Conditions using Elastic Finite Element Stress Analysis", ASME-PVP Conference, Pittsburgh, Vol. 136, pp. 3-9.

28. Seshadri, R., and Fernando, C. P. D., 1992, "Limit Loads of Mechnanical Components and Structures using the GLOSS R-Node Method", ASME J. Pressure Vessel Technology, Vol. 114, pp. 201-208.

29. Kraus H., 1980, *Creep Analysis*, John Eiley & Sons.

30. Mackenzie, D., and Boyle, J. T., 1993, "A Method of Estimating Limit Loads Using Elastic Analysis, I: Simple Examples", Int. J. Pressure Vessel Piping, Vol. 53, pp. 77-85.

31. Seshadri, R., 1991, "The Generalized Local Stress Strain GLOSS Analysis - Theory and Applications", ASME J. Pressure Vessel Technology, Vol 113, pp. 219-227.

32. Mackenzie, D., Shi, J. and Boyle, J. T., 1994, "Finite Element Modeling for Limit Analysis by the Elastic Compensation Method", Computers and Structures, Vol. 51, No. 4, pp. 403-410.

33. Boyle, J. T., Hamilton, R., Shi, J., and Mackenzie, D., 1997, "A Simple Method for Calculatiing Limit Loads for Axisymmetric Thin Shells", ASME J. Pressure Vessel Technology, Vol. 15, pp. 236-242.

34. Hamilton, R., Boyle, J. T., Shi, J., Mackenzie, D., 1996, "A Simple upper-bound method for calculating approximate shakedown loads", ASME J. Pressure Vessel Technology, Vol. 120, pp. 195-199.

35. Nadarajah, C., Mackenzie, D. and Boyle, J. T., 1996, "Limit and shakedown analysis of nozzle/cylinder Intersections under Internal Pressure and In-plane Moment Loading", Int. J. Pressure Vessels and Piping, Vol.68, pp. 261-272.

36. Ponter, A. R. S. and Carter, K. F., 1997, "Limit State Solutions, Based upon Linear Elastic Solutions with a Spatially Varying Elastic Modulus", Computer Methods in Applied Mechanics and Engineering, Vol.140, pp. 237-258.

37. Desai, C. S., and Abel, J. F., 1972, Introduction to the finite element method: A numerical method for engineering analysis, van Nostrand Reinhold Company, New York.

38. Spyrakos, C. C. and Raftoyiannia, J, 1997, *Linear ans Nonlinear Finite Element Analysis in Engineering Practice*, Algore Inc., Pittsburgh, PA

39. Smith, G.N., 1974, *Elements of Soil Mechanics for Civil and Mining Engineers*, Crosby Lockwood Staples, London.

40. Adibi-Asl, R., 2008, *Simplified Limit Load Determination for Integrity Assessment*, Ph.D. Thesis, Faculty of Engineering and Applied Sciences, Memorial University of Newfoundland.

41. Wilun, Z. and Starzewski, K., 1975, *Soil Mechanics in Foundation Engineering*, Surrey university press, London.

42. Helwany, S., 2007, *Applied Soil Mechanics with ABAQUS Applications*, Wiley, Hoboken, New Jersey.

43. Boussinesq, J., 1885, *Application des potentials a lèquilibre et de movement des solids elastiques*, Gauthier-Villars, Paris.

44. Steinbrenner, W., 1934, ``Tafeln zur setzungsberechnung``, Die Strasse, Vol. 1, pp. 121-124.

45. Fadam, R. E., 1941, *Influence Values for Vertical Stresses in a Semi-Infinite Solid due to Surface Loads*, School of Engineering, Harvard University.

46. Jurgenson, L., 1934, The Application of Theories of Elasticity and Plasticity to Foundation Problems, Proceedings Boston Society of Civil Engineers, Boston.

47. Fanous, I. F. Z. and Seshadri, R., 2009, "Limit Load Analysis Using the Reference Volume Concepts", Int. J. Pressure Vessel and Piping, Vol. 86, pp. 291-295.

48. Reinhardt, W. D., and Mangalaramanan, S. P., 2001, "Effective Tube-sheet Design Using Repeated Elastic Limit Analysis", ASME J. Pressure Vessel Technology, Vol. 123, pp.197-202.

49. Shih, C. F. and Lee, D., 1978, "Further Developments in Anisotropic Plasticity", J. Engineering Materials and Technology, Vol. 100, pp. 294-302.

50. Valliappan, S., Boonlaulohr, P. and Lee, I. K., 1976, "Non-linear Analysis for Anisotropic Materials", Int. J. for Numerical Methods in Engineering, Vol. 10, pp. 597-606.

51. Reinhardt, W. D. and Mangalaramanan, S. P., 1999, "Effective Tube-Sheet Design Using Repeated Elastic Limit Analysis", Proceedings of ASME Pressure Vessels and Piping Conference, Vol. 385, pp.141-149.

52. Reinhardt, W. D. and Mangalaramanan, S. P., 2001, "Plastic Limit Analysis of a Tube-Sheet Using an Elastic Modulus Modification Method", ASME J. Pressure VesselsTechnology, Vol. 123, pp. 197-202.

53. Indermohan, H., Reinhardt, W. D. and Seshadri. R., 2004, "Limit Load of Anisotropic Components Using the m-Beta Multiplier Method", J. Pressure Vessel Technology, Vol. 126, No. 4, Nov 2004, pp.455-460.

54. Seshadri, R. and Indermohan, H., 2004, "Lower Bound Limit Load Determination: The m_β–Multiplier Method," ASME J. Pressure Vessel Technology, Vol. 126, pp. 237-240.

55. William, F. and Hosford. R., 2005, *Mechanical Behavior of Materials*, Cambridge University Press, New York.

56. Adibi-Asl, R., and Seshadri, R., 2009, "Simplified Estimation Method for Inelastic Energy Release Rate,", Proceedings of 12th International Conference on Fracture (ICF-12), Ottawa, Canada.

57. Kim. Y. J., Huh. N. S. and Kim. Y. J., 2001, "Enhanced Reference Stress Based J and COD Estimation Method for LBB Analysis and Comparison With GE/EPRI Method", J. Fatigue and Fracture of Engineering Material and Structures, Vol. 24(a), pp. 243–254.

58. Kim, Y. J., Huh, N. S., and Kim, Y. J., 2001, ''Effect of Luders Strain on Engineering Crack Opening Displacement Estimations: Finite Element Study,'' J. Fatigue and Fracture of Engineering Material and Structures, Vol. 24(b), pp. 617–624.

59. Kim. Y. J., Huh. N. S., Kim. Y. J., Choi.Y. H., and Yang. J. S, 2004, "On Relevant Ramberg-Osgood Fit to Engineering Nonlinear Fracture Mechanics Analysis", ASME J. Pressure Vessel Technology, Vol. 126, pp. 277-283.

60. Adibi-Asl, R., and Seshadri, R., 2007, "Limit Load Analysis of Cracked Components Using the Reference Volume Method", ASME J. Pressure Vessel Technology, Vol. 129, pp.391-399.

61. ANSYS, 2008, Ver. 11.0 Online User Guide, ANSYS, Inc., Canonsburg, Pennsylvania.

Appendix-A
ANSYS COMMAND LISTING

Macro's for Linear Elastic Finite Element Analysis:

Following are some of the sample macro's used for doing linier elastic analysis in the research:

1) Thick Walled Cylinder

```
!*****************************************************************!
!   A program to analyze the thick cylinder with internal pressure   !
!*****************************************************************!

/prep7
*set, ri, 65              ! Internal radius=65mm
*set, ro, 90              ! External radius=90mm
*set, ys, 300             ! Yield stress=300mpa
*set, ym, 200e3           ! Young's modulus=200e3mpa
*set, pr, 0.47            ! Poisson's ratio=0.47
*set, p, 50               ! Internal pressure=50mpa

et, 1, plane82,,, 2,,     ! Defining axi-symmetric element

                          ! Defining material properties
mp, ex, 1, ym
mp, prxy, 1, pr

immed, 1                  ! Creating the model

k, 10, 0, 0
k, 1, ri, 0
k, 2, ro, 0
k, 3, 0, ro
k, 4, 0, ri
k, 5, ro, ro

lstr, 1, 2
larc, 2, 3, 10, ro
lstr, 3, 4
larc, 4, 1, 10, ri
lstr, 10, 5

lsbl, 2, 5,, delete, keep
lsbl, 4, 5,, delete, delete
lstr, 6, 7
```

```
lsel, s, line,, 1,2,1
lsel, a, line,, 4,6,2
al, all
lsel, all

lsel, s, line,, 3,4,1
lsel, a, line,, 7,8,1
al, all
lsel, all

aglue, 1, 2

esize, 2
mshkey, 1
amesh, all

lsel, s, line,, 1              ! Applying boundary conditions
dl, all,, symm
lsel, all

lsel, s, line,, 3
dl, all,, symm
lsel, all


lsel, s, line,, 2,8,6          ! Applying load
sfl, all, pres, p
lsel, all

esel, all

/quit                          ! End of prep7 commands

/solu                          ! Entering solver
solve                          ! Solving the problem
/quit                          ! Exiting solver

/post1                         ! Entering post1 post processor

pldisp, 1                      ! Plotting displacement
/wait, 3

plnsol, u, sum, 0              ! Plotting 'u' sum
/replot
/wait, 3
```

```
plnsol, s, eqv, 0                    ! Plotting stresses (equivalent)
/replot
/wait,3

plnsol, epto, eqv, 0                 ! Plotting total strains (equivalent)
/replot
```

2) Torispherical head

```
!*************************************************************!
!   A program to analyze Torospherical head subjected to Uniform Pressure   !
!*************************************************************!
/prep7

*set, pi, 3.1415926536
*set, ym, 262e03
*set, ys, 262
*set, pr, 0.47
*set, prsr, 5
*set, t, 50
*set, lsbyd, 0.8
*set, rbyd, 0.12
*set, tbyd, 1/40
*set, phitwo, asin((0.5-rbyd)/(lsbyd-rbyd))*180/pi
*set, phi1, 90.0-phitwo
*set, d, 2000
*set, rk, rbyd*d
*set, rh, lsbyd*d
*set, hh, rh-(rh-rk)*cos(phitwo*pi/180)
*set, a, d/2-rk
*set, ri, d/2.0
*set, ro, ri+t
*set, h, 6*sqrt(d*t/2)
*set, ndiv1, 5
*set, ndiv2, 70
*set, ndiv3, 30
*set, ndiv4, 120

antype, 0
et, 1, 82,,,1
mp, ex, 1, ym
mp, nuxy,, pr
k, 1, ri
k, 2, ro
k, 3, ri, h
```

```
k, 4, ro, h

!local coordinate system for knuckle

local, 11, 1, a, h
csys, 11
k, 5, rk, phi1
k, 6, rk+t, phi1
csys, 0

!local coordinate system for the head

local, 12, 1, 0, h+hh-rh
csys, 12
k, 7, rh, 90
k, 8, rh+t,90

csys, 0
l, 1, 2, ndiv1
l, 3, 4, ndiv1
l, 5, 6, ndiv1
l, 7, 8, ndiv1
l, 1, 3, ndiv2
l, 2, 4, ndiv2

csys, 11
l, 3, 5, ndiv3
l, 4, 6, ndiv3

csys, 12
l, 5, 7, ndiv4
l, 6, 8, ndiv4

csys, 0
a, 1,2,4,3
csys11
a, 3,4,6,5
csys, 12
a, 5,6,8,7
aglue, 1, 2, 3
amesh, all

csys, 0
nsel,, loc,x,0
d, all, ux, 0
nsel, all
```

```
nsel,, loc,y,0
d, all, uy, 0
nsel, all

csys, 0
sfl, 5, pres, prsr
csys, 11
sfl, 7, pres, prsr
csys, 0
csys, 12
sfl, 9, pres, prsr
csys, 0

finish
/solution
solve
/quit
```

3) Unreinforced Axi-symmetric Nozzle

```
!****************************************************************!
!            A program to analyze Unreinforced Axi-symmetric Nozzle         !
!****************************************************************!

/prep7

! Inner Radius of head(R) =914.4mm
! Nominal wall thickness (t) =82.55mm
! Inside radius of nozzle(r) =136.525mm
! Nominal wall thickness (tn) =25.4mm
! Required minimum wall thickness of head (tr) =76.835mm
! Required minimum wall thickness of nozzle (trn) =24.308mm
! Internal pressure (p) =24.132Mpa
! Young's modulus (YM) = 262Gpa
! Yield stress (YS) = 262MPa
! Poisson ratio (PR) = 0.47
! Height of the nozzle (h) =10*sqrt(R*trn) =1490.8801(or) 30"=762


!****Setting up of parameters****

*set, hr, 914.4
*set, ht, 82.55
*set, nr, 136.525
*set, nt, 25.4
```

```
*set, p, 24.132
*set, YM, 262e03
*set, PR, 0.47
*set, nh, 762
*set, ys, 262

!****Defining the Element type****

ET, 1, plane82,,, 1          !Defining the axi symmetric type of the element
                             ! Change the value to 0 for plain stress
                             ! Change the value to 3 for with thickness


!****Defining of material properties****

mptemp, 1, 0                 !Defining the material properties
mpdata, ex, 1,, YM
mpdata, prxy, 1,, PR

!****Creation of model****

IMMED, 1                     ! Creating the model

k, 10, 0, 0
k, 1, hr, 0                  ! Creating the corner key points
k, 2, (hr+ht), 0
k, 3, (nr+nt), (hr+ht)
k, 4, (nr+nt), (hr+ht+nh)
k, 5, nr, (hr+ht+nh)
k, 6, nr, hr

lstr, 1, 2, 6                !Creating four faces of rectangle
larc, 2, 3, 10, (hr+ht)
lstr, 3, 6, 6
larc, 6, 1, 10, hr
lstr, 3, 4
lstr, 4, 5, 6
lstr, 5, 6


lsel, s, line,, 1, 4, 1
al, all
lsel, all

lsel, s, line,, 3
lsel, a, line,, 5, 7, 1
```

```
al, all
lsel, all
aglue, 1, 2

esize, 10
mshkey, 1
amesh, all

!lrefine, 3,,, 4, 3, smooth

lsel, s, line,, 1
lplot
nsll, r, 1
nplot
d, all, uy, 0
nsel, all
lsel, all

lsel, s, line,, 4
lsel, a, line,, 7
nsll, r, 1
sf, all, pres, p
nsel, all
lsel, all

*****Entering the solver processor****

/solu                          ! Solving the problem
solve
/quit
```

4) Reinforced Axi-symmetric Nozzle

```
!*************************************************************!
!          A program to analyze Reinforced Axi-symmetric Nozzle          !
!*************************************************************!
/prep7

! Inner Radius of head(R) =914.4mm
! Nominal wall thickness (t) =82.55mm
! Inside radius of nozzle(r) =136.525mm
! Nominal wall thickness (tn) =25.4mm
! Required minimum wall thickness of head (tr) =76.835mm
! Required minimum wall thickness of nozzle (trn) =24.308mm
! Internal pressure (p) =24.132Mpa
! Young's modulus (YM) = 262Gpa
```

```
! Yield stress (YS) = 262MPa
! Poisson ratio (PR) = 0.47
! Height of the nozzle (h) =10*sqrt(R*trn) =1490.8801(or) 30"=762
! rei-bou-rad(Ln)=143.51mm

!****Setting up of parameters****

*set, hr, 914.4
*set, ht, 82.55
*set, hnt, 76.835
*set, nr, 136.525
*set, nt, 25.4
*set, nnt, 24.308
*set, ln, 143.51
*set, p, 24.132
*set, YM, 262e03
*set, PR, 0.47
*set, nh, 762
*set, ys, 262
*set, r1, 10.312
*set, r2, 83.312
*set, r3, 115.214
*set, t2, 54.61

!****Defining the Element type****

et,1,plane82,,,1          !Defining the axi symmetric type of the element
                          ! Change the value to 0 for plain stress
                          ! Change the value to 3 for with thickness

!****Defining of material properties****

mptemp, 1, 0              !Defining the material properties
mpdata, ex, 1,, YM
mpdata, prxy, 1,, PR

!****Creation of model****

IMMED, 1                  ! Creating the model

k, 10, 0, 0
k, 1, hr, 0               ! Creating the corner key points
k, 2, (hr+ht), 0
k, 100, (nr+nnt), (hr+hnt)
k, 3, (nr+nt+t2), (hr+ht)
k, 4, nr, hr
```

```
k, 5, (nr+nt), (hr+hnt+nh)
k, 6, nr, (hr+hnt+nh)
k, 7, (nr+nt), (hr+ht)

larc, 1, 4, 10, hr
larc, 2, 3, 10, (hr+ht)
lstr, 5, 7
lstr, 6, 4

circle, 100, ln
lsbl, 1, 8,, delete, keep2
lsbl, 2, 8,, delete, delete
lsbl, 3, 5,, delete, delete
lsbl, 4, 6,, delete, delete
lsel, s, line,, 3
lsel, a, line,, 7, 8, 1
lsel, a, line,, 10, 11, 1
ldele, all,,, 1
lsel, all
k, 16, (nr+nt+t2), (hr+ht)
k, 17, (nr+nt+t2), (hr+ht+ln-t2)
k, 18, nr, 887.0535          !this value is taken from ansys point at the same level as 13
larc, 14, 16, 10, (hr+ht)
lstr, 16, 17
k, 200, (nr+nnt), (hr+hnt)
larc, 17, 15, 200, -r3
lstr, 15, 8, 6
lstr, 8, 18
lstr, 18, 13
lstr, 13, 14, 6

lfillt, 3, 4, r2
lfillt, 8, 10, r1

lstr, 1, 2, 6
lstr, 5, 6, 6

lsel, s, line,, 3, 4, 1
lsel, a, line,, 6
lsel, a, line,, 12
lcomb, all,, 0
lsel, all

lsel, s, line,, 8
lsel, a, line,, 10
lsel, a, line,, 13
```

```
lcomb, all,, 0
lsel, all

lsel, s, line,, 1
lsel, a, line,, 9, 11, 2
lsel, a, line,, 14
al, all
lsel, all

lsel, s, line,, 3
lsel, a, line,, 7, 8, 1
lsel, a, line,, 11
al, all
lsel, all

lsel, s, line,, 2
lsel, a, line,, 5, 7, 2
lsel, a, line,, 15
al, all
lsel, all

mshkey, 1
esize, 20
amesh, all

lsel, s, line,, 14
lplot
nsll, r, 1
nplot
d, all, uy, 0
nsel, all
lsel, all


lsel, s, line,, 5
lsel, a, line,, 8, 9, 1
nsll, r, 1
sf, all, pres, p
nsel, all
lsel, all

*****Entering the solver processor****

/solu                          ! Solving the problem
solve
/quit
```

5) **Pressure Vessel Support Skirt**

```
!***************************************************************!
!          A program to analyze Pressure Vessel Support Skirt          !
!***************************************************************!
/prep7

! Inner Radius of Cylinder (cyi) =1240mm
! Outer Radius of Cylinder (cyo) =1290mm
! Inner Radius of Cone (ci) =1400mm
! Outer Radius of Cylinder (co)=1450mm
! Wall thickness (t) =50mm
! Axial pressure (p) =77.362Mpa
! Young's modulus (YM) = 275.8Gpa
! Yield stress (YS) = 275.8MPa
! Poisson ratio (PR) = 0.47
! Height of the cylinder (cyh) =760mm
! Height of the cone (ch) =0.16/tan(18.05)=0.4909m=490.9mm


!****Setting up of parameters****

*set, cyi, 1240
*set, cyo, 1290
*set, ci, 1400
*set, co, 1450
*set, t, 50
*set, p, 77.362
*set, YM, 275.8e03
*set, PR, 0.47
*set, ys, 275.8
*set, cyh, 760
*set, ch, 490.9

!****Defining the Element type****

et, 1, plane82,,, 1          !Defining the axi symmetric type of the element
                             ! Change the value to 0 for plain stress
                             ! Change the value to 3 for with thickness

!****Defining of material properties****

mptemp, 1, 0                 !Defining the material properties
mpdata, ex, 1,, YM
mpdata, prxy, 1,, PR
```

```
!****Creation of model****

immed, 1                        ! Creating the model

k, 1, cyi, 0                    ! Creating the corner key points
k, 2, cyo, 0
k, 3, cyo, cyh
k, 4, co, (cyh+ch)
k, 5, ci, (cyh+ch)
k, 6, cyi, cyh

lstr, 1, 2, 6                   !Creating four faces of rectangle
lstr, 2, 3
lstr, 3, 4
lstr, 4, 5
lstr, 5, 6, 6
lstr, 6, 1
lfillt, 5, 6, t
lstr, 3, 7, 6
lstr, 3, 8, 6

lsel, s, line,, 1, 2, 1
lsel, a, line,, 6, 9, 3
al, all
lsel, all

lsel, s, line,, 7, 9, 1
al, all

lsel, s, line,, 3, 5, 1
lsel, a, line,, 8
al, all
lsel, all

aglue, 1, 2, 3

lsel, all

mshkey, 1
esize, 5
amesh, all

!krefine,3,,,1,1,smooth,on

lsel, s, line,, 4
```

```
lplot
nsll, r, 1
nplot
d, all, all
nsel, all
lsel, all


lsel, s, line,, 1
nsll, r, 1
sf, all, pres, p
nsel, all
lsel, all

!*****Entering the solver processor****

/solu                          ! Solving the problem
solve
/quit
```

6) CT Specimen

```
!***************************************************************!
!                 A program to analyze CT Specimen              !
!***************************************************************!
/prep7

! Height (h) =125 mm
! Width (W) =100 mm
! Tensile load = 10KN
! Young's modulus (YM) = 211Gpa
! Yield stress (YS) = 250MPa
! Poisson ratio (PR) = 0.47
! Thickness (t) =3mm
! Crack length (a) = 46mm

!****Setting up of parameters****

*set, h, 62.5
*set, w1, -25
*set, w, 100
*set, t, 3
*set, tl, 10e03          !total load should be divided with
                         !thickness when ever we are using with plain stress option
                         !and plain stress with thickness option is being used we can
                         !use the total value of load
```

```
*set, ym, 211e03
*set, pr, 0.47
*set, a, 46
*set, ys, 250
*set, d1, 20
*set, d2, 25
*set, s, 3
*set, c, 27.5
*set, r, 12.5


!****Defining the Element type****

et, 1, plane82,,, 3
r, 1, 3


!****Defining of material properties****

mptemp, 1, 0                !Defining the material properties
mpdata, ex, 1,, ym
mpdata, prxy, 1,, pr

!****Creation of model****

immed, 1                    !creating the model

k, 1, a, 0                  ! Creating the corner key points
k, 2, w, 0
k, 3, w, h
k, 4, 0, h
k, 5, w1, h
k, 6, w1, s
k, 7, 0, s
k, 8, d1, s
k, 9, d2, 0
k, 10, 0, c

lstr, 1, 2, 25              !Creating four faces of rectangle
lstr, 2, 3, 32
lstr, 3, 4, 50
lstr, 4, 5, 13
lstr, 5, 6, 32
lstr, 6, 7, 13
lstr, 7, 8, 10
lstr, 8, 9, 2
```

```
lstr, 9, 1, 15

circle, 10, r,, 4,, 16
lsel, s, line,, 10, 25, 1
lesize, all,,, 5
lsel, all

lsel, s, line,, 1, 9, 1
al, all
lsel, all

lsel, s, line,, 10, 25, 1
al, all
lsel, all

asba, 1, 2,, delete, delete

esize, 5
type, 1
kscon, 1, 5, 1, 9,
amesh, 3

lsel, s, line,, 1
lplot
nsll, r, 1
nplot
d, all, uy
nsel,all
lsel,all

lsel, s, line,, 10
lsel, a, line,, 25
nsll, r, 1
*get, nn, node, 0, count
f, all, fy, TL/nn
nsel, all
lsel, all

!****Entering the solver processor****

/solu                          ! Solving the problem
solve
/quit
```

7) **Single Edge Notch bend**

```
!*****************************************************************!
!        A program to analyze Single Edge Notch Bend problem      !
!*****************************************************************!
/prep7

*set, s, 200                 ! Total span=400mm
*set, w, 100                 ! Width=100mm
*set, ys, 488.43             ! Yield stress=488.43MPa
*set, ym, 211e3              ! Young's modulus=211E3MPa
*set, pr, 0.47               ! Poisson's ratio=0.47
*set, pl, 12000/3            ! Internal pressure=12KN
*set, a, 50                  ! Crack tip length=50mm

et, 1, plane82,,, 3          !Defining plain stress with thickness
r, 1, 3

                             ! Defining material properties
mp, ex, 1, ym
mp, prxy, 1, pr

immid, 1                     !Creation of model


k, 1, 0, 0                   !Creation of end points
k, 2, 197.5, 0
k, 3, 197.5, 15
k, 4, 200, 25
k, 5, 200, 50
k, 6, 200, 100
k, 7, 0, 100
k, 8, 175, 0
k, 9, 175, 100


lstr, 1, 8
lstr, 8, 2
lstr, 2, 3
lstr, 3, 4
lstr, 4, 5
lstr, 5, 6
lstr, 6, 9
lstr, 9, 7
lstr, 7, 1
lstr, 8, 9
```

```
lsel, s, line,, 2, 7, 1
lsel, a, line,, 10
al, all
lsel, all

lsel, s, line,, 1
lsel, a, line,, 8, 10, 1
al, all
lsel, all

aglue, all

esize, 2
mshkey, 1
amesh, 2

mshkey, 0
kscon, 5, 1, 1, 6, 2
amesh, 1

nsel, s, loc, x, 0
!nsel, r, loc, y, 0
d, all, uy, 0
nsel, all

lsel, s, line,, 6
nsll, r, 1
dsym, symm, x
lsel, all
nsel, all

lsel, s, line,, 6
nsll, r, 1
*get, nn, node, 0, count
f, all, fy, -pl/nn
lsel, all
nsel, all

/quit                    !end of prep7 commands

/solu                    !entering solver
solve                    !solving the problem
/quit                    !exiting solver
```

8) **Plate with Multiple Crack**

```
!***************************************************************!
!         A program to analyze Plate with Multiple Crack problem         !
!***************************************************************!
/prep7

! Height (h) =100 mm                    Actual height is 200mm
! Width (W) =100 mm
! Tensile stress = 100Mpa
! Young's modulus (YM) = 211Gpa
! Yield stress (YS) = 250MPa
! Poisson's ratio (PR) = 0.47
! Thickness (t) =3mm
! Crack length (a) = 10mm

!****Setting up of parameters****

*set, H, 100
!*set, W1, 25
*set, W, 50
*set, T, 3
*set, c, 10                             !b,c and d are to locate
*set, d, 20                             !inclined cracks
*set, b, 21.2
*set, TL,-100                           !here stress is given
                                        !so no need to divide the total load
                                        !by thickness
*set, YM, 211e03
*set, PR, 0.47
*set, a, 10
*set, ys, 250

!****Defining the Element type****

et, 1 , plane82,,, 3            !Defining the type of the element
r, 1, 3
                                !change the value to 0 for plain stress
                                !change the value to 3 for with thickness

!****Defining of material properties****

mptemp, 1, 0                    !Defining the material properties
mpdata, ex, 1,, YM
mpdata, prxy, 1,, PR
```

```
!****Creation of model****

immed, 1                    !creating the model

k, 1, 0, 0                  !creating the corner key points
k, 2, 10, 0
k, 3, 15, 0
k, 4, 25, 0
k, 5, 32.5, 0
k, 6, 40, 0
k, 7, 50, 0
k, 8, 0, 5
k, 9, 15, 5
k, 10, 27.5, 5
k, 11, 32.5, 5
k, 12, 50, 5
k, 13, 20, 10
k, 14, 27.5, 17.5
k, 15, 35, 25
k, 16, 27.5, 17.5
k, 17, 0, 10
k, 18, 27.5, 50
k, 19, 50, 40
k, 20, 50, 50
k, 21, 50, 100
k, 22, 0, 100

A, 1, 2, 3, 9, 8
A, 3, 4, 5, 11, 10, 9
A, 5, 6, 7, 12, 11
A, 8, 9, 13, 14, 18, 17
A, 9, 10, 16, 13
A, 10, 11, 12, 19, 15, 16
A, 14, 15, 19, 20, 18
A, 17, 18, 20, 21, 22


kscon, 2, 0.25, 1, 12
kscon, 13, 0.25, 1, 6
kscon, 15, 0.25, 1, 6


esize, 1
lesize, 2,,, 8
```

```
amesh,1, 2

esize, 2
lesize, 15,,, 10
lesize, 23,,, 15
lesize, 16,,, 12
lesize, 21,,, 12
lesize, 24,,, 12
lesize, 25,,, 12

amesh, 3
amesh, 4, 5
amesh, 6, 7

esize, 2
amesh, 8

nsel, s, loc, x, 0
d, all, ux, 0
nsel, all

nsel, s, loc, y, 0
nsel, r, loc, x, 10, 50
d, all, uy, 0
nsel, all

nsel, s, loc, y, 100
sf, all, pres, tl
nsel, all

/solu
antype,0
solve
finish
```

9) Middle Tension Panel

```
!*****************************************************************!
!          A program to analyze Middle Tension Panel problem       !
!*****************************************************************!
/prep7

! Height (h) =300 mm
! Width (w) =125 mm
! Tensile load = 100Mpa
! Young's modulus (ym) = 211Gpa
```

```
! Yield stress (ys) = 250MPa
! Poisson's ratio (pr) = 0.47
! Thickness (t) =3mm
! Crack length (a) = 25mm

!****Setting up of parameters****

*set, h, 300
!*set, w1, 25
*set, w, 125
*set, t, 3
*set, tl, 100                ! Here stress is given
                             !so no need to divide the total load
                             !by thickness
*set, ym, 211e03
*set, pr, 0.47
*set, a, 25
*set, ys, 250

!****Defining the Element type****

et, 1, plane82,,, 3          !Defining the type of the element
r, 1, 3
                             ! Change the value to 0 for plain stress
                             ! Change the value to 3 for with thickness

!****Defining of material properties****

mptemp, 1, 0                 !Defining the material properties
mpdata, ex, 1,, ym
mpdata, prxy, 1,, pr

!****Creation of model****

immed, 1                     !Creating the model

k, 1, a, 0                   !Creating the corner key points
k, 2, a+a/2, 0
k, 3, w, 0
k, 4, w, h
k, 5, 0, h
k, 6, 0, a+a/2
k, 7, 0, 0
k, 8, a+a/2, a+a/2
k, 9, w, a+a/2
```

```
lstr, 1, 2                    !Creating four faces of rectangle
lstr, 2, 3
lstr, 3, 9
lstr, 9, 4
lstr, 4, 5
lstr, 5, 6
lstr, 6, 7
lstr, 7, 1
lstr, 6, 8
lstr, 8, 9
lstr, 8, 2


lsel, s, line,, 2, 3, 1
lsel, a, line,, 10, 11, 1
al, all
lsel, all

lsel, s, line,, 4, 6, 1
lsel, a, line,, 9, 10, 1
al, all
lsel, all

lsel, s, line,, 7, 9, 1
lsel, a, line,, 1
lsel, a, line,, 11
al, all
lsel, all

aglue, all
lccatt, 9, 10

mshkey, 0
esize, 5
kscon, 1, 4, 1, 9
amesh, 3

mshkey, 1
amesh, 1
amesh, 2

lsel, s, line,, 1, 2, 1
lplot
nsll, r, 1
nplot
dsym, symm, y
```

```
nsel, all
lsel, all

lsel, s, line,, 6, 7, 1
lplot
nsll, r, 1
nplot
dsym, symm, x
nsel, all
lsel, all

lsel, s, line,, 5
nsll, r, 1
sf, all, pres, -tl
nsel, all
lsel, all

*****Entering the solver processor****

/solu                          ! Solving the problem
solve
/quit
```

10) Plate with a Hole

```
!******************************************************************!
!          A program to analyze Plate with a Hole problem          !
!******************************************************************!

/prep7

! Height (2h) =300 mm
! Width (2w) =150 mm
! Hole radius(r) =23 mm
! Tensile stress = 100 Mpa
! Young's modulus (ym) = 152.95 Gpa
! Yield stress (ys) = 131.90 MPa
! Poisson's ratio (pr) = 0.47


!****Setting up of parameters****

*set, h, 300/2
*set, w, 150/2
*set, tl, 100                ! Here stress is given
                             !so no need to divide the total load
                             !by thickness
```

```
*set, ym, 152.95e03
*set, pr, 0.47
*set, r, 23
*set, ys, 131.90

!****Defining the Element type****

et, 1, plane82,,, 0          ! Defining the type of the element
                             ! Change the value to 0 for plain stress
                             ! Change the value to 3 for with thickness

!****Defining of material properties****

mptemp, 1, 0                 ! Defining the material properties
mpdata, ex, 1,, ym
mpdata, prxy, 1,, pr
!mpdata, dens, 1,, d

!****Creation of model****

immed, 1                     ! Creating the model

k, 10, 0, 0
k, 1, r, 0                   ! Creating the corner key points
k, 2, w, 0
k, 3, w, w
k, 4, w, h
k, 5, 0, h
k, 6, 0, w
k, 7, 0, r

lstr, 1, 2                   ! Creating four faces of rectangle
lstr, 2, 3
lstr, 3, 4
lstr, 4, 5
lstr, 5, 6
lstr, 6, 7
lstr, 3, 6
larc, 7, 1, 10, r

lsel, s, line,, 1, 2, 1
lsel, a, line,, 6, 7, 1
lsel, a, line,, 8
al, all
lsel, all
```

```
lsel, s, line,, 3, 5, 1
lsel, a, line,, 7
al, all
lsel, all

aglue, 1, 2
lccat, 2, 7

!r, 1, 3                        ! 3-Plain stress with thickness
esize, 4
!mshape, 0, 2D
mshkey, 1
amesh, all

lsel, s, line,, 1
lplot
nsll, r, 1
nplot
dsym, symm, y
nsel, all
lsel, all

lsel, s, line,, 5, 6, 1
lplot
nsll, r, 1
nplot
dsym, symm, x
nsel, all
lsel, all

lsel, s, line,, 4
nsll, r, 1
sf, all, pres, -tl
nsel, all
lsel, all

*****Entering the solver processor****

/solu                           ! Solving the problem
solve
/quit
```

11) Indeterminate Beam

```
!*************************************************************!
!          A program to analyze Indeterminate Beam problem          !
!*************************************************************!
/prep7

! Length (l)=508mm
! Width (w)=25.4mm
! Pressure (p) = 1Mpa
! Young's modulus (ym) = 206E3 N/mm2
! Poisson's ratio (pr) = 0.47
! Density (d) = 2500 n/mm3

!****Setting up of parameters****

*set, l, 508
*set, w, 25.4
*set, p, 1
*set, ym, 206.85e3
*set, pr, 0.47
*set, ys, 206.85
*set, d, 2500

!****Defining the Element type****

et, 1, plane82,,, 3          !Defining the type of the element
r, 1, 1

!****Defining of material properties****

mptemp, 1, 0                 ! Defining the material properties
mpdata, ex, 1,, ym
mpdata, prxy, 1,, pr
mpdata, dens, 1,, d

immed, 1                     ! Creating the model

k, 1, 0, 0, 0                ! Creating the corner key points
k, 2, l, 0
k, 3, l, w
k, 4, 0, w

lstr, 1, 2                   ! Creating four faces of rectangle
lstr, 2, 3
lstr, 3, 4
```

```
lstr, 4, 1

al, 1, 2, 3, 4                !Creating the area
                              ! Area defined using previously defined lines

!****Meshing****

esize, 1
mshkey, 1
amesh, all                    !Meshing the Area


!****Applying Boundary conditions (Left End)*****

lsel, s, loc, x, 0            ! Selecting a line with the help of location
lplot
nsll, r, 1                    ! Selecting the nodes attached to the previous
                              ! Selected line including the keypoint nodes
nplot

d, all, all                   ! Constraining all above picked nodes in all directions

nsel, all                     ! Reselecting all nodes and lines
nplot
lplot
lsel,all
/replot

!****Applying boundary conditions (Right End)****

lsel, s, loc, x, 1
lplot
nsll, r, 1
nplot
d, all, uy
nsel, all
nplot
lsel, all
lplot

!****Applying pressure load on the top layer of beam****

lsel, s, loc, y, w
lplot
nsll, r, 1
```

```
nplot
nsel, all
nplot
lplot
sfl, all, pres, p
lsel, all
lplot

/quit                         ! End of Prep7 commands


!****Entering the solver processor****

/solu                         ! Solving the problem
solve
/quit
```

12) Oblique Nozzle

```
!***************************************************************!
!            A program to analyze Oblique Nozzle Problem          !
!***************************************************************!

/prep7

*set, ri, 300                 ! Internal radius of cylinder =300
*set, ro, 306                 ! External radius of cylinder =306
*set, rni, 156.5              ! Internal radius of nozzle=156.5
*set, rno, 162.5              ! External radius of nozzle=162.5
*set, ys, 339.4               ! Yield stress=339.4mpa
*set, ym, 108.08e3            ! Young's modulus=108.08e3mpa
*set, pr, 0.47                ! Poisson's ratio=0.47
*set, p, 3.0                  ! Internal pressure=3.0mpa
*set, l1, 2400                ! Length of cylinder
*set, l2, 1200                ! Length of nozzle
*set, t, 6                    ! Thickness of cylinder
*set, t, 6                    ! Thickness of nozzle
*set, h1, 175                 ! Cylinder cap
*set, h2, 106                 ! Nozzle cap

et,1,solid95                  !Defining  element
                              ! Defining material properties
mp, ex, 1, ym
mp, prxy, 1, pr


immid,1                       !creation of model
```

```
cylind, ri, ro, -(l1/2), (l1/2), 90, 270
wpoffs,, (ri+(t/2))
wprota, ,-30            !rotation of workplane, change this angle for different
csys, wp                !nozzle angles
cylind, rni, rno, -(l2/2), (l2/2), 90, 270
vsba, 1, 10
vsba, 2, 19
vdele, 1, 3, 2, 1
vadd, 4, 5
wprota,, 30
wpoffs,, -(ri+(t/2))
csys, wp

wpoffs,,, -(l1/2)       ! Creating right cap
wprota,,, 90
csys, wp
k, 49, 0, 0, 0
k, 50, 42.25, 290.4738
k, 51, 84.5, 259.8076
k, 52, 126.75, 198.4313
k, 53, 169.00,0
k, 54, 175, 0
k, 55, 131.25, 202.4
k, 56, 87.50, 265.0038
k, 57, 43.75, 296.2832
spline, 2, 50, 51, 52, 53
l, 53, 54
spline, 54, 55, 56, 57, 1
l, 1, 2
lsel, s, line,, 1
lsel, a, line,, 31, 34, 1
lsel, a, line,, 37
lsel, a,  line,, 40, 43, 1
al, all
vrotat, 16,,,,,, 53, 54, -180, 1
lsel, all
wprota,,, -90
wpoffs,,, (l1/2)


wpoffs,,, (l1/2)        ! Creating left cap
wprota,,, -90
csys, wp
k, 99, 0, 0, 0
k, 100, 42.25, 290.4738
```

```
k, 101, 84.5, 259.8076
k, 102, 126.75, 198.4313
k, 103, 169.00, 0
k, 104, 175, 0
k, 105, 131.25, 202.4
k, 106, 87.50, 265.0038
k, 107, 43.75, 296.2832
spline, 8, 100, 101, 102, 103
l, 103, 104
spline, 104, 105, 106, 107, 5
l, 5, 8
lsel, s, line,, 8
lsel, a, line,, 61, 69, 1
al, all
vrotat, 28,,,,,, 103, 104, +180, 1
lsel, all
wprota,,, 90
wpoffs,,, -(l1/2)
csys, wp

wpoffs,, (ri+(t/2))
wprota,, -30                        ! Creating nozzle cap
csys, wp
wpoffs,,, (l2/2)
wprota,,, -90
csys, wp
k, 199, 0, 0, 0
k, 200, 25, 151.5305
k, 201, 50, 135.5330
k, 202, 75, 103.5150
k, 203, 100, 0
k, 204, 106, 0
k, 205, 79.50, 107.7291
k, 206, 53, 140.7291
k, 207, 26.50, 157.3399
spline, 16, 200, 201, 202, 203
l, 203, 204
spline, 204, 205, 206, 207, 13
l, 13, 16
lsel, s, line,, 20
lsel, a, line,, 87, 95, 1
al, all
vrotat, 39,,,,,, 203, 204, 180, 1
lsel, all
wprota,,, 90
wpoffs,,, -(l2/2)
```

```
wprota,, 30
wpoffs,, -(ri+(t/2))
csys,wp


vadd, 1, 2, 3, 4
esize, 15
mshkey, 0
mshape, 1
vmesh, 5

asel, s, area,, 3, 4, 1
asel, a, area,, 6, 7, 1
asel, a, area,, 10, 16, 6
asel, a, area,, 13, 14, 1
asel, a, area,, 28
asel, a, area,, 39
asel, a, area,, 56, 58, 1
aplot
da, all, symm
allsel

asel, s, area,, 9
asel, a, area,, 11, 12, 1
asel, a, area,, 15, 19, 4
asel, a, area,, 20, 22, 2
asel, a, area,, 31, 33, 1
asel, a, area,, 42, 44, 1
asel, a, area,, 50, 53, 3
asel, a, area,, 55
aplot
sfa, all,, pres, p              ! Application of pressure
allsel

nsel, s, loc, z, 780, 820
nsel, a, loc, z, -780, -820
nsel, r, loc, x, 0,- 80
nsel, u, loc, y, 0, 3000
d, all, uy
d, all, uz
allsel
/quit                           ! End of prep7 commands

/solu                           ! Entering solver
solve                           ! Solving the problem
/quit                           ! Exiting solver
```

Macro's for Non-Linear Elastic Finite Element Analysis:

The macro for the non-linear analysis can be obtained by doing some minor changes to the linear elastic analysis macros. The changes will be in the material property definition and the load definition.

The generalized macros for these changes are given below:

Material Properties:

```
*set, ys, 339.4              ! Yield stress=339.4mpa
*set, ym, 108.08e3           ! Young's modulus=108.08e3mpa
*set, pr, 0.47               ! Poisson's ratio=0.47

!****Defining of material properties****!
mptemp, 1,0
mpdata, ex, 1,, ym
mpdata, prxy, 1,, pr
tb, bkin, 1, 1,, 1
tbtemp, 1, 1
tbdata, 1, ys, 0

!**** Apllication of load and solving****!
/solu                        ! Entering solver
antype, static

lsel, s, line,, 10           !Sample load application
lsel, a, line,, 25
nsll, r, 1
*get, nn, node, 0, count
f, all, fy, 10*TL/nn         ! Load is increases 10 folds so multiplier
nsel, all                    ! should be multiplied by 10.
lsel, all
solcontrol, on
outres, all, all
time, 1
autots, on
nsubst,100
lswrite,1

lssolve,1                    !Solving the problem
/quit
```

Macro for EMAP Iterations:

The EMAP iterations are used to obtain the converged solution. The following is the generalized macro used to do the EMAP iterations, in the current research a '*q*' value of 0.1 is used, but this macro can be used with any value of fixed '*q*'.

```
!***********************************************************
!macro for finding out multipliers;
!***********************************************************

/post 1

*ask, NI, Required Number Of Iterations,1
*ask, q, Enter the 'q'val 1 for plane strain and 2 for plane stress, 1
! NI _ number of iterations to be run
! Input the number of iterations to be run

*dim, enub, array, nd2, nd1        ! Def. an array for writing the element numbers.
*get, ecou, elem, 0, count
*dim, eval, array, ecou, NI+1      ! Def. Eval array
*vget, eval(1,1), elem,, attr, mat
*do, i, 1, ecou, 1
*if, eval(i,1), eq, 1, then
eval(i,1 ) = ym
*endif
*if, eval(i,1), eq, 2, then
eval(i,1) = ym/3
*endif
*enddo

*dim, ests, array, ecou, 5         ! Def. array for element stress.
*dim, ests2, array, ecou, 5
*dim, vol, array, ecou, 1


! Getting the centroidal location of the elements

*dim, loe, array, ecou, 3
*do, lo, 1, ecou, 1
*get, loe(lo,1), elem, lo, cent, x
*get, loe(lo,2), elem, lo, cent, y
*get, loe(lo,3), elem, lo, cent, z
*enddo
```

```
tvol = 0
*do, v, 1, ecou, 1                    ! Reading volumes of each element and summing
*get, vol(v,1), elem, v, volu         ! them up.
tvol = tvol + vol(v,1)
*enddo

*do, gp, 1, NI, 1
sp = gp+1


etable, sigc, s, eqv                  ! Reading stress into element table.
etable, sot, s, eqv                   ! Sorting of element stresses.
esort, etab, sot, 0, 0
*get, meqs, sort, 0, max
etable, eqst, epto, eqv               ! Reading strain values into element table.

trn = 0                               ! Calculation of reference stress.
*do, k, 1, ecou, 1
*get, els, etab, 1, elem, k
rn = els * els * vol(k,1)
trn = trn + rn
*enddo
srv = (trn/tvol)
sr = sqrt(srv)


!******* finding out the multiplyer values************************

ML=ys/meqs                            ! Calculation of lower bound multiplier

MUN2=0
MUD2=0

M01D2=0
M01D=0
M01N2=0
M01N=0

M02N2=0
M02N=0
M02D2=0
M02D=0

*do, z, 1, ecou, 1
*get, elsa, etab, 1, elem, z
*get, elst, etab, 3, elem, z
```

```
MUN1 = elst * vol(z,1)              ! Calculation of upper bound multiplier
MUN2 = MUN2 + MUN1
MUD1 = elsa * elst * vol(z,1)
MUD2 = MUD2 + MUD1

M01N1 = vol(z,1)
M01N2 = M01N2 + M01N1
M01D1 = vol(z,1) * elsa**2          ! Calculation of M01 multiplier
M01D2 = M01D2 + M01D1

M02N1 = vol(z,1) / eval(z,gp)       ! Calculation of M02 multiplier
M02N2 = M02N2 + M02N1
M02D1 = elsa * elsa * vol(z,1) / eval(z,gp)
M02D2 = M02D2 + M02D1

*enddo

MU = ys * MUN2 / MUD2

M01N = sqrt(M01N2)
M01D = sqrt(M01D2)
M01 = ys * M01N / M01D


M02N = sqrt(M02N2)
M02D = sqrt(M02D2)
M02 = ys * M02N / M02D

*SET, JETA, (M02/ML)
*SET, Tan_theta, 0.2929  ! This is the fixed value shown in the formula of paper

*if, JETA, LE, (1 + sqrt(2)), then
MAT =  m02 / (1 + (Jeta - 1) * Tan_theta)
*endif

*if, JETA, GT, (1 + sqrt(2)), then
cee = 0.2929 * (JETA - 1)
JETAF = (1 + cee) + sqrt(((1 + cee) * ( 1 + cee)) - 1)
MAT =  M02 / (1 + (Jetaf-1) * Tan_theta)
*endif

!*cfopen, MULT%gp%   !Writing out the multipliers
*cfopen, MULT,,, append
*vwrite, gp
(f9.4)
```

```
!(1x,'ITERATION NO : ',f9.4)
*vwrite, ML
(f9.4)
!(1x,'Multiplier ML : ',f9.4)
*vwrite, MU
(f9.4)
!(1x,'Multiplier MU : ',f9.4)
*vwrite, M01
(f9.4)
!(1x,'Multiplier M01 : ',f9.4)
*vwrite, M02
(f9.4)
!(1x,'Multiplier M02 : ',f9.4)
*vwrite, MAT
(f9.4)
!(1x,'Multiplier MAT : ',f9.4)
!*cfclos

*do, k, 1, ecou, 1
*get, ests(k,1), etab, 1, elem, k
*enddo

!*if, gp, eq, 1, or, gp, eq, 10, then
*cfopen, ESTS%gp%                    ! Opening a file to write element stress.
*do, k, 1, ecou, 1
*get, elsts, etab, 1, elem, k
!*get, elst, etab, 3, elem, k
*set, ymv, eval(k,gp)
*set, volu, vol(k,1)
*set, lx, loe(k,1)
*set, ly, loe(k,2)
*set, lz, loe(k,3)
*vwrite, k, elsts, volu, ymv, lx, ly, lz ! Writing element stresses to a ESTS1 file.
(f7.0,3x,f9.4,3x,f11.3,3x,e21.10,2x,f11.4,2x,f11.4,2x,f11.4)
*enddo
*cfclos
!*endif

*do, c, 1, ecou, 1                   !Def. the values of eval.
*set, eval(c,gp+1), eval(c,gp)
*enddo
```

```
!****EMAP PART****

*do, m, 1, ecou, 1
ests(m,3) = sr / ests(m,1)          ! Dividing limit stress with individual stresses.
ests(m,4) = (ests(m,3)**q)          ! Elastic Adjustment parameter
eval(m,gp+1) = eval(m,gp) * ests(m,4)
*enddo

/quit
/prep7

*do, x, 1, ecou, 1
mp, ex, x, eval(x,gp+1)
*if, gp, eq, 1, then
mp, prxy, x, 0.47
*endif                              ! Creating suppurate material properties
emodif, x, mat, x                   !for individual element.
*enddo

/quit
/solu                               ! Resolving the problem with new
Solve                               ! material properties
/quit
/post1

*enddo                              ! Closing of Iterative loop.
```

The out put from theses macros will be two types of files, one is MULT, which contains the multiplier values and the second is ESTS that contain element stresses and location values in them. Further these two files will be processed using MATLAB to obtain the required plots and multipliers. For using in MATLAB these files need to be converted to text tiles which can be easily done by renaming them. The MATLAB files used for the research are provided in Appendix B.

Appendix-B
MATLAB COMMAND LISTING

The following MATLAB macros are used to process the output files from the ANSYS. The MULT file should be renamed as MULT.txt file. We can choose any file Iteration files and name them as b.txt, b2.txt, b3.txt, b4.txt, b5.txt files.

Macro for Single Iteration

```
%m_alfa tangent plot(macro with mref=m0-(volrat)*(mo-ml))
%this macro is to plot m0 vs sqrt(volrat).
%enter number of iterations(noi) and actual multiplier(mact)
%gat the mult file from ansys and correct it and save as a text file in
the
%same directory as this file is

clear
load mult.txt
load b.txt
b=sortrows(b,-2);

noi=18                        % Number of Iterations
mact=0.81                     % multiplier from non-linear analysis
en=2674                       % Number of Elements
sig_y=250                     % Yield Stress
tot_vol=0;

%m-alfa triangle formation
aa=1:0.0001:1+sqrt(2);
bb=aa;
d=1:0.0001:1+sqrt(2);
for i=1:14143
c(i)=(d(i)^4+4*d(i)^2-1)/(4*d(i)^2+2*sqrt(d(i)*(d(i)-1)^2*(d(i)-
1+sqrt(2))*(1+sqrt(2)-d(i))));
end
f=1:0.0001:1+sqrt(2);
for i=1:14143
    e(i)=1+sqrt(2);
end
j=1
for i=1:6:noi*6
    ml(j)=mult(i+1);
    mu(j)=mult(i+2);
    m01(j)=mult(i+3);
    m02(j)=mult(i+4);
    mat(j)=mult(i+5)
    ma(j)=mact
    j=j+1;
end

for k=1:noi
    m0byml(k)=m02(k)/ml(k);
    %if (m0byml(k)<=1+sqrt(2))
```

```
            lam(k)=(1/m0byml(k))^2;
            %else
            %lam(k)=0.171;
            %end
        m2bar(k)=(2*sqrt(lam(k))*m02(k))/(1+lam(k));
        m0bym2bar(k)=m02(k)/m2bar(k);
        m0bym(k)=m02(k)/ma(k);
end
%m0bml=m0byml(1)
for i=1:noi
if (m0byml(i)<=1+sqrt(2))
    malft(i)=m02(i)/(1+0.2929*(m0byml(i)-1));
    m0byml(i);
    lim(i)=m0byml(i);
else
    m0bymlf(i)=((2+0.5858*(m0byml(i)-1))+sqrt((2+0.5858*(m0byml(i)-
1))^2-4))/2;
    %m0bymlf(i)=(1+0.2929*(m0byml(i)-1))+sqrt((1+0.2929*(m0byml(i)-
1))^2-1);
    malft(i)=m02(i)/(1+0.2929*(m0bymlf(i)-1));
    m0bymlf(i);
    lim(i)=m0bymlf(i);
end
end
g=1
part1=-(((g^2+2)^2-5)*(8*g)-16*g^3*(g^2+2))/((g^2+2)^2-5)^2
part2=-(((g^2+2)^2-5)*((g-1)*(-3*g^2+4*g+1)+2*(-g^3+2*g^2+g))-
8*g^2*(g^2+2)*(g-1)*(1+sqrt(2)-g)*(g-1+sqrt(2)))/(((g^2+2)^2-
5)^2*sqrt(g*(g-1+sqrt(2))*(1+sqrt(2)-g)))
s=part1+part2;
z=1:0.001:5;
li=s*(z-1)+1;


%%%%%%%%%%%%%%%%%%%%%%%%%%%%%%%%%%%%%%%%%%%%%%%%%%%%%%%%%%%%%%%%%%%%%%%%%%%%%%%%
%%%%%%%%%%%%%%%%%%%%%%%%%%%%%%%%%%%%%%%%%%%%%%%%%%%%%%%%%%%%%%%%%%%%%%%%%%%%%%%%
%Calicúlating the total volume of the component
vol=0
for i=1:en
    vol=vol+b(i,3);
    voli(i,1)=vol;
end
tot_vol=voli(en,1);

for i=1:en
    vol_rat(i,1)=voli(i,1)/tot_vol;
    sq_vol_rat(i,1)=sqrt(voli(i,1)/tot_vol);
end

%caliculation of total denominator
tot_din=0;
for i=1:en
    din1(i,1)=(b(i,2)*b(i,2)*b(i,3))/(b(i,4));
    tot_din=tot_din+din1(i,1);
    num1(i,1)=b(i,3)/b(i,4);
end
```

```
din=0
num=0

%caliculation of mo with step by step increase of volume;
for i=1:en
    num=num+num1(i,1);
    nu(i,1)=num;
    din=din+din1(i,1);
    di(i,1)=din;
    mo(i,1)=sig_y*sqrt(nu(i,1))/(sqrt(di(i,1)));
    m0bm1(i,1)=mo(i,1)/mo(1,1);
    end
   mactbml=mact/mo(1,1);

%calculation of ml for individual elements
for i=1:en
    ml1(i,1)=sig_y/b(i,2);
    ml1_vol(i,1)=tot_vol-voli(i,1);
    ml1_volrat(i,1)=ml1_vol(i,1)/tot_vol;
    sq_ml1_volrat(i,1)=sqrt(ml1_volrat(i,1));
end

 hh=(1/en);

%caliculation of average m0(trapizoidal method)
%  mrefn=0
%  for i=1:en-1
%       mrefn=mrefn+((mo(i+1,1)+mo(i,1))*(vol_rat(i+1,1)-
vol_rat(i,1)))/2;
%  end
%  mref=mrefn
 mr1=0
 mrow=0
 %mrw=0
 for i=2:en
     mr1=mr1+(vol_rat(i,1)-vol_rat(i-1,1))*(mo(i,1)-mo(1,1));
     %mrw=mrw+(vol_rat(i,1)-vol_rat(i-1,1))*(mo(i,1)+mo(i-1,1))/2;
     mr(i-1,1)=mr1;
 end
       mr(en,1)=mr1;
     mrow=mo(1,1)+mr1;
 for i=1:en
    if (mrow>=mo(i,1))
        vrreq=vol_rat(i,1);
    end
end
mref=mrow;
mrefbml=mref/mo(1,1);
for i=1:en
    if (mref>=mo(i,1))
       mreq=mo(i,1);
       vreq=vol_rat(i,1);
   end
end

%caliculation of average m0(trapizoidal method)
```

```
% mrefn1=0
% for i=1:en-1
%     mrefn1=mrefn1+((mo(i+1,1)+mo(i,1))*(sq_vol_rat(i+1,1)-
sq_vol_rat(i,1)))/2;
% end
% mref1=mrefn1
 mr2=0
 mrow1=0
 %mrw1=0
 for i=2:en
     mr2=mr2+(sq_vol_rat(i,1)-sq_vol_rat(i-1,1))*(mo(i,1)-mo(1,1));
     %mrw1=mrw1+(sq_vol_rat(i,1)-sq_vol_rat(i-1,1))*(mo(i,1)+mo(i-
1,1))/2;
 end
    mrow1=mo(1,1)+mr2;
 for i=1:en
    if (mrow1>=mo(i,1))
        vrreq1=sq_vol_rat(i,1);
    end
end
mref1=mrow1;
mref1bm1=mrow1/mo(1,1);

  for i=1:en
    if  (mref1>=mo(i,1))
       mreq1=mo(i,1);
       vreq1=sq_vol_rat(i,1);
   end
  end
ge1=0;
geh=0;
ge=0;
gee=0;
vreeq=0;
ge2=0;
mge=0;
mge1=0;
mge2=0;
  for i=1:en
    geh=ge1+((((mo(en,1)*b(i,2)/sig_y)^2-1)^2)*b(i,3))/(4*tot_vol);
    ge=sqrt(geh);
    sig_ref=(b(1,2)+(mo(en,1)/sig_y))/2;
    ge1=sqrt(((((mref*sig_ref/sig_y)^2-1)^2)*vreq)/(4));
    if (mref>=mo(i,1))
       gee=gee+((((mo(en,1)*b(i,2)/sig_y)^2-1)^2)*b(i,3))/(4*tot_vol);
    end
    ge2=sqrt(gee);
  end

  mge=mo(en,1)/(1+ge);
  mge1=mref/(1+ge1);
  mge2=mref/(1+ge2);

%construction of st.line for finding out new mavg
x1=vol_rat(en,1)
y1=mo(en,1)
```

```
x2=vreq
y2=mreq
slope=(y2-y1)/(x2-x1)
yint=y1-(x1*slope)
for i=1:en  %no of elements from end to control the extent of line
    xco(i,1)=vol_rat(i,1);
    yco(i,1)=slope*xco(i,1)+yint;
end
m=yint+slope*vreq

%construction of st.line for finding out new mavg
x11=sq_vol_rat(en,1)
y11=mo(en,1)
x21=vreq1
y21=mreq1
slope1=(y21-y11)/(x21-x11)
yint1=y11-(x11*slope1)
for i=1:en  %no of elements from end to control the extent of line
    xco1(i,1)=sq_vol_rat(i,1);
    yco1(i,1)=slope1*xco1(i,1)+yint1;
end
m1=yint1+slope1*vreq1

%plotting mo vs volume ratio
figure(1)
hold on
i=1:en;
h=plot(vol_rat(i,1),mo(i,1),'k')
for j=0:0.01:1
plot(j,mref,'-+k')
plot(j,mact,'-*k')
end
xlabel('V_R/V_T','FontAngle','Italic','FontSize',12)
ylabel('m^0','FontAngle','Italic','FontSize',12)
legend('\it m^0','\it m^0(V_R_p)','\it m_n_o_n',0)
title('Plot of m^0 vs V_R/V_T','FontAngle','Italic','FontSize',12)
saveas(h,'mref.fig')
hold off

%plotting mo/ml vs volume ratio
figure(2)
hold on
i=1:en;
h=plot(vol_rat(i,1),m0bml(i,1),'k')
for j=0:0.01:1
plot(j,mrefbml,'-+k')
plot(j,mactbml,'-*k')
end
xlabel('V_R/V_T','FontAngle','Italic','FontSize',12)
ylabel('m^0/m_L','FontAngle','Italic','FontSize',12)
legend('\it m^0','\it m^0(V_R_p)','\it m_n_o_n',0)
title('Plot of m^0/m_L vs V_R/V_T','FontAngle','Italic','FontSize',12)
saveas(h,'mobml.fig')
hold off

%plotting mo vs sqrt(volume ratio)
```

```
figure(3)
hold on
i=1:en;
h=plot(sq_vol_rat(i,1),mo(i,1),'k')
for j=0:0.01:1
plot(j,mref1,'-+k')
plot(j,mact,'-*k')
end
xlabel('\surd (V_R / V_T)','FontAngle','Italic','FontSize',12)
ylabel('m^0','FontAngle','Italic','FontSize',12)
legend('\it m^0','\it m^0(\surd (V_R_p))','\it m_n_o_n',0)
title('Plot of m^0 vs \surd (V_R /
V_T)','FontAngle','Italic','FontSize',12')
saveas(h,'mref1.fig')
hold off

%plotting mo/ml vs sqrt(volume ratio)
figure(4)
hold on
i=1:en;
h=plot(sq_vol_rat(i,1),m0bml(i,1),'k')
for j=0:0.01:1
plot(j,mref1bml,'-+k')
plot(j,mactbml,'-*k')
end
xlabel('\surd (V_R / V_T)','FontAngle','Italic','FontSize',12)
ylabel('m^0/m_L','FontAngle','Italic','FontSize',12)
legend('\it m^0/m_L','\it m^0(\surd (V_R_p))','\it m_n_o_n',0)
title('Plot of m^0/m_L vs \surd
(V_R/V_T)','FontAngle','Italic','FontSize',12)
saveas(h,'mobml1.fig')
hold off

% % caliculating ml for individual element
% for i=1:en
%     ml1(i,1)=(sig_y*sqrt(b(i,3)))/sqrt(din1(i,1));
% end
%
%countor plots at different %of max stresses

ps1=0.01*b(1,2)
ps2=0.02*b(1,2)
ps3=0.03*b(1,2)
ps4=0.04*b(1,2)
ps5=0.05*b(1,2)

omrefn=0
tmrefn=0
thmrefn=0
fmrefn=0
fimrefn=0

for i=1:en
    if (b(i,2)>ps1)
        ops(i,1)=b(i,2);
        omo(i,1)=mo(i,1);
```

```
        opmo=omo(i,1);
        opmobym=omo(i,1)/mact;
        omrefn=mo(i,1);
    else
        ops(i,1)=0;
        omo(i,1)=0;

    end

    if (b(i,2)>ps2)
        tps(i,1)=b(i,2);
        tmo(i,1)=mo(i,1);
        tpmo=tmo(i,1);
        tpmobym=tmo(i,1)/mact;
        tmrefn=mo(i,1);
    else
        tps(i,1)=0;
        tmo(i,1)=0;

    end

    if (b(i,2)>ps3)
        thps(i,1)=b(i,2);
        thmo(i,1)=mo(i,1);
        thpmo=thmo(i,1);
        thpmobym=thmo(i,1)/mact;
        thmrefn=mo(i,1);

    else
        thps(i,1)=0;
        thmo(i,1)=0;

    end


    if (b(i,2)>ps4)
        fps(i,1)=b(i,2);
        fmo(i,1)=mo(i,1);
        fpmo=fmo(i,1);
        fpmobym=fmo(i,1)/mact;
        fmrefn=mo(i,1);
    else
        fps(i,1)=0;
        fmo(i,1)=0;

    end

    if (b(i,2)>ps5)
        fips(i,1)=b(i,2);
        fimo(i,1)=mo(i,1);
        fipmo=fimo(i,1);
        fipmobym=fimo(i,1)/mact;
        fimrefn=mo(i,1);
    else
        fips(i,1)=0;
```

```
        fimo(i,1)=0;
    end

end

omref=omrefn;
tmref=tmrefn;
thmref=thmrefn;
fmref=fmrefn;
fimref=fimrefn;

%%%%%%%%%%%%%%%%%%%%%%%%%%%%%%%%%%%%%%%%%%%%%%%%%%%%%%%%%%%%%%%%%%%%%

%Plotting M-alfa triangle
figure(5)
plot(aa,bb)
daspect('auto')
XLim('auto')
YLim([1 5])
ZLim('auto')
hold on
h=plot(d,c)
plot(e,f)
plot(z,li)
plot(m0byml,m0bym2bar,'-b')
plot(m0byml,m0bym,'*g')
xlabel('m^0/m_L','FontAngle','Italic','FontSize',12)
ylabel('m^0/m','FontAngle','Italic','FontSize',12)
title('plot of m^0/m vs m^0/ml','FontAngle','Italic','FontSize',12)
saveas(h,'malfa triangle.fig')
hold off

figure(6)
j=1:noi
hold on
xlim([1 noi])
ylim([mo(1,1)-0.02 mo(en,1)+0.02])
Zlim([1 noi])
h=plot(j,m01,'+-k')
plot(j,m02,'x-k')
%plot(j,mu,'o-k')
plot(j,ma,'.-k')
plot(j,mat,'.k')
plot(j,ml,'*-k')
xlabel('Iteration Number','FontAngle','Italic','FontSize',12)
ylabel('Multiplier','FontAngle','Italic','FontSize',12)
legend('\it m^0_1','\it m^0_2','\it m_n_o_n','\it m^\propto_T','\it
m_L',0)
title('plot of Multipliers vs
Iter.No','FontAngle','Italic','FontSize',12)
saveas(h,'mult_vs_iter.fig')
hold off


figure(7)
```

```
i=1:en
w1=plot(vol_rat(i,1),ops(i,1),vol_rat(i,1),tps(i,1),vol_rat(i,1),thps(i
,1),vol_rat(i,1),fps(i,1),vol_rat(i,1),fips(i,1))
xlabel('V_R/V_T','FontAngle','Italic','FontSize',12)
ylabel('Stresses','FontAngle','Italic','FontSize',12)
legend('1%','2%','3%','4%','5%',0)
title('stresses vs V_R/V_T','FontAngle','Italic','FontSize',12)

figure(8)
i=1:en;
w2=plot(vol_rat(i,1),omo(i,1),vol_rat(i,1),tmo(i,1),vol_rat(i,1),thmo(i
,1),vol_rat(i,1),fmo(i,1),vol_rat(i,1),fimo(i,1))
xlabel('V_R/V_T','FontAngle','Italic','FontSize',12)
ylabel('m^0','FontAngle','Italic','FontSize',12)
legend('1%','2%','3%','4%','5%',0)
title('m^0 vs V_R/V_T','FontAngle','Italic','FontSize',12)


figure(9)
i=1:en;
 xlin=linspace(min(b(i,5)),max(b(i,5)),60);
 ylin=linspace(min(b(i,6)),max(b(i,6)),60);
 [X,Y]=meshgrid(xlin,ylin);
 Z=griddata(b(i,5),b(i,6),ops(i,1),X,Y,'cubic');
 contour3(X,Y,Z,60)
 k=surface(X,Y,Z,'EdgeColor',[.8 .8 .8],'FaceColor','none')
 grid off
 view(0,90)
 colormap cool
 colorbar
 title('stress profile 1% peak
stress','FontAngle','Italic','FontSize',12)
 saveas(k,'sp1.fig')

figure(10)
i=1:en;
xlin=linspace(min(b(i,5)),max(b(i,5)),60);
ylin=linspace(min(b(i,6)),max(b(i,6)),60);
[X,Y]=meshgrid(xlin,ylin);
Z=griddata(b(i,5),b(i,6),tps(i,1),X,Y,'cubic');
contour3(X,Y,Z,60)
k=surface(X,Y,Z,'EdgeColor',[.8 .8 .8],'FaceColor','none')
grid off
view(0,90)
colormap cool
colorbar
title('stress profile 2% peak
stress','FontAngle','Italic','FontSize',12)
saveas(k,'sp2.fig')

figure(11)
i=1:en;
xlin=linspace(min(b(i,5)),max(b(i,5)),60);
ylin=linspace(min(b(i,6)),max(b(i,6)),60);
[X,Y]=meshgrid(xlin,ylin);
Z=griddata(b(i,5),b(i,6),thps(i,1),X,Y,'cubic');
```

```
contour3(X,Y,Z,60)
k=surface(X,Y,Z,'EdgeColor',[.8 .8 .8],'FaceColor','none')
grid off
view(0,90)
colormap cool
colorbar
title('stress profile 3% peak
stress','FontAngle','Italic','FontSize',12)
saveas(k,'sp3.fig')

figure(12)
i=1:en;
xlin=linspace(min(b(i,5)),max(b(i,5)),60);
ylin=linspace(min(b(i,6)),max(b(i,6)),60);
[X,Y]=meshgrid(xlin,ylin);
Z=griddata(b(i,5),b(i,6),fps(i,1),X,Y,'cubic');
contour3(X,Y,Z,60)
k=surface(X,Y,Z,'EdgeColor',[.8 .8 .8],'FaceColor','none')
grid off
view(0,90)
colormap cool
colorbar
title('stress profile 4% peak
stress','FontAngle','Italic','FontSize',12)
saveas(k,'sp4.fig')

figure(13)
i=1:en;
xlin=linspace(min(b(i,5)),max(b(i,5)),60);
ylin=linspace(min(b(i,6)),max(b(i,6)),60);
[X,Y]=meshgrid(xlin,ylin);
Z=griddata(b(i,5),b(i,6),fips(i,1),X,Y,'cubic');
contour3(X,Y,Z,60)
k=surface(X,Y,Z,'EdgeColor',[.8 .8 .8],'FaceColor','none')
grid off
view(0,90)
colormap cool
colorbar
title('stress profile 5% peak
stress','FontAngle','Italic','FontSize',12)
saveas(k,'sp5.fig')

figure(14)
i=1:en;
xlin=linspace(min(b(i,5)),max(b(i,5)),60);
ylin=linspace(min(b(i,6)),max(b(i,6)),60);
[X,Y]=meshgrid(xlin,ylin);
Z=griddata(b(i,5),b(i,6),b(i,2),X,Y,'cubic');
contour3(X,Y,Z,60)
k=surface(X,Y,Z,'EdgeColor',[.8 .8 .8],'FaceColor','none')
grid off
view(0,90)
colormap cool
colorbar
title('stress profile','FontAngle','Italic','FontSize',12)
saveas(k,'sp.fig')
```

Macro for Multiple Iterations

```
%m_alfa tangent plot(macro with mref=m0-(volrat)*(mo-ml))
%this macro is to plot m0 vs sqrt(volrat).
%enter number of iterations(noi) and actual multiplier(mact)
%gat the mult file from ansys and correct it and save as a text file in
the
%same directory as this file is

clear
load mult.txt
load b.txt
load b2.txt
load b3.txt
load b4.txt
load b5.txt

noi=18                          % number of Iterations
mact=0.81                       % Multiplier from non-linear analysis
en=2674                         % Number of Elements
sig_y=250                       % Yield Stress
tot_vol=0;


seq=[1,4,8,12,18]                     %for fix-q
%seq=[1,2,3,4,5]                      %for var-q

for ind=1:5

    if ind==1
            b=sortrows(b,-2);
    elseif ind==2
            b=sortrows(b2,-2);
    elseif ind==3
            b=sortrows(b3,-2);
    elseif ind==4
            b=sortrows(b4,-2);
    else
            b=sortrows(b5,-2);
    end

%m-alfa triangle formation
aa=1:0.0001:1+sqrt(2);
bb=aa;
d=1:0.0001:1+sqrt(2);
for i=1:14143
c(i)=(d(i)^4+4*d(i)^2-1)/(4*d(i)^2+2*sqrt(d(i)*(d(i)-1)^2*(d(i)-
1+sqrt(2))*(1+sqrt(2)-d(i))));
end
f=1:0.0001:1+sqrt(2);
for i=1:14143
    e(i)=1+sqrt(2);
end
j=1
```

```
for i=1:6:noi*6
    ml(j)=mult(i+1);
    mu(j)=mult(i+2);
    m01(j)=mult(i+3);
    m02(j)=mult(i+4);
    ma(j)=mact
    malf(j)=mult(i+5);
    j=j+1;
end

for k=1:noi
    m0byml(k)=m02(k)/ml(k);
    %if (m0byml(k)<=1+sqrt(2))
        lam(k)=(1/m0byml(k))^2;
        %else
        %lam(k)=0.171;
        %end
    m2bar(k)=(2*sqrt(lam(k))*m02(k))/(1+lam(k));
    m0bym2bar(k)=m02(k)/m2bar(k);
    m0bym(k)=m02(k)/ma(k);
end
%m0bml=m0byml(1)
for i=1:noi
if (m0byml(i)<=1+sqrt(2))
    malft(i)=m02(i)/(1+0.2929*(m0byml(i)-1));
    m0byml(i)
else
    m0bymlf(i)=((2+0.5858*(m0byml(i)-1))+sqrt((2+0.5858*(m0byml(i)-
1))^2-4))/2;
    %m0bymlf(i)=(1+0.2929*(m0byml(i)-1))+sqrt((1+0.2929*(m0byml(i)-
1))^2-1);
    malft(i)=m02(i)/(1+0.2929*(m0bymlf(i)-1));
    m0bymlf(i)
end
end
g=1
part1=-(((g^2+2)^2-5)*(8*g)-16*g^3*(g^2+2))/((g^2+2)^2-5)^2
part2=-(((g^2+2)^2-5)*((g-1)*(-3*g^2+4*g+1)+2*(-g^3+2*g^2+g))-
8*g^2*(g^2+2)*(g-1)*(1+sqrt(2)-g)*(g-1+sqrt(2)))/(((g^2+2)^2-
5)^2*sqrt(g*(g-1+sqrt(2))*(1+sqrt(2)-g)))
s=part1+part2;
z=1:0.001:5;
li=s*(z-1)+1;

%%%%%%%%%%%%%%%%%%%%%%%%%%%%%%%%%%%%%%%%%%%%%%%%%%%%%%%%%%%%%%%%%%%%%%%%%%%%%%%%%
%%%%%%%%%%%%%%%%%%%%%%%%%%%%%%%%%%%%%%%%%%%%%%%%%%%%%%%%%%%%%%%%%%%%%%%%%%%%%%%%%
for i=1:en
    voli(i,1)=0;
    vol_rat(i,1)=0;
    sq_vol_rat(i,1)=0;
end
%Caliculating the total volume of the component
vol=0
for i=1:en
    vol=vol+b(i,3);
    voli(i,1)=vol;
```

```
end
tot_vol=voli(en,1);

for i=1:en
    vol_rat(i,1)=voli(i,1)/tot_vol;
    sq_vol_rat(i,1)=sqrt(vol_rat(i,1));
end

%caliculation of total denominator
tot_din=0;
for i=1:en
    din1(i,1)=(b(i,2)*b(i,2)*b(i,3))/(b(i,4));
    tot_din=tot_din+din1(i,1);
    num1(i,1)=b(i,3)/b(i,4);
end
din=0
num=0

for i=1:en
    mo(i,1)=0;
    mobm1(i,1)=0;
    refmbm1(i,1)=0;
    refm1bm1(i,1)=0;
end

%caliculation of mo with step by step increase of volume;
for i=1:en
    num=num+num1(i,1);
    nu(i,1)=num;
    din=din+din1(i,1);
    di(i,1)=din;
    mo(i,1)=sig_y*sqrt(nu(i,1))/(sqrt(di(i,1)));
    mobm1(i,1)=mo(i,1)/mo(1,1);
    if ind==1
        moo(i,1)=mo(i,1);
        bs(i,1)=b(i,2);
        bv(i,1)=b(i,3);
        vvr(i,1)=vol_rat(i,1);
        vvr1(i,1)=sq_vol_rat(i,1);
    end
end
m0bm1=mo(en,1)/mo(1,1);

%%%%%%%%%%%%%%%%%%%%%%%%%%%%%%%%%%%%%%%%%%%%%%%%%%%%%%%%
% contour plots at different %of max stresses
%%%%%%%%%%%%%%%%%%%%%%%%%%%%%%%%%%%%%%%%%%%%%%%%%%%%%%%%

ps1=0.01*b(1,2)
ps2=0.02*b(1,2)
ps3=0.03*b(1,2)
ps4=0.04*b(1,2)
ps5=0.05*b(1,2)

for i=1:en
    if (b(i,2)>ps1)
```

```
ops(i,1)=b(i,2);
    omo(i,1)=mo(i,1);
    opmo=omo(i,1);
    opmobym=omo(i,1)/mact;
    omrefn=mo(i,1);
else
    ops(i,1)=0;
    omo(i,1)=0;

end

if (b(i,2)>ps2)
    tps(i,1)=b(i,2);
    tmo(i,1)=mo(i,1);
    tpmo=tmo(i,1);
    tpmobym=tmo(i,1)/mact;
    tmrefn=mo(i,1);
else
    tps(i,1)=0;
    tmo(i,1)=0;

end

if (b(i,2)>ps3)
    thps(i,1)=b(i,2);
    thmo(i,1)=mo(i,1);
    thpmo=thmo(i,1);
    thpmobym=thmo(i,1)/mact;
    thmrefn=mo(i,1);

else
    thps(i,1)=0;
    thmo(i,1)=0;

end


if (b(i,2)>ps4)
    fps(i,1)=b(i,2);
    fmo(i,1)=mo(i,1);
    fpmo=fmo(i,1);
    fpmobym=fmo(i,1)/mact;
    fmrefn=mo(i,1);
else
    fps(i,1)=0;
    fmo(i,1)=0;

end


if (b(i,2)>ps5)
    fips(i,1)=b(i,2);
    fimo(i,1)=mo(i,1);
    fipmo=fimo(i,1);
    fipmobym=fimo(i,1)/mact;
```

```
        fimrefn=mo(i,1);
        fivrefn=sq_vol_rat(i,1);
    else
        fips(i,1)=0;
        fimo(i,1)=0;
    end

end

omref(ind,1)=omrefn;
tmref(ind,1)=tmrefn;
thmref(ind,1)=thmrefn;
fmref(ind,1)=fmrefn;
fimref(ind,1)=fimrefn;
fimrefv(ind,1)=fivrefn;

%%%%%%%%%%%%%%%%%%%%%%%%%%%%%%%%%%%%%%%%%%%%%%%%%%%%%%%%%%%%%%%
%calculation of ml for individual elements
%%%%%%%%%%%%%%%%%%%%%%%%%%%%%%%%%%%%%%%%%%%%%%%%%%%%%%%%%%%%%%%

for i=1:en
    ml1(i,1)=sig_y/b(i,2);
    ml1_vol(i,1)=tot_vol-voli(i,1);
    ml1_volrat(i,1)=ml1_vol(i,1)/tot_vol;
    sq_ml1_volrat(i,1)=sqrt(ml1_volrat(i,1));
end

 hh=1/en;


%caliculation of average m0(trapizoidal method)
%  mrefn=0
%  mref=0
%  for i=2:en
%       mrefn=mrefn+(((mo(i-1,1)+mo(i,1))/2)*(vol_rat(i,1)-vol_rat(i-
1,1)));
%  end
%  mref=mrefn
mref=0
mr1=0
mrow=0
 for i=2:en
     mr1=mr1+(vol_rat(i,1)-vol_rat(i-1,1))*(mo(i,1)-mo(1,1));
     mrw(i,1)=mo(1,1)+mr1;
 end
     mrow=mo(1,1)+mr1;
mref=mrow;
vrreq=0;
reffv=0;

for i=1:en
    if (mact>=mo(i,1))
        vrreq=vol_rat(i,1);
    end
%      if (mref>=mo(i,1))
```

```
%          reffv=vol_rat(i,1);
%      end
end
reqvr(ind)=vrreq;
% refv(ind)=reffv;

for i=1:en
     refm(i,1)=mref;
     refmbml(i,1)=mref/mo(1,1);
end

%caliculation of average m0(trapizoidal method)
%  mrefn1=0
%  mref1=0
%  for i=2:en
%       mrefn1=mrefn1+(((mo(i-1,1)+mo(i,1))/2)*(sq_vol_rat(i,1)-
sq_vol_rat(i-1,1)));
%  end
%  mref1=mrefn1

 mref1=0
 mr2=0
 mrow1=0
 for i=2:en
      mr2=mr2+(sq_vol_rat(i,1)-sq_vol_rat(i-1,1))*(mo(i,1)-mo(1,1));
      mrw1(i,1)=mo(1,1)+mr2;
 end
 mrow1=mo(1,1)+mr2;
 mref1=mrow1;

vrreq1=0;
reffv1=0;
for i=1:en
    if (mact>=mo(i,1))
         vrreq1=sq_vol_rat(i,1);
    end
%      if (mref1>=mo(i,1))
%            reffv1=sq_vol_rat(i,1);
%      end
end

mrefbml=mref1/mo(1,1);
reqvr1(ind)=vrreq1;
% refv1(ind)=reffv1;

for i=1:en
    refm1(i,1)=mref1;
    refm1bml(i,1)=mref1/mo(1,1);
    mat(i,1)=mact;
    matbml(i,1)=mact/mo(1,1);
end


%calculating malf tan for iterations Vr/Vt
mz1(ind,1)=mref;
```

```
mal1(ind,1)=mo(1,1);
mzbymal1=mz1(ind,1)/mal1(ind,1);

if (mzbymal1<=1+sqrt(2))
    malftan1(ind,1)=mz1(ind,1)/(1+0.2929*(mzbymal1-1))
    mzbymal1
else
    mzbymalf1=((2+0.5858*(mzbymal1-1))+sqrt((2+0.5858*(mzbymal1-1))^2-
4))/2;
    malftan1(ind,1)=mz1(ind,1)/(1+0.2929*(mzbymalf1-1))
    mzbymalf1
end

%calculating malf tan for iterations sqrt(Vr/Vt)
mz2(ind,1)=mref1;
mal2(ind,1)=mo(1,1);
mzbymal2=mz2(ind,1)/mal2(ind,1);

if (mzbymal2<=1+sqrt(2))
    malftan2(ind,1)=mz2(ind,1)/(1+0.2929*(mzbymal2-1))
    mzbymal2
else
    mzbymalf2=((2+0.5858*(mzbymal2-1))+sqrt((2+0.5858*(mzbymal2-1))^2-
4))/2;
    malftan2(ind,1)=mz2(ind,1)/(1+0.2929*(mzbymalf2-1))
    mzbymalf2
end

%calculating malf tan for iterations sqrt(Vr/Vt)
mz3(ind,1)=fimrefn;
mal3(ind,1)=mo(1,1);
mzbymal3=mz3(ind,1)/mal3(ind,1);

if (mzbymal3<=1+sqrt(2))
    malftan3(ind,1)=mz3(ind,1)/(1+0.2929*(mzbymal3-1))
    mzbymal3
else
    mzbymalf3=((2+0.5858*(mzbymal3-1))+sqrt((2+0.5858*(mzbymal3-1))^2-
4))/2;
    malftan3(ind,1)=mz3(ind,1)/(1+0.2929*(mzbymalf3-1))
    mzbymalf3
end

% for j=1:en
%       if (mref>=mo(j,1))
%           refv(ind,1)=vvr(j,1);
%     end
%     if (mref1>=mo(j,1))
%         refv1(ind,1)=vvr1(j,1);
%     end
%         if (mact>=mo(j,1))
%         rv(ind,1)=vvr(j,1);
%         rrv(ind,1)=vvr1(j,1);
%     end
% end
```

```
%plotting mo vs volume ratio
figure(1)
hold on
i=1:en;
if ind==1
        h=plot(vol_rat(i,1),mo(i,1),'-k')
        plot(vol_rat(i,1),mat(i,1),'-k','linewidth',3.5)
        plot(vol_rat(i,1),refm(i,1),'--k')
    elseif ind==2
        %h=plot(vol_rat(i,1),mo(i,1),':b')
         h= plot(vol_rat(i,1),refm(i,1),':k')

    elseif ind==3
        %h=plot(vol_rat(i,1),mo(i,1),'-.b')
         h= plot(vol_rat(i,1),refm(i,1),'-.k')

    elseif ind==4
        %h=plot(vol_rat(i,1),mo(i,1),'--b')
          h=plot(vol_rat(i,1),refm(i,1),'-k','linewidth',1.5)

    else
        %h=plot(vol_rat(i,1),mo(i,1),'-b','linewidth',1.5)
         h= plot(vol_rat(i,1),refm(i,1),'-k','linewidth',2.5)
         legend('\it m^0','\it m_n_o_n','\it iter 1','\it iter4','\it
iter 8','\it iter 12','\it iter 16',0)

end
xlabel('V_R/V_T','FontAngle','Italic','FontSize',12)
ylabel('m^0','FontAngle','Italic','FontSize',12)
title('Plot of m^0 vs V_R/V_T','FontAngle','Italic','FontSize',12)
saveas(h,'mrefiter.fig')
hold off

figure(2)
hold on
i=1:en;
if ind==1
        h=plot(sq_vol_rat(i,1),mo(i,1),'-k')
        plot(sq_vol_rat(i,1),mat(i,1),'-k','linewidth',3.5)
        plot(sq_vol_rat(i,1),refm1(i,1),'--k')

    elseif ind==2
        %h=plot(sq_vol_rat(i,1),mo(i,1),':b')
          h=plot(sq_vol_rat(i,1),refm1(i,1),':k')

    elseif ind==3
        %h=plot(sq_vol_rat(i,1),mo(i,1),'-.b')
          h=plot(sq_vol_rat(i,1),refm1(i,1),'-.k')
    elseif ind==4
        %h=plot(sq_vol_rat(i,1),mo(i,1),'--b')
           h=plot(sq_vol_rat(i,1),refm1(i,1),'-k','linewidth',1.5)
    else
        %h=plot(sq_vol_rat(i,1),mo(i,1),'-b','linewidth',1.5)
           h=plot(sq_vol_rat(i,1),refm1(i,1),'-k','linewidth',2.5)
```

```
        legend('\it m^0/m_L','\it m_n_o_n','\it iter 1','\it
iter4','\it iter 8','\it iter 12','\it iter 16',0)
    end
xlabel('\surd (V_R / V_T)','FontAngle','Italic','FontSize',12)
ylabel('m^0','FontAngle','Italic','FontSize',12)
title('Plot of m^0 vs \surd (V_R /
V_T)','FontAngle','Italic','FontSize',12')
saveas(h,'mrefliter.fig')
%hold off

% caliculating ml for individual element
for i=1:en
    ml1(i,1)=(sig_y*sqrt(b(i,3)))/sqrt(din1(i,1));
end

%%%%%%%%%%%%%%%%%%%%%%%%%%%%%%%%%%%%%%%%%%%%%%%%%%%%%%%%%
%%%%%%%%%%%%%%%%%%%%%%%%%%%%%%%%%%%%%%%%%%%%%%%%%%%%%%%%%


%Plotting M-alfa triangle
figure(3)
h=plot(aa,bb)
daspect('auto')
XLim('auto')
YLim([1 5])
ZLim('auto')
hold on
plot(d,c)
plot(e,f)
plot(z,li)
%plot(m0byml,m0bym2bar,'-b')
plot(m0byml,m0bym,'*g')
xlabel('m^0/m_L','FontAngle','Italic','FontSize',12)
ylabel('m^0/m','FontAngle','Italic','FontSize',12)
title('Plot of m^0/m vs m^0/ml','FontAngle','Italic','FontSize',12)
saveas(h,'malfa triangle1.fig')
hold off

%Plotting variation of multipliers with iteration number
figure(4)
j=1:noi
hold on
h=plot(j,m01,'+-r')
daspect('auto')
xlim([1 noi])
plot(j,m02,'x-b')
%plot(j,mu,'o-y')
plot(j,ma,'.-k')
%plot(j,malf,'.k')
plot(j,ml,'*-g')
xlabel('Iteration Number','FontAngle','Italic','FontSize',12)
ylabel('Multiplier','FontAngle','Italic','FontSize',12)
legend('\it m^0_1','\it m^0_2','\it m_n_o_n','\it m_L',0)
title('Plot of Multipliers vs
Iter.No','FontAngle','Italic','FontSize',12)
saveas(h,'mult_vs_iter1.fig')
```

```
hold off

figure(5)
i=1:en
hold on
if ind==1
        h=plot(vol_rat(i,1),b(i,2),'--k')
    elseif ind==2
        h=plot(vol_rat(i,1),b(i,2),':k')
    elseif ind==3
        h=plot(vol_rat(i,1),b(i,2),'-.k')
    elseif ind==4
        h=plot(vol_rat(i,1),b(i,2),'-k','linewidth',1.5)
    else
       h=plot(vol_rat(i,1),b(i,2),'-k','linewidth',2.5)
     end
xlabel('V_R/V_T','FontAngle','Italic','FontSize',12)
ylabel('Stresses','FontAngle','Italic','FontSize',12)
%legend('\it iter 1','\it iter4','\it iter 8','\it iter 12','\it iter
18',0)
legend('\it iter 1','\it iter4','\it iter 8','\it iter 12','\it iter
18',0)
title('Stresses vs V_R/V_T','FontAngle','Italic','FontSize',12)
saveas(h,'str_vs_volrat.fig')

figure(6)
i=1:en
hold on
if ind==1
        h=plot(vol_rat(i,1),mo(i,1),'--k')
    elseif ind==2
        h=plot(vol_rat(i,1),mo(i,1),':k')
    elseif ind==3
        h=plot(vol_rat(i,1),mo(i,1),'-.k')
    elseif ind==4
        h=plot(vol_rat(i,1),mo(i,1),'-k','linewidth',1.5)
    else
       h=plot(vol_rat(i,1),mo(i,1),'-k','linewidth',2.5)
     end
xlabel('V_R/V_T','FontAngle','Italic','FontSize',12)
ylabel('m^0','FontAngle','Italic','FontSize',12)
title('Plot of m^0 vs V_R / V_T','FontAngle','Italic','FontSize',12)
%legend('\it iter 1','\it iter 2','\it iter 3','\it iter 4','\it iter
5',0)
legend('\it iter 1','\it iter4','\it iter 8','\it iter 12','\it iter
18',0)
saveas(h,'m0_vs_volrat.fig')

figure(7)
i=1:en
hold on
if ind==1
        h=plot(sq_vol_rat(i,1),b(i,2),'--k')
    elseif ind==2
        h=plot(sq_vol_rat(i,1),b(i,2),':k')
    elseif ind==3
```

```
        h=plot(sq_vol_rat(i,1),b(i,2),'-.k')
    elseif ind==4
        h=plot(sq_vol_rat(i,1),b(i,2),'-k','linewidth',1.5)
    else
       h=plot(sq_vol_rat(i,1),b(i,2),'-k','linewidth',2.5)
     end
xlabel('\surd (V_R/V_T)','FontAngle','Italic','FontSize',12)
ylabel('Stresses','FontAngle','Italic','FontSize',12)
%legend('\it iter 1','\it iter 2','\it iter 3','\it iter 4','\it iter
5',0)
legend('\it iter 1','\it iter4','\it iter 8','\it iter 12','\it iter
18',0)
title('Stresses vs \surd (V_R/V_T)','FontAngle','Italic','FontSize',12)
saveas(h,'str_vs_sqrtvolrat.fig')

figure(8)
i=1:en
hold on
if ind==1
        h=plot(sq_vol_rat(i,1),mo(i,1),'--k')
    elseif ind==2
        h=plot(sq_vol_rat(i,1),mo(i,1),':k')
    elseif ind==3
        h=plot(sq_vol_rat(i,1),mo(i,1),'-.k')
    elseif ind==4
        h=plot(sq_vol_rat(i,1),mo(i,1),'-k','linewidth',1.5)
    else
       h=plot(sq_vol_rat(i,1),mo(i,1),'-k','linewidth',2.5)
     end
xlabel('\surd (V_R/V_T)','FontAngle','Italic','FontSize',12)
ylabel('m^0','FontAngle','Italic','FontSize',12)
title('Plot of m^0 vs \surd (V_R /
V_T)','FontAngle','Italic','FontSize',12')
%legend('\it iter 1','\it iter 2','\it iter 3','\it iter 4','\it iter
5',0)
legend('\it iter 1','\it iter4','\it iter 8','\it iter 12','\it iter
18',0)
saveas(h,'m0_vs_sqrtvolrat.fig')
end


for i=1:5
    refv(i)=0;
    refv1(i)=0;
end

for i=1:5
  for j=1:en
     if (mz1(i,1)>=moo(j,1))
         refv(i)=vvr(j,1);
    end
    if (mz2(i,1)>=moo(j,1))
        refv1(i)=vvr1(j,1);
    end
    if (mact>=moo(j,1))
        rv(i)=vvr(j,1);
```

```
        rrv(i)=vvr1(j,1);
    end
    end
end


figure(9)
i=1:5
w2=plot(seq,malftan1,'+-g',seq,mz1,'*-b',seq,mact,'o-k')
daspect('auto')
xlim([1 noi])
xlabel('Iteration Number','FontAngle','Italic','FontSize',12)
ylabel('Multiplier','FontAngle','Italic','FontSize',12)
legend('\it m^T_\propto(V_R_p)','\it m^0(V_R_p)','\it m_n_o_n',0)
title('Plot of Multipliers vs
Iter.No','FontAngle','Italic','FontSize',12)

figure(10)
i=1:5
w2=plot(seq,malftan2,'+-g',seq,mz2,'*-b',seq,mact,'o-k')
daspect('auto')
xlim([1 noi])
xlabel('Iteration Number','FontAngle','Italic','FontSize',12)
ylabel('Multiplier','FontAngle','Italic','FontSize',12)
legend('\it m^T_\propto(V_R_p)','\it m^0(V_R_p)','\it m_n_o_n',0)
title('Plot of Multipliers vs
Iter.No','FontAngle','Italic','FontSize',12)

figure(11)
i=1:5
w2=plot(seq,refv,'+-b',seq,rv,'*-k')
daspect('auto')
xlim([1 noi])
xlabel('Iteration Number','FontAngle','Italic','FontSize',12)
ylabel('V_R/V_T','FontAngle','Italic','FontSize',12)
legend('\it (V_R/V_T)_p','\it (V_R/V_T)_n_o_n',0)
title('Plot of V_R/V_T vs Iter.No','FontAngle','Italic','FontSize',12)

figure(12)
i=1:5
w2=plot(seq,refv1,'+-b',seq,rrv,'*-k')
daspect('auto')
xlim([1 noi])
xlabel('Iteration Number','FontAngle','Italic','FontSize',12)
ylabel('\surd (V_R/V_T)','FontAngle','Italic','FontSize',12)
legend('\it \surd (V_R/V_T)_p','\it \surd (V_R/V_T)_n_o_n',0)
title('Plot of \surd (V_R/V_T) vs
Iter.No','FontAngle','Italic','FontSize',12)

figure(13)
i=1:5
w2=plot(seq,malftan3,'+-g',seq,mz3,'*-b',seq,mact,'o-k')
daspect('auto')
xlim([1 noi])
xlabel('Iteration Number','FontAngle','Italic','FontSize',12)
ylabel('Multiplier','FontAngle','Italic','FontSize',12)
```

```
legend('\it m^T_\propto(V_R_e)','\it  m^0(V_R_e)','\it m_n_o_n',0)
title('Plot of Multipliers vs
Iter.No','FontAngle','Italic','FontSize',12)

figure(14)
i=1:5
w2=plot(seq,fimrefv,'+-k')
daspect('auto')
xlim([1 noi])
xlabel('Iteration Number','FontAngle','Italic','FontSize',12)
ylabel('V_R/V_T','FontAngle','Italic','FontSize',12)
legend('\it (V_R/V_T)_e',0)
title('Plot of V_R/V_T vs Iter.No','FontAngle','Italic','FontSize',12)
```

Sample macro for simultaneous correction of peak stress and dead volume effect

```
clear
load mult.txt
noi=50
mact=1.35
j=1
l=1
for i=1:6:noi*6
    ml(j,1)=mult(i+1);
    mu(j,1)=mult(i+2);
    m01(j,1)=mult(i+3);
    m02(j,1)=mult(i+4);
    mat(j,1)=mult(i+5);
    ma(j,1)=mact;
    mobml(j,1)=m02(j,1)/ml(j,1);

    if l==1
    crit1(l,i)=1;
    else
    crit1(l,1)=(m02(l-1,1)-m02(l,1))/m02(l-1,1);
    if (crit1(l,1)>=0.01)
        iter1=l;
    end
    end
    l=l+1;

    if j==1
    crit2(j,i)=1;
    else
    crit2(j,1)=(mat(j,1)-mat(j-1,1))/mat(j-1,1);
    if (crit2(j,1)>=0.01)
        iter2=j;
    end
    end
    j=j+1;
 end

for i=1:1:50
    gei(i,1)=m02(i,1)/ml(i,1);
```

```
    if (gei(i,1)>=1+sqrt(2))
    Robd(i,1)=(1+(gei(i,1)*gei(i,1)))/(2*gei(i,1));
    Rob(i,1)=1+0.2929*(gei(i,1)-1);
    mac(i,1)=m02(i,1)*(Rob(i,1)/Robd(i,1));
    gef(i,1)=((1+0.2929*(gei(i,1)-1))+sqrt((1+0.2929*(gei(i,1)-1))^2-
1));
    %gef(i,1)=((2+0.5858*(gei(i,1)-1))+sqrt((2+0.5858*(gei(i,1)-1))^2-
4))/2;
    malf(i,1)=mac(i,1)/(1+0.2929*(gef(i,1)-1));
    else
    malf(i,1)=m02(i)/(1+0.2929*(gei(i,1)-1));
    mac(i,1)=m02(i,1);
    end
    if i==1
    crit3(i,1)=1;
    else
    crit3(i,1)=(malf(i,1)-malf(i-1,1))/malf(i-1,1);
    if (crit3(i,1)>=0.01)
        iter3=i;
    end
    end
end

i=1
mc(i,1)=mac(i,1);
malc(i,1)=malf(i,1);
mlc(i,1)=ml(i,1);
i=i+1;
for j=5:5:20
mc(i,1)=mac(j,1);
malc(i,1)=malf(j,1);
mlc(i,1)=ml(j,1);
i=i+1;
end

figure(1)
j=1:noi
daspect('auto')
XLim([1 noi])
hold on
plot(j,m01,'+-r')
h=plot(j,m02,'x-b')
plot(j,ma,'.-k')
plot(j,malf,'.k')
plot(j,ml,'*-g')
plot(j,mat,'.g')
xlabel('Iteration
Number','FontAngle','Italic','FontWeight','bold','FontSize',12)
ylabel('Multiplier','FontAngle','Italic','FontWeight','bold','FontSize'
,12)
%legend('\it m^0_1','\it m^0_2','\it m_a_c_t','\it m_L',0)
title('Plot of Multipliers vs
Iter.No','FontAngle','Italic','FontWeight','bold','FontSize',12)
saveas(h,'mult_vs_iter3.fig')
hold off
```

```
figure(2)
k=1:20
daspect('auto')
XLim([1 20])
% YLim([1 15])
% ZLim('auto')
hold on
plot(k,m01(k,1),'+-r')
h=plot(k,m02(k,1),'x-b')
plot(k,ma(k,1),'.-k')
plot(k,malf(k,1),'.k')
plot(k,ml(k,1),'*-g')
%plot(j,mat(j,1),'.g')
xlabel('Iteration
Number','FontAngle','Italic','FontWeight','bold','FontSize',12)
ylabel('Multiplier','FontAngle','Italic','FontWeight','bold','FontSize'
,12)
legend('\it m^0_1','\it m^0_2','\it m_a_c_t','\it m^\propto_T','\it
m_L',0)
title('Plot of Multipliers vs
Iter.No','FontAngle','Italic','FontWeight','bold','FontSize',12)
saveas(h,'mult_vs_iter4.fig')
hold off
```

Appendix-C

EMAP Iteration Results for All Examples

In the Following Section the EMAP analysis results if all the problems, upto fifty iterations have been provided. For the EMAP analysis a 'q' of 0.1 has been used. It can be seen from the results that even after fifty Iterations of EMAP the solutions are not completely converged onto non-linear, where as using the methods developed in the thesis they are converging much faster.

The convergemce criterion used for different methods in this thesis are:

S. NO	Method	Category of Component	Convergence Criterion
1	Elastic Reference volume Method	Any Category	$\frac{m_\alpha^T(V_{\mathrm{Re}})_\xi - m_\alpha^T(V_{\mathrm{Re}})_{\xi-1}}{m_\alpha^T(V_{\mathrm{Re}})_\xi} \le 0.01$
2	Plastic Reference Volume Method	1st Category	$\frac{m^0(V_{Rp})_\xi - m^0(V_{Rp})_{\xi-1}}{m^0(V_{Rp})_\xi} \le 0.01$
		2nd Category	$\frac{m_\alpha^T(V_{Rp})_\xi - m_\alpha^T(V_{Rp})_{\xi-1}}{m_\alpha^T(V_{Rp})_\xi} \le 0.01$
3	Lower bounded m_α^T Method	2nd Category	$\frac{(m_\alpha^T)_\xi - (m_\alpha^T)_{\xi-1}}{(m_\alpha^T)_\xi} \le 0.01$

	Thick Walled Cylinder			Torispherical Head			Unreinforced Axi-symmetric Nozzle		
Iteration	m_1^0	m_2^0	m_L	m_1^0	m_2^0	m_L	m_1^0	m_2^0	m_L
1	2.2941	2.2941	1.7061	3.0293	3.0293	1.4584	1.8704	1.8704	0.9215
2	2.2937	2.2865	1.7507	3.029	3.0126	1.5109	1.8704	1.8686	0.9682
3	2.2927	2.2804	1.7923	3.0279	2.9979	1.5623	1.8702	1.8671	1.013
4	2.2912	2.2754	1.8312	3.0262	2.9849	1.6126	1.87	1.8656	1.0558
5	2.2895	2.2714	1.8673	3.0239	2.9734	1.6615	1.8696	1.8644	1.0965
6	2.2876	2.2681	1.9007	3.0213	2.9632	1.7089	1.8693	1.8632	1.1351
7	2.2855	2.2654	1.9316	3.0183	2.954	1.7549	1.8689	1.8621	1.1639
8	2.2835	2.2633	1.9601	3.0151	2.9459	1.7993	1.8685	1.8612	1.1853
9	2.2814	2.2616	1.9863	3.0117	2.9386	1.8421	1.8682	1.8602	1.2038
10	2.2794	2.2602	2.0104	3.0082	2.932	1.8833	1.8678	1.8594	1.2214
11	2.2775	2.259	2.0325	3.0045	2.9261	1.9228	1.8674	1.8586	1.2383
12	2.2757	2.2581	2.0527	3.0008	2.9208	1.9608	1.867	1.8578	1.2544
13	2.2739	2.2574	2.0712	2.9971	2.916	1.9972	1.8667	1.857	1.2698
14	2.2723	2.2568	2.0881	2.9934	2.9117	2.032	1.8663	1.8563	1.2832
15	2.2707	2.2563	2.1036	2.9897	2.9078	2.0654	1.866	1.8556	1.2954
16	2.2693	2.2559	2.1176	2.9859	2.9042	2.0972	1.8656	1.8549	1.3072
17	2.268	2.2556	2.1304	2.9822	2.901	2.1276	1.8653	1.8542	1.3186
18	2.2668	2.2553	2.142	2.9786	2.8981	2.1567	1.865	1.8535	1.3296
19	2.2657	2.2551	2.1526	2.9749	2.8955	2.1844	1.8648	1.8529	1.3401
20	2.2646	2.255	2.1622	2.9714	2.8932	2.2108	1.8645	1.8522	1.3503
21	2.2637	2.2548	2.171	2.9678	2.891	2.236	1.8642	1.8516	1.3602
22	2.2628	2.2547	2.1789	2.9643	2.8891	2.26	1.864	1.8509	1.3697
23	2.262	2.2546	2.1861	2.9609	2.8873	2.2829	1.8637	1.8503	1.3789
24	2.2613	2.2546	2.1926	2.9575	2.8857	2.3047	1.8635	1.8497	1.3878
25	2.2607	2.2545	2.1985	2.9541	2.8843	2.3254	1.8632	1.849	1.3964
26	2.2601	2.2545	2.2038	2.9508	2.883	2.3451	1.863	1.8484	1.4047
27	2.2595	2.2544	2.2087	2.9475	2.8818	2.3639	1.8628	1.8478	1.4127
28	2.259	2.2544	2.213	2.9443	2.8807	2.3818	1.8626	1.8472	1.4205
29	2.2586	2.2544	2.217	2.9412	2.8797	2.3989	1.8624	1.8466	1.4281
30	2.2582	2.2544	2.2206	2.9381	2.8787	2.4151	1.8622	1.846	1.4354
31	2.2578	2.2544	2.2238	2.9352	2.8779	2.4305	1.862	1.8454	1.4425
32	2.2575	2.2544	2.2268	2.9323	2.8771	2.4452	1.8618	1.8448	1.4493
33	2.2572	2.2544	2.2294	2.9295	2.8763	2.4592	1.8616	1.8442	1.4557
34	2.2569	2.2543	2.2318	2.9269	2.8756	2.4725	1.8614	1.8436	1.4617
35	2.2567	2.2543	2.234	2.9243	2.875	2.4852	1.8613	1.843	1.4675
36	2.2564	2.2543	2.236	2.9218	2.8744	2.4973	1.8611	1.8424	1.4731
37	2.2562	2.2543	2.2378	2.9195	2.8738	2.5088	1.8609	1.8418	1.4786
38	2.2561	2.2543	2.2394	2.9172	2.8733	2.5198	1.8607	1.8412	1.484
39	2.2559	2.2543	2.2408	2.915	2.8728	2.5303	1.8605	1.8406	1.4892
40	2.2557	2.2543	2.2421	2.913	2.8723	2.5403	1.8604	1.84	1.4943
41	2.2556	2.2543	2.2433	2.911	2.8719	2.5498	1.8602	1.8394	1.4992
42	2.2555	2.2543	2.2444	2.9091	2.8714	2.5589	1.86	1.8388	1.504
43	2.2554	2.2543	2.2453	2.9073	2.871	2.5604	1.8599	1.8382	1.5087
44	2.2553	2.2543	2.2462	2.9056	2.8706	2.5315	1.8597	1.8377	1.5133
45	2.2552	2.2543	2.247	2.904	2.8703	2.5076	1.8595	1.8371	1.5178
46	2.2551	2.2543	2.2477	2.9024	2.8699	2.4881	1.8593	1.8365	1.5221
47	2.255	2.2543	2.2484	2.9009	2.8696	2.4723	1.8592	1.8359	1.5264
48	2.255	2.2543	2.2489	2.8995	2.8693	2.4596	1.859	1.8353	1.5305
49	2.2549	2.2543	2.2495	2.8981	2.8689	2.4496	1.8588	1.8348	1.5345
50	2.2548	2.2543	2.2499	2.8968	2.8686	2.4419	1.8587	1.8342	1.5385

	Reinforced Axi-symmetric Nozzle			Pressure Vessel Support Skirt			CT Specimen		
Iteration	m_1^0	m_2^0	m_L	m_1^0	m_2^0	m_L	m_1^0	m_2^0	m_L
1	2.011	2.011	1.2478	3.6136	3.6136	1.5219	1.5496	1.5496	0.1084
2	2.0109	2.0086	1.3003	3.6129	3.5935	1.5788	1.5502	1.5034	0.1205
3	2.0107	2.0064	1.3507	3.6114	3.5753	1.6347	1.5485	1.463	0.1336
4	2.0105	2.0046	1.3991	3.6091	3.5586	1.6893	1.545	1.4272	0.1475
5	2.0101	2.0029	1.4453	3.6062	3.5434	1.7424	1.5399	1.3952	0.1623
6	2.0097	2.0015	1.4893	3.6028	3.5293	1.7938	1.5338	1.3663	0.178
7	2.0093	2.0002	1.5311	3.5991	3.5162	1.8436	1.5267	1.3399	0.1944
8	2.0088	1.999	1.5706	3.5951	3.5041	1.8915	1.519	1.3158	0.2116
9	2.0084	1.9979	1.608	3.591	3.4927	1.9375	1.5108	1.2935	0.2296
10	2.008	1.9969	1.6432	3.5867	3.482	1.9816	1.5023	1.2729	0.2481
11	2.0076	1.9959	1.6763	3.5824	3.472	2.0239	1.4935	1.2538	0.2672
12	2.0072	1.9951	1.7075	3.5781	3.4625	2.0643	1.4846	1.2359	0.2867
13	2.0068	1.9942	1.7366	3.5738	3.4535	2.1029	1.4757	1.2192	0.3066
14	2.0064	1.9934	1.7639	3.5695	3.4449	2.1397	1.4668	1.2035	0.3265
15	2.006	1.9927	1.769	3.5653	3.4367	2.1748	1.458	1.1888	0.3464
16	2.0057	1.9919	1.768	3.5611	3.429	2.2082	1.4493	1.1749	0.3663
17	2.0054	1.9912	1.7673	3.5571	3.4215	2.2401	1.4407	1.1617	0.3859
18	2.0051	1.9906	1.7669	3.5531	3.4144	2.2705	1.4323	1.1492	0.4053
19	2.0048	1.9899	1.7666	3.5491	3.4075	2.2994	1.4241	1.1374	0.4245
20	2.0046	1.9892	1.7666	3.5453	3.4009	2.327	1.4161	1.1261	0.4433
21	2.0043	1.9886	1.7667	3.5415	3.3946	2.3533	1.4083	1.1154	0.4618
22	2.0041	1.988	1.767	3.5377	3.3886	2.3785	1.4007	1.1052	0.4799
23	2.0039	1.9874	1.7675	3.534	3.3827	2.4025	1.3934	1.0955	0.4976
24	2.0037	1.9867	1.768	3.5304	3.3771	2.4255	1.3863	1.0862	0.5148
25	2.0035	1.9861	1.7687	3.5267	3.3717	2.4475	1.3795	1.0773	0.5315
26	2.0033	1.9855	1.7694	3.5231	3.3665	2.4686	1.3729	1.0687	0.5476
27	2.0031	1.985	1.7702	3.5195	3.3616	2.4888	1.3665	1.0606	0.5631
28	2.003	1.9844	1.771	3.5159	3.3568	2.5082	1.3604	1.0527	0.5781
29	2.0028	1.9838	1.772	3.5122	3.3522	2.5269	1.3546	1.0452	0.5925
30	2.0027	1.9832	1.7729	3.5086	3.3478	2.5449	1.3489	1.038	0.6062
31	2.0025	1.9826	1.7739	3.5049	3.3435	2.5622	1.3435	1.031	0.6193
32	2.0024	1.9821	1.7749	3.5012	3.3395	2.5789	1.3383	1.0243	0.6318
33	2.0023	1.9815	1.776	3.4974	3.3356	2.595	1.3333	1.0179	0.6437
34	2.0022	1.9809	1.7771	3.4937	3.3319	2.6105	1.3284	1.0117	0.6497
35	2.0021	1.9804	1.7781	3.4898	3.3283	2.6256	1.3238	1.0057	0.6519
36	2.002	1.9798	1.7792	3.4859	3.3248	2.6401	1.3194	0.9999	0.6543
37	2.0019	1.9793	1.7803	3.482	3.3215	2.6542	1.3151	0.9944	0.6569
38	2.0018	1.9787	1.7814	3.4781	3.3184	2.6678	1.311	0.989	0.6596
39	2.0017	1.9782	1.7825	3.4741	3.3153	2.6809	1.307	0.9839	0.6623
40	2.0016	1.9776	1.7836	3.4701	3.3124	2.6937	1.3032	0.9789	0.6651
41	2.0015	1.9771	1.7847	3.4661	3.3096	2.706	1.2996	0.9741	0.6678
42	2.0014	1.9765	1.7858	3.4621	3.3068	2.718	1.2961	0.9694	0.6706
43	2.0014	1.976	1.7869	3.4581	3.3042	2.7295	1.2927	0.9649	0.6734
44	2.0013	1.9755	1.7879	3.4541	3.3016	2.7406	1.2894	0.9606	0.6761
45	2.0012	1.9749	1.789	3.4501	3.2992	2.7512	1.2863	0.9564	0.6788
46	2.0011	1.9744	1.79	3.4461	3.2968	2.7616	1.2833	0.9524	0.6814
47	2.0011	1.9739	1.7911	3.4422	3.2944	2.7715	1.2804	0.9484	0.6839
48	2.001	1.9733	1.7921	3.4383	3.2922	2.7812	1.2776	0.9447	0.6864
49	2.0009	1.9728	1.7931	3.4345	3.29	2.7905	1.275	0.941	0.6888
50	2.0009	1.9723	1.7941	3.4308	3.2879	2.7996	1.2724	0.9375	0.6912

	Single Edge Notch Bend			Plate with multiple Cracks			Plate with a Hole		
Iteration	m_1^0	m_2^0	m_L	m_1^0	m_2^0	m_L	m_1^0	m_2^0	m_L
1	4.7588	4.7588	0.2015	2.3588	2.3588	0.1974	1.2214	1.2214	0.4811
2	4.761	4.4382	0.221	2.359	2.3433	0.2138	1.2214	1.2162	0.4963
3	4.7586	4.145	0.2417	2.3588	2.3282	0.2314	1.2213	1.2112	0.5114
4	4.7524	3.8769	0.2637	2.3583	2.3134	0.2501	1.2211	1.2062	0.5263
5	4.7428	3.6324	0.2868	2.3574	2.2987	0.2698	1.2208	1.2014	0.5411
6	4.7304	3.4098	0.3111	2.3562	2.2842	0.2906	1.2205	1.1967	0.5557
7	4.7157	3.2075	0.3363	2.3548	2.2697	0.3122	1.2202	1.1921	0.57
8	4.6991	3.0242	0.3626	2.3532	2.2552	0.3347	1.2198	1.1875	0.5841
9	4.6811	2.8585	0.3896	2.3513	2.2406	0.3581	1.2193	1.183	0.5978
10	4.6621	2.7089	0.4174	2.3494	2.226	0.3821	1.2189	1.1786	0.6112
11	4.6426	2.5741	0.4459	2.3472	2.2114	0.4068	1.2184	1.1743	0.6242
12	4.6228	2.4529	0.4749	2.345	2.1966	0.4321	1.218	1.17	0.6369
13	4.603	2.3441	0.5043	2.3426	2.1817	0.4579	1.2175	1.1658	0.6492
14	4.5835	2.2465	0.534	2.3401	2.1667	0.4841	1.217	1.1617	0.661
15	4.5645	2.1591	0.5639	2.3376	2.1517	0.5107	1.2164	1.1575	0.6725
16	4.5459	2.081	0.594	2.335	2.1365	0.5375	1.2159	1.1535	0.6836
17	4.528	2.0111	0.6239	2.3323	2.1212	0.5644	1.2154	1.1495	0.6943
18	4.5108	1.9485	0.6537	2.3296	2.1059	0.5913	1.2149	1.1455	0.7045
19	4.4943	1.8927	0.6833	2.3269	2.0904	0.6183	1.2143	1.1417	0.7144
20	4.4785	1.8427	0.7124	2.3241	2.075	0.6324	1.2138	1.1378	0.7238
21	4.4634	1.798	0.7411	2.3213	2.0594	0.6446	1.2133	1.134	0.7329
22	4.4492	1.758	0.7692	2.3185	2.0439	0.658	1.2128	1.1303	0.7416
23	4.4356	1.7221	0.7966	2.3156	2.0283	0.6724	1.2122	1.1266	0.7499
24	4.4227	1.6899	0.8232	2.3128	2.0126	0.6877	1.2117	1.1229	0.7578
25	4.4106	1.6609	0.8491	2.31	1.9971	0.7037	1.2112	1.1193	0.7654
26	4.3991	1.6349	0.8741	2.3071	1.9815	0.7204	1.2107	1.1158	0.7726
27	4.3883	1.6114	0.8982	2.3043	1.9659	0.7375	1.2102	1.1123	0.7795
28	4.378	1.5902	0.9213	2.3015	1.9505	0.7551	1.2097	1.1088	0.786
29	4.3684	1.571	0.9304	2.2987	1.935	0.7729	1.2092	1.1054	0.7923
30	4.3593	1.5535	0.9358	2.296	1.9197	0.791	1.2088	1.102	0.7982
31	4.3507	1.5376	0.9415	2.2933	1.9045	0.8093	1.2083	1.0987	0.8039
32	4.3426	1.5232	0.9475	2.2906	1.8894	0.8277	1.2078	1.0955	0.8093
33	4.335	1.51	0.9536	2.2879	1.8744	0.846	1.2074	1.0922	0.8144
34	4.3279	1.4979	0.9597	2.2853	1.8596	0.8644	1.2069	1.0891	0.8193
35	4.3211	1.4868	0.9659	2.2828	1.8449	0.8826	1.2065	1.086	0.8239
36	4.3148	1.4765	0.9721	2.2802	1.8304	0.9007	1.2061	1.0829	0.8283
37	4.3088	1.4671	0.9783	2.2777	1.8161	0.9187	1.2057	1.0799	0.8324
38	4.3032	1.4584	0.9844	2.2753	1.802	0.9364	1.2053	1.0769	0.8364
39	4.2979	1.4503	0.9904	2.2729	1.7881	0.9538	1.2049	1.074	0.8401
40	4.293	1.4429	0.9964	2.2706	1.7744	0.9709	1.2045	1.0711	0.8437
41	4.2884	1.4359	1.0022	2.2683	1.7609	0.9877	1.2041	1.0683	0.8471
42	4.2841	1.4295	1.008	2.266	1.7477	1.0041	1.2037	1.0655	0.8503
43	4.2801	1.4235	1.0137	2.2639	1.7347	1.0202	1.2034	1.0627	0.8533
44	4.2764	1.4179	1.0192	2.2617	1.722	1.0358	1.203	1.0601	0.8562
45	4.2733	1.4128	1.0247	2.2597	1.7095	1.051	1.2027	1.0574	0.859
46	4.2707	1.4081	1.0301	2.2576	1.6973	1.0657	1.2023	1.0548	0.8616
47	4.2686	1.4038	1.0354	2.2557	1.6854	1.08	1.202	1.0523	0.864
48	4.2681	1.4002	1.0408	2.2538	1.6737	1.0938	1.2017	1.0498	0.8664
49	4.2692	1.3974	1.0462	2.2519	1.6623	1.1071	1.2014	1.0473	0.8686
50	4.2706	1.3948	1.0516	2.2501	1.6512	1.1199	1.2011	1.0449	0.8707

	Indeterminate Beam			Oblique Nozzle 30^0			Oblique Nozzle 45^0		
Iteration	m_1^0	m_2^0	m_L	m_1^0	m_2^0	m_L	m_1^0	m_2^0	m_L
1	2.649	2.649	0.6132	1.8673	1.8673	0.1265	2.4004	2.4004	0.2422
2	2.6475	2.5359	0.6456	1.8699	1.8106	0.1413	2.402	2.3639	0.2632
3	2.6428	2.4393	0.6781	1.871	1.7542	0.1563	2.4028	2.3267	0.2838
4	2.6354	2.3565	0.7106	1.8709	1.6984	0.1714	2.403	2.2884	0.3041
5	2.6255	2.2853	0.7428	1.8697	1.6432	0.1864	2.4026	2.2493	0.3238
6	2.6136	2.2237	0.7746	1.8675	1.5888	0.2012	2.4015	2.2091	0.3431
7	2.6	2.1702	0.8059	1.8644	1.5353	0.2158	2.3998	2.1679	0.3618
8	2.5851	2.1236	0.8366	1.8604	1.4829	0.2301	2.3976	2.1258	0.38
9	2.5692	2.0829	0.8666	1.8555	1.4318	0.2439	2.3947	2.0829	0.3976
10	2.5526	2.0471	0.8958	1.8498	1.3821	0.2575	2.3911	2.0393	0.409
11	2.5355	2.0155	0.9241	1.8431	1.334	0.2706	2.3868	1.9952	0.4186
12	2.5182	1.9875	0.9514	1.8355	1.2877	0.2834	2.3817	1.9506	0.4288
13	2.501	1.9625	0.9778	1.8269	1.2432	0.2959	2.3756	1.9059	0.4395
14	2.4839	1.9402	1.0031	1.8172	1.2008	0.3081	2.3685	1.8613	0.4507
15	2.4671	1.9202	1.0274	1.8062	1.1604	0.32	2.3602	1.8168	0.4625
16	2.4508	1.9022	1.0507	1.7938	1.1222	0.3317	2.3505	1.7729	0.4748
17	2.435	1.8859	1.073	1.7799	1.0863	0.3433	2.3393	1.7297	0.4876
18	2.4198	1.871	1.0942	1.7642	1.0526	0.3516	2.3265	1.6873	0.5009
19	2.4053	1.8574	1.1145	1.7467	1.0213	0.36	2.3119	1.6461	0.5147
20	2.3914	1.845	1.1337	1.7272	0.9922	0.3687	2.2955	1.6061	0.5289
21	2.3783	1.8336	1.1521	1.7057	0.9654	0.3778	2.2773	1.5676	0.5436
22	2.3659	1.8231	1.1695	1.6824	0.9408	0.3872	2.2574	1.5305	0.5585
23	2.3542	1.8133	1.186	1.6572	0.9183	0.397	2.236	1.4951	0.5738
24	2.3433	1.8042	1.2016	1.6304	0.8979	0.4071	2.2133	1.4613	0.5893
25	2.333	1.7958	1.2165	1.6022	0.8794	0.4173	2.1895	1.4292	0.605
26	2.3234	1.7879	1.2306	1.573	0.8628	0.4278	2.1649	1.3989	0.6151
27	2.3144	1.7805	1.2439	1.5431	0.8479	0.4196	2.1396	1.3704	0.5941
28	2.306	1.7735	1.2566	1.5127	0.8346	0.4118	2.1141	1.3435	0.5765
29	2.2982	1.767	1.2686	1.4822	0.8228	0.4058	2.0884	1.3184	0.5618
30	2.2909	1.7608	1.2799	1.452	0.8123	0.4013	2.0628	1.295	0.5496
31	2.2842	1.755	1.2907	1.4221	0.8031	0.3981	2.0374	1.2732	0.5398
32	2.2779	1.7494	1.3009	1.3929	0.795	0.3962	2.0124	1.253	0.532
33	2.2721	1.7442	1.3106	1.3644	0.7879	0.3953	1.9879	1.2343	0.5259
34	2.2667	1.7392	1.3198	1.3369	0.7817	0.3953	1.9639	1.217	0.5215
35	2.2617	1.7344	1.3285	1.3104	0.7763	0.3951	1.9405	1.2011	0.5185
36	2.2571	1.7299	1.3368	1.285	0.7716	0.3956	1.9178	1.1865	0.5167
37	2.2527	1.7256	1.3446	1.2606	0.7675	0.3969	1.8957	1.1731	0.516
38	2.2487	1.7215	1.3521	1.2374	0.764	0.3988	1.8743	1.1608	0.5163
39	2.245	1.7175	1.3592	1.2154	0.761	0.4013	1.8535	1.1495	0.515
40	2.2416	1.7137	1.3659	1.1944	0.7584	0.4042	1.8334	1.1392	0.5143
41	2.2384	1.7101	1.3724	1.1744	0.7561	0.4076	1.814	1.1298	0.5144
42	2.2354	1.7066	1.3785	1.1555	0.7542	0.4113	1.7952	1.1212	0.5154
43	2.2327	1.7033	1.3843	1.1376	0.7525	0.4153	1.7769	1.1134	0.5171
44	2.2301	1.7001	1.3899	1.1206	0.7511	0.4195	1.7592	1.1063	0.5195
45	2.2277	1.697	1.3952	1.1045	0.7498	0.424	1.7421	1.0998	0.5226
46	2.2255	1.694	1.4003	1.0893	0.7488	0.4286	1.7255	1.0939	0.5261
47	2.2234	1.6911	1.4051	1.0748	0.7479	0.4334	1.7094	1.0884	0.5302
48	2.2215	1.6883	1.4097	1.0611	0.7471	0.4382	1.6938	1.0835	0.5347
49	2.2197	1.6857	1.4141	1.0481	0.7464	0.4431	1.6786	1.079	0.5396
50	2.218	1.6831	1.4172	1.0358	0.7459	0.4476	1.6638	1.0749	0.5448

	Oblique Nozzle 60^0			Oblique Nozzle 90^0			Orthotropic Thick walled Cylinder		
Iteration	m_1^0	m_2^0	m_L	m_1^0	m_2^0	m_L	m_1^0	m_2^0	m_L
1	2.5581	2.5581	0.3508	2.6244	2.6244	0.5133	0.7798	0.7798	0.5574
2	2.5592	2.531	0.3746	2.6253	2.6023	0.536	0.7797	0.7777	0.5702
3	2.5598	2.5037	0.3978	2.6258	2.5804	0.5485	0.7795	0.776	0.582
4	2.5601	2.4761	0.4203	2.6261	2.5586	0.5612	0.7791	0.7745	0.593
5	2.5599	2.448	0.4423	2.6261	2.5369	0.5743	0.7787	0.7733	0.6032
6	2.5593	2.4195	0.4637	2.6258	2.5152	0.5877	0.7782	0.7723	0.6127
7	2.5584	2.3905	0.4844	2.6253	2.4935	0.6015	0.7777	0.7714	0.6214
8	2.557	2.3609	0.5034	2.6245	2.4717	0.6156	0.7772	0.7706	0.6294
9	2.5552	2.3307	0.5147	2.6234	2.4497	0.63	0.7767	0.77	0.6367
10	2.5528	2.3001	0.5265	2.6219	2.4277	0.6449	0.7762	0.7694	0.6435
11	2.55	2.2689	0.5389	2.6201	2.4055	0.6602	0.7758	0.7689	0.6497
12	2.5465	2.2374	0.5519	2.6179	2.3832	0.6759	0.7753	0.7685	0.6554
13	2.5424	2.2054	0.5654	2.6153	2.3608	0.6921	0.7749	0.7681	0.6606
14	2.5374	2.1732	0.5794	2.612	2.3384	0.7088	0.7745	0.7677	0.6653
15	2.5315	2.1408	0.5941	2.6082	2.3159	0.7261	0.7741	0.7674	0.6697
16	2.5246	2.1083	0.6093	2.6036	2.2935	0.7439	0.7737	0.7671	0.6736
17	2.5165	2.0759	0.625	2.5981	2.2711	0.7622	0.7734	0.7668	0.6773
18	2.5071	2.0436	0.6413	2.5918	2.2488	0.781	0.7731	0.7666	0.6805
19	2.4964	2.0115	0.658	2.5845	2.2267	0.8003	0.7728	0.7663	0.6836
20	2.4843	1.9798	0.6752	2.5762	2.2047	0.82	0.7725	0.7661	0.6863
21	2.4708	1.9485	0.6928	2.5668	2.1829	0.8401	0.7723	0.7658	0.6888
22	2.4561	1.9177	0.7106	2.5565	2.1612	0.8604	0.7721	0.7656	0.691
23	2.4401	1.8875	0.7287	2.5453	2.1398	0.8809	0.7719	0.7654	0.6931
24	2.4232	1.8578	0.7467	2.5332	2.1187	0.9015	0.7717	0.7652	0.695
25	2.4054	1.8289	0.7643	2.5204	2.0977	0.9221	0.7715	0.765	0.6967
26	2.3869	1.8006	0.7802	2.507	2.077	0.9427	0.7714	0.7647	0.6982
27	2.3679	1.7731	0.7467	2.4931	2.0565	0.9631	0.7712	0.7645	0.6996
28	2.3487	1.7465	0.7185	2.4789	2.0363	0.9833	0.7711	0.7643	0.7009
29	2.3294	1.7206	0.6948	2.4645	2.0164	1.0032	0.771	0.7641	0.702
30	2.3102	1.6956	0.675	2.4501	1.9968	1.0228	0.7709	0.7639	0.7031
31	2.2911	1.6715	0.6586	2.4357	1.9774	1.0224	0.7708	0.7637	0.7039
32	2.2724	1.6482	0.6452	2.4215	1.9584	0.9961	0.7707	0.7635	0.7045
33	2.254	1.6259	0.6344	2.4076	1.9397	0.973	0.7706	0.7633	0.705
34	2.2362	1.6045	0.626	2.394	1.9214	0.9527	0.7706	0.7631	0.7053
35	2.2188	1.584	0.6197	2.3808	1.9034	0.9351	0.7705	0.7629	0.7055
36	2.202	1.5644	0.6152	2.368	1.8858	0.9198	0.7704	0.7627	0.7057
37	2.1857	1.5457	0.6124	2.3557	1.8686	0.9066	0.7704	0.7625	0.7058
38	2.17	1.5279	0.6111	2.3438	1.8518	0.8955	0.7703	0.7623	0.7058
39	2.1549	1.511	0.6111	2.3325	1.8354	0.8861	0.7703	0.7621	0.7059
40	2.1403	1.4949	0.6122	2.3216	1.8194	0.8785	0.7703	0.7619	0.7059
41	2.1263	1.4797	0.6145	2.3112	1.8039	0.8724	0.7702	0.7618	0.7058
42	2.1128	1.4652	0.6177	2.3013	1.7888	0.8678	0.7702	0.7616	0.7058
43	2.0997	1.4515	0.6218	2.2919	1.7742	0.8646	0.7702	0.7614	0.7058
44	2.0871	1.4386	0.6267	2.2829	1.76	0.8626	0.7701	0.7612	0.7058
45	2.075	1.4264	0.6322	2.2743	1.7462	0.8617	0.7701	0.761	0.7057
46	2.0633	1.4149	0.6383	2.2661	1.7329	0.8619	0.7701	0.7608	0.7057
47	2.0519	1.404	0.645	2.2583	1.7201	0.8621	0.7701	0.7606	0.7056
48	2.041	1.3938	0.6521	2.2509	1.7076	0.862	0.7701	0.7604	0.7056
49	2.0304	1.3841	0.6597	2.2438	1.6956	0.8627	0.77	0.7602	0.7056
50	2.0201	1.3751	0.6676	2.237	1.6841	0.8643	0.77	0.76	0.7055

	Transversely Isotropic Bridgman notch bar			Transversely Isotropic Plate with a hole			Cylinder Bilinear Hardening		
Iteration	m_1^0	m_2^0	m_L	m_1^0	m_2^0	m_L	m_1^0	m_2^0	m_L
1	1.1105	1.1105	0.4767	5.3165	5.3165	1.9849	3.0394	3.0394	2.2123
2	1.1107	1.1081	0.4976	5.3162	5.2911	2.0531	3.0389	3.0293	2.2748
3	1.1107	1.1059	0.5179	5.3154	5.2666	2.1213	3.0375	3.0211	2.3333
4	1.1106	1.1038	0.5377	5.3142	5.2429	2.1892	3.0356	3.0145	2.3879
5	1.1105	1.1018	0.5569	5.3127	5.22	2.2566	3.0333	3.0091	2.4387
6	1.1104	1.0998	0.5755	5.3109	5.1977	2.3232	3.0307	3.0048	2.4858
7	1.1101	1.098	0.5934	5.3088	5.176	2.389	3.028	3.0013	2.5293
8	1.1099	1.0962	0.6106	5.3065	5.1548	2.4537	3.0253	2.9984	2.5695
9	1.1096	1.0945	0.6271	5.3041	5.1341	2.5172	3.0225	2.9961	2.6066
10	1.1093	1.0929	0.643	5.3015	5.1139	2.5793	3.0199	2.9942	2.6406
11	1.1089	1.0913	0.6582	5.2989	5.0941	2.6399	3.0173	2.9927	2.6718
12	1.1086	1.0897	0.6727	5.2961	5.0747	2.6989	3.0149	2.9915	2.7004
13	1.1082	1.0882	0.6866	5.2933	5.0557	2.7563	3.0125	2.9905	2.7266
14	1.1078	1.0867	0.6998	5.2905	5.037	2.8119	3.0104	2.9897	2.7505
15	1.1074	1.0853	0.7124	5.2876	5.0187	2.8658	3.0083	2.9891	2.7723
16	1.107	1.0839	0.7244	5.2847	5.0007	2.9178	3.0064	2.9885	2.7922
17	1.1066	1.0826	0.7358	5.2818	4.9831	2.9679	3.0047	2.9881	2.8103
18	1.1062	1.0813	0.7466	5.2789	4.9657	3.0163	3.0031	2.9878	2.8268
19	1.1058	1.08	0.7569	5.276	4.9487	3.0627	3.0016	2.9875	2.8418
20	1.1054	1.0787	0.7666	5.2731	4.9319	3.1073	3.0002	2.9873	2.8555
21	1.105	1.0775	0.7759	5.2702	4.9154	3.1501	2.9989	2.9871	2.8679
22	1.1046	1.0762	0.7846	5.2674	4.8993	3.191	2.9978	2.987	2.8791
23	1.1042	1.0751	0.7929	5.2646	4.8834	3.2302	2.9967	2.9869	2.8893
24	1.1038	1.0739	0.8008	5.2618	4.8677	3.2676	2.9958	2.9868	2.8986
25	1.1034	1.0727	0.8083	5.2591	4.8524	3.3034	2.9949	2.9867	2.9069
26	1.103	1.0716	0.8153	5.2564	4.8373	3.3375	2.9941	2.9866	2.9145
27	1.1026	1.0705	0.822	5.2537	4.8225	3.37	2.9934	2.9866	2.9214
28	1.1022	1.0694	0.8284	5.2511	4.8079	3.401	2.9927	2.9866	2.9276
29	1.1018	1.0683	0.8344	5.2486	4.7936	3.4305	2.9921	2.9865	2.9333
30	1.1015	1.0672	0.8401	5.246	4.7795	3.4585	2.9916	2.9865	2.9384
31	1.1011	1.0662	0.8455	5.2436	4.7657	3.4852	2.9911	2.9865	2.943
32	1.1008	1.0651	0.8505	5.2412	4.7521	3.5105	2.9907	2.9865	2.9472
33	1.1004	1.0641	0.8551	5.2388	4.7388	3.5346	2.9903	2.9865	2.951
34	1.1001	1.0631	0.8595	5.2365	4.7257	3.5574	2.9899	2.9865	2.9544
35	1.0997	1.0621	0.8635	5.2342	4.7129	3.5791	2.9896	2.9865	2.9575
36	1.0994	1.0611	0.8673	5.232	4.7003	3.5997	2.9893	2.9865	2.9603
37	1.0991	1.0602	0.8709	5.2298	4.6879	3.6192	2.989	2.9865	2.9628
38	1.0988	1.0592	0.8741	5.2277	4.6757	3.6377	2.9888	2.9865	2.9651
39	1.0985	1.0583	0.8772	5.2256	4.6638	3.6553	2.9885	2.9865	2.9672
40	1.0982	1.0573	0.8802	5.2236	4.6521	3.6719	2.9883	2.9865	2.969
41	1.0979	1.0564	0.8829	5.2216	4.6406	3.6877	2.9882	2.9865	2.9707
42	1.0976	1.0555	0.8855	5.2196	4.6293	3.7027	2.988	2.9865	2.9722
43	1.0973	1.0546	0.8879	5.2177	4.6183	3.7169	2.9878	2.9865	2.9736
44	1.097	1.0537	0.8903	5.2159	4.6074	3.7303	2.9877	2.9865	2.9749
45	1.0967	1.0528	0.8925	5.2141	4.5968	3.7431	2.9876	2.9865	2.976
46	1.0965	1.0519	0.8945	5.2123	4.5864	3.7552	2.9875	2.9865	2.977
47	1.0962	1.0511	0.8965	5.2106	4.5762	3.7667	2.9874	2.9865	2.9779
48	1.0959	1.0502	0.8984	5.2089	4.5661	3.7776	2.9873	2.9865	2.9787
49	1.0957	1.0494	0.9002	5.2073	4.5563	3.7879	2.9872	2.9865	2.9795
50	1.0954	1.0485	0.9019	5.2057	4.5467	3.7977	2.9871	2.9865	2.9802

	Cylinder Ramberg-Osgood			CT Specimen Bilinear Hardening			CT Specimen Ramberg-Osgood		
Iteration	m_1^0	m_2^0	m_L	m_1^0	m_2^0	m_L	m_1^0	m_2^0	m_L
1	2.9715	2.9715	2.1629	2.0835	2.0835	0.2179	2.0233	2.0233	0.2116
2	2.971	2.9616	2.224	2.0865	2.0219	0.2367	2.0261	1.9634	0.2299
3	2.9697	2.9536	2.2812	2.0863	1.9673	0.2565	2.026	1.9104	0.2491
4	2.9678	2.9472	2.3346	2.0835	1.9182	0.2773	2.0232	1.8627	0.2692
5	2.9655	2.9419	2.3842	2.0786	1.8738	0.2989	2.0184	1.8196	0.2903
6	2.963	2.9377	2.4303	2.0719	1.8331	0.3215	2.012	1.7801	0.3122
7	2.9604	2.9342	2.4728	2.0639	1.7957	0.3448	2.0042	1.7437	0.3349
8	2.9577	2.9314	2.5121	2.0548	1.761	0.3689	1.9953	1.7101	0.3582
9	2.955	2.9292	2.5483	2.0449	1.7288	0.3936	1.9857	1.6788	0.3822
10	2.9524	2.9273	2.5816	2.0344	1.6987	0.4187	1.9756	1.6496	0.4066
11	2.9499	2.9259	2.6121	2.0236	1.6706	0.4441	1.965	1.6223	0.4312
12	2.9475	2.9247	2.6401	2.0124	1.6442	0.47	1.9542	1.5966	0.4564
13	2.9452	2.9237	2.6657	2.0012	1.6193	0.4962	1.9433	1.5725	0.4818
14	2.9431	2.9229	2.689	1.9899	1.5959	0.5226	1.9323	1.5497	0.5075
15	2.9411	2.9223	2.7104	1.9786	1.5738	0.549	1.9214	1.5283	0.5331
16	2.9393	2.9218	2.7298	1.9674	1.5529	0.5752	1.9105	1.508	0.5586
17	2.9375	2.9214	2.7476	1.9564	1.5331	0.601	1.8998	1.4887	0.5836
18	2.936	2.921	2.7637	1.9456	1.5143	0.6259	1.8893	1.4705	0.6078
19	2.9345	2.9208	2.7784	1.935	1.4965	0.6502	1.879	1.4532	0.6314
20	2.9332	2.9206	2.7917	1.9246	1.4795	0.6738	1.8689	1.4367	0.6543
21	2.9319	2.9204	2.8038	1.9144	1.4634	0.6966	1.859	1.421	0.6764
22	2.9308	2.9202	2.8148	1.9045	1.448	0.7186	1.8494	1.4061	0.6978
23	2.9298	2.9201	2.8248	1.8949	1.4334	0.7397	1.8401	1.392	0.7183
24	2.9289	2.92	2.8338	1.8855	1.4195	0.7601	1.831	1.3785	0.7381
25	2.928	2.92	2.842	1.8764	1.4063	0.7797	1.8221	1.3656	0.7571
26	2.9272	2.9199	2.8494	1.8676	1.3936	0.7985	1.8136	1.3533	0.7754
27	2.9265	2.9199	2.8562	1.859	1.3816	0.8164	1.8052	1.3416	0.7928
28	2.9259	2.9198	2.8622	1.8507	1.37	0.8336	1.7971	1.3304	0.8095
29	2.9253	2.9198	2.8678	1.8426	1.359	0.8499	1.7893	1.3197	0.8254
30	2.9248	2.9198	2.8728	1.8349	1.3485	0.8655	1.7818	1.3095	0.8404
31	2.9243	2.9198	2.8773	1.8273	1.3385	0.8802	1.7745	1.2998	0.8548
32	2.9238	2.9198	2.8814	1.8201	1.3289	0.8925	1.7674	1.2905	0.8666
33	2.9235	2.9198	2.8851	1.813	1.3197	0.9018	1.7606	1.2816	0.8757
34	2.9231	2.9198	2.8884	1.8062	1.311	0.9107	1.754	1.273	0.8844
35	2.9228	2.9198	2.8914	1.7997	1.3026	0.9193	1.7476	1.2649	0.8927
36	2.9225	2.9197	2.8942	1.7933	1.2945	0.9275	1.7415	1.2571	0.9007
37	2.9222	2.9197	2.8966	1.7872	1.2869	0.9353	1.7355	1.2496	0.9083
38	2.922	2.9197	2.8989	1.7813	1.2795	0.9428	1.7298	1.2425	0.9155
39	2.9218	2.9197	2.9009	1.7756	1.2725	0.9488	1.7243	1.2356	0.9214
40	2.9216	2.9197	2.9027	1.7701	1.2657	0.9493	1.7189	1.2291	0.9218
41	2.9214	2.9197	2.9044	1.7648	1.2593	0.95	1.7138	1.2228	0.9225
42	2.9212	2.9197	2.9058	1.7597	1.2531	0.951	1.7088	1.2168	0.9235
43	2.9211	2.9197	2.9072	1.7548	1.2472	0.9523	1.704	1.2111	0.9247
44	2.921	2.9197	2.9084	1.75	1.2415	0.9537	1.6994	1.2056	0.9261
45	2.9208	2.9197	2.9095	1.7454	1.236	0.9552	1.6949	1.2003	0.9276
46	2.9207	2.9197	2.9105	1.741	1.2308	0.9568	1.6906	1.1952	0.9292
47	2.9206	2.9197	2.9114	1.7367	1.2258	0.9585	1.6865	1.1903	0.9308
48	2.9206	2.9197	2.9122	1.7326	1.221	0.9603	1.6825	1.1857	0.9325
49	2.9205	2.9198	2.9129	1.7286	1.2164	0.962	1.6786	1.1812	0.9342
50	2.9204	2.9198	2.9136	1.7248	1.212	0.9638	1.6749	1.1769	0.9359

	Indeterminate Beam Bilinear Hardening			Indeterminate Beam Ramberg-Osgood		
Iteration	m_1^0	m_2^0	m_L	m_1^0	m_2^0	m_L
1	3.2997	3.2997	0.7638	3.4533	3.4533	0.7993
2	3.2978	3.1588	0.8042	3.4513	3.3058	0.8416
3	3.292	3.0385	0.8447	3.4452	3.1799	0.884
4	3.2827	2.9354	0.8851	3.4355	3.072	0.9263
5	3.2704	2.8466	0.9252	3.4226	2.9791	0.9683
6	3.2556	2.7699	0.9649	3.4071	2.8988	1.0098
7	3.2387	2.7033	1.0039	3.3894	2.8291	1.0506
8	3.2201	2.6453	1.0421	3.37	2.7684	1.0906
9	3.2003	2.5945	1.0795	3.3492	2.7152	1.1297
10	3.1796	2.5499	1.1158	3.3275	2.6686	1.1677
11	3.1583	2.5105	1.151	3.3053	2.6274	1.2046
12	3.1368	2.4757	1.1851	3.2828	2.5909	1.2402
13	3.1153	2.4446	1.2179	3.2603	2.5584	1.2746
14	3.094	2.4168	1.2495	3.238	2.5293	1.3076
15	3.0731	2.3919	1.2798	3.2161	2.5032	1.3394
16	3.0528	2.3694	1.3088	3.1948	2.4797	1.3697
17	3.0331	2.3491	1.3365	3.1742	2.4584	1.3987
18	3.0142	2.3306	1.363	3.1544	2.439	1.4264
19	2.9961	2.3137	1.3882	3.1355	2.4214	1.4528
20	2.9788	2.2982	1.4122	3.1175	2.4052	1.4779
21	2.9625	2.284	1.435	3.1004	2.3903	1.5018
22	2.9471	2.2709	1.4567	3.0842	2.3765	1.5245
23	2.9325	2.2587	1.4773	3.069	2.3638	1.546
24	2.9189	2.2474	1.4968	3.0547	2.352	1.5665
25	2.906	2.2369	1.5153	3.0413	2.341	1.5858
26	2.8941	2.227	1.5329	3.0287	2.3307	1.6042
27	2.8829	2.2178	1.5495	3.017	2.321	1.6216
28	2.8724	2.2091	1.5653	3.0061	2.312	1.6381
29	2.8627	2.201	1.5802	2.9959	2.3034	1.6537
30	2.8537	2.1933	1.5944	2.9865	2.2954	1.6685
31	2.8453	2.186	1.6078	2.9777	2.2878	1.6826
32	2.8375	2.1791	1.6205	2.9695	2.2805	1.6959
33	2.8302	2.1726	1.6325	2.9619	2.2737	1.7085
34	2.8235	2.1664	1.644	2.9549	2.2672	1.7205
35	2.8173	2.1605	1.6548	2.9484	2.261	1.7318
36	2.8115	2.1548	1.6651	2.9423	2.2551	1.7426
37	2.8061	2.1495	1.6749	2.9367	2.2495	1.7529
38	2.8011	2.1443	1.6842	2.9315	2.2441	1.7626
39	2.7965	2.1394	1.6931	2.9266	2.239	1.7718
40	2.7922	2.1347	1.7015	2.9221	2.234	1.7806
41	2.7882	2.1302	1.7095	2.918	2.2293	1.789
42	2.7845	2.1258	1.7171	2.9141	2.2248	1.797
43	2.7811	2.1217	1.7244	2.9105	2.2204	1.8046
44	2.7779	2.1176	1.7313	2.9072	2.2162	1.8119
45	2.7749	2.1138	1.7379	2.904	2.2122	1.8188
46	2.7721	2.1101	1.7442	2.9011	2.2083	1.8254
47	2.7696	2.1065	1.7502	2.8984	2.2045	1.8317
48	2.7672	2.1031	1.756	2.8959	2.2009	1.8377
49	2.7649	2.0997	1.7615	2.8936	2.1974	1.8435
50	2.7628	2.0965	1.7653	2.8914	2.1941	1.8474